CHAPTER 4:
COMPUTER SIMULATION OF THE NOx ABATEMENT PROCESS AS AN EQUILIBRIUM-REACTION MODEL

4.1 Introduction

4.1.1 An Overview

The previous chapter graphically displays the shortcomings of the conversion-reaction model and explained the reasons for those shortcomings. We ask ourselves if any changes to process parameters could improve the performance of the conversion-reaction model. The answer is no; we need an inherent change in the way the model deals with chemical reactions.

The next step we choose to take is to treat the reactions in the scrubber/absorber and catalyst vessel as equilibrium reactions. That is to say, we define for ASPEN Plus the reactants, products, and reaction stoichiometry. ASPEN Plus calculates the chemical equilibrium of the system using thermodynamics. This change results, surprisingly, in a marked reduction in flowsheet complexity and in the amount of user effort involved. The use of equilibrium reactions allows us to represent the entire scrubber/absorber tower as a single reactive-distillation unit. The two scrubber stages are incorporated as equilibrium trays. Now, instead of specifying the number of theoretical stages and finding reaction conversions by trial and error, we let ASPEN Plus calculate the reaction results, and we use trial and error to determine the number of theoretical stages required for the specified separation.

This arrangement gives rise to two different equilibrium models. The only difference between the two models is the specification of stage efficiencies for the second model. The first model has 100% efficient equilibrium stages. This model results in a requirement of a mere three stages for the base-case NOx removal. We compare that number to the eighteen total stages (counting the two scrubber sections as stages) in the actual scrubber/absorber. If the model is accurate, it gives an overall column efficiency of 17%.

We then specify vaporization efficiencies for the stages to arrive at the second equilibrium model. The specification of vaporization efficiencies of 2.5 for NO, NO_2, and N_2O_4 brings the tray number in the ASPEN Plus simulation up to equal the actual tray number of eighteen. Recall that the reactions are in equilibrium in the model (which we will show is a reasonable assumption for the real system as well) and that the vaporization efficiencies only affect the vapor-liquid equilibrium. This fact tells us that the mass transfer between phases represents the main resistance to absorption, whereas the reaction equilibria constitute the main driving force.

The equilibrium model performs the simulation of the scrubber/absorber quite well. However, the equilibrium model cannot satisfactorily simulate the behavior of the SCR. It fails because of mathematical limitations in ASPEN Plus. We find the maximum value for a reaction equilibrium constant in ASPEN Plus to be $1x10^{20}$. The equilibrium constants for the SCR reactions are above this value, however, ASPEN Plus assigns the maximum value to such constants. Therefore, the ratio of products to reactants is limited such that ASPEN Plus does not allow the actual product concentration to be reached. The failure of the equilibrium model to simulate the SCR motivates us to develop the kinetic model of the following chapter.

4.1.2 Motivation for an Equilibrium-Absorption Model

The conversion-reaction model ASPEN simulation matches the mass-balance data for the base case very well. This modeling approach cannot match the system sensitivity to variables, such as temperature and pressure changes. This inability makes it an unsatisfactory tool for analyzing retrofit design options on the NOx abatement system.

Reaction equilibria predominates in the liquid region (Jethani et.al., 1992; Miller, 1987; Thomas et al., 1997). Reaction rates and reaction equilibria constitute the driving force for NOx absorption. Gas solubilities and mass-transfer rates are secondary as driving forces (although primary in the resistance to equilibrium absorption) in that they supply the reactants to the proper

phase in which they participate in their respective reactions. This situation itself sets NOx absorption apart from most absorption processes.

Due to the fast reactions in the gas and liquid phases, reaction equilibrium dominates in the NOx and water system. Column-tray efficiency ultimately depends on the rate at which the mass transfer supplies these reactants to the proper phase, as well as the rates at which the reactions achieve equilibrium. Because the reactions are fast and assumed to reach instantaneous equilibrium, mass transfer represents the rate-limiting step in the absorption of NOx when NO_2 is the dominant NOx species.

Reactions modeled by simply specifying conversion values cannot incorporate dependence on temperature, pressure, or concentration in the reacting phase. The last point may be easily overlooked. Most of the key reactions that drive absorption take place in the liquid phase. Therefore, reactions in a vapor-liquid system depend on the concentration of the reactants and products in the phase in which the reactions take place.

Defining a conversion for a stage where the reactants predominate in the vapor, whereas the reactions take place in the liquid, contains an inherent logical flaw. Increasing vapor-phase concentrations of reactants does not necessarily increase liquid-phase concentrations proportionately or immediately. Making such an assumption removes mass transfer as the essential link in the chain reaction mechanism of NOx absorbing into water. Reaction is the driving force for NOx absorption, but mass transfer is the barrier that slows the process.

4.1.3 Complexities of NOx Absorption

Even as recently as 1994, researchers recognized the complexity of NOx absorption. Suchak and Joshi (1994) state that “absorption of NOx gas is probably the most complex when compared with other absorption operations.” Miller states that “the chemistry, although extremely complex, has been treated extensively in the literature [but] gas-liquid mass transfer of the primary reactants, however, is less well understood.” He goes on to say that “in particular,

data for prediction of plant-scale performance has been lacking" (Miller, 1987). Even after minimal perusal of the literature, it becomes clear that the very simple set of reactions proposed by RFAAP and used in the conversion model will not suffice. Figure 4.1 shows the proposed absorption and reaction network presented in one example of the literature (Newman and Carta, 1988).

The reader can see from Figure 4.1 that neither NO and NO_2 do not absorb directly into water, nor do they directly react to form nitric acid. They first must react to form the NOx species, N_2O_3 or N_2O_4. These new species do absorb into the liquid phase and subsequently react to form nitric acid.

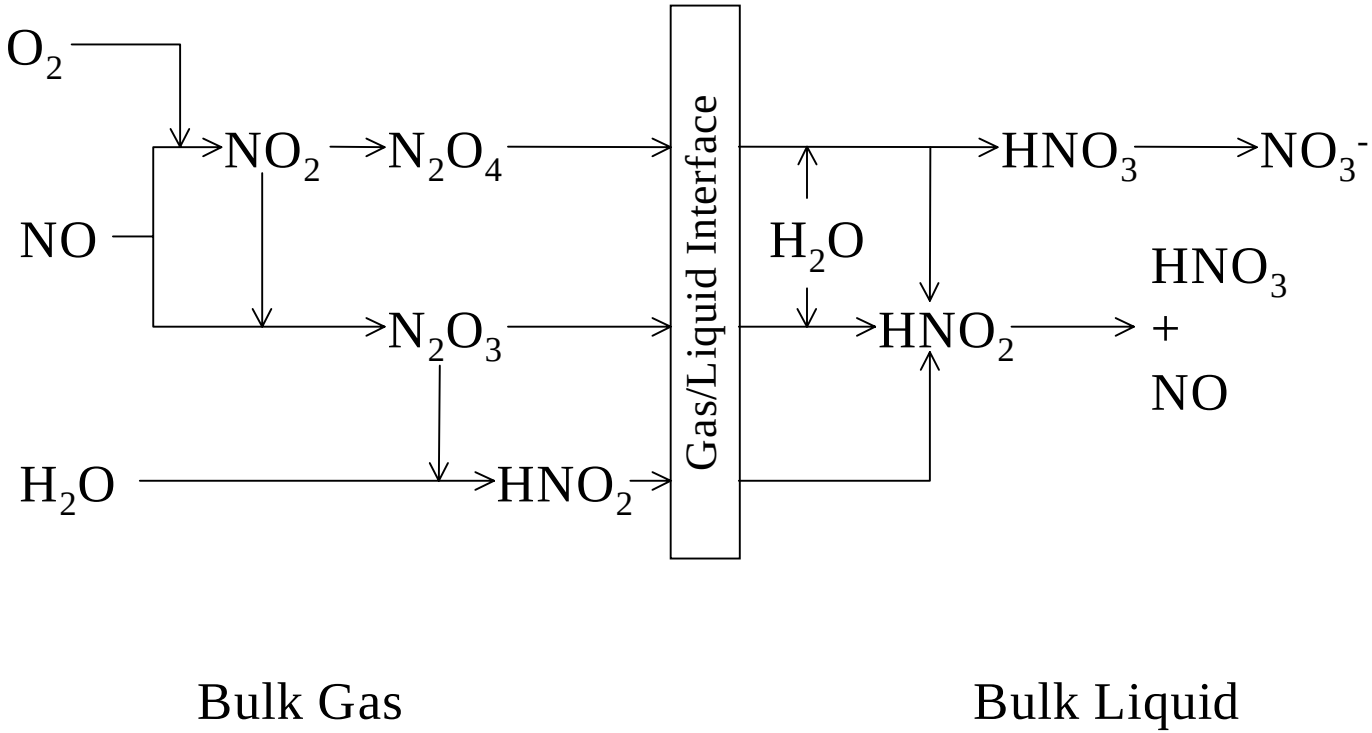

Figure 4.1. Actual diffusion/reaction network for absorption of nitrogen oxides in water (Newman and Carta, 1988).

The first thing that the reader must understand when approaching the challenge of NOx removal by absorption is that removal of NO and removal of NO_2 are very different, even somewhat antagonistic processes. Figure 4.1 illustrates this fact. NO_2 absorption into water results in the production of HNO_3 and NO. HNO_3, the product of NO_2 absorption, obviously hinders removal of NO_2. However, some evidence exists suggesting that HNO_3 improves removal of NO (Thomas and Vanderschuren, 1997). NO absorption into nitric acid solutions results in the production of NO_2. The implications are bewildering for researchers merely attempting to understand this process. The engineer charged with actually doing something about it will be lost without an understanding of the subtle trade-offs involved.

Attempts to remove NO by absorption will be disappointing because NO_2 is produced in the process. This NO_2 then reacts in water to reproduce the NO in equal proportions to the NO originally absorbed. NO must therefore be converted in a way that does not return equal amounts of NO. Oxidation of NO to NO_2 in air, and subsequent absorption of NO_2 in water, still evolves NO. However, NO oxidizes to produce NO_2 in a one-to-one proportion. Then the absorption of 3 moles of NO_2 produces one mole of NO. The first lesson that the reader learns is to maximize NO removal by oxidation and NO_2 removal by absorption. The regeneration of NO in NOx absorption cannot be avoided. However, the engineer can stack the deck to affect the maximum total NOx reduction. Reduction of total NOx should remain the final objective for general NOx abatement.

4.1.4 Simplification of Reaction Mechanism

Chapter 2 discusses the important reactions of NOx absorption, and we have listed them in Table 4.1. Table 4.2 summarizes the important characteristics of the key components in the NOx absorption system. Table 4.3 shows some of the qualitative aspects of the important reactions involved in the system. We use the properties in Tables 4.2 and 4.3 to simplify the full reaction mechanism proposed by Miller (1987) to a manageable size.

Table 4.1. Full reaction and absorption mechanism for NOx and water (Miller, 1987).

N_2O_4 Path	N_2O_3 Path	NO_2 Path
Gas Phase	Gas Phase	Gas Phase
$2NO + O_2 \leftrightarrow 2NO_2$ (4.1) $2NO_2 \leftrightarrow N_2O_4$ (4.2)	$NO + NO_2 \leftrightarrow N_2O_3$ (4.6)	$NO_{2(g)} \leftrightarrow NO_{2(l)}$ (4.10) $2NO_{2(l)} + H_2O \leftrightarrow HNO_3 + HNO_2$ (4.11)
Transport	Transport	Transport
$N_2O_{4(g)} \leftrightarrow N_2O_{4(l)}$ (4.3)	$N_2O_{3(g)} \leftrightarrow N_2O_{3(l)}$ (4.7)	$HNO_{3(g)} \leftrightarrow HNO_{3(l)}$ (4.12)
Liquid Phase	Liquid Phase	Liquid Phase
$N_2O_{4(l)} + H_2O \leftrightarrow HNO_3 + HNO_2$ (4.4) $3HNO_2 \leftrightarrow HNO_3 + H_2O + 2NO_{(g)}$ (4.5)	$N_2O_{3(g)} + H_2O \leftrightarrow 2HNO_2$ (4.8) $2HNO_2 + O_2 \leftrightarrow 2HNO_3$ (4.9)	$3NO_2 + H_2O \leftrightarrow 2HNO_3 + NO$ (4.13)

Note: (l) refers to liquid phase and (g) refers to gas phase

Table 4.2. NOx absorption chemistry: key component descriptions.

Compound	Conc.	Solubility	Stability
NO	High	Negligible	Stable
NO_2	High	Low	Reactive
N_2O_3	Low	Moderate	Reactive/Dissociates easily
N_2O_4	Moderate	Moderate	Reactive/Dissociates easily
HNO_2	Low	Highly	Reactive/Unstable
HNO_3	High	Extremely	Unstable/Dissociates easily
$NO3^-$	High	Completely	Stable

Table 4.3. NOx absorption chemistry: key reaction descriptions.

Reactions	Rate	Equilibrium
$2NO + O_2 <=> 2NO_2$	Slow	Irreversible
$NO + NO_2 <=> N_2O_3$	Fast	NO, NO_2, favored heavily
$2NO_2 <=> N_2O_4$	Fast	NO_2 favored moderately
$N_2O_4 + H_2O <=> HNO_2 + HNO_3$	Fast	Products favored heavily
$3HNO_2 <=> HNO_3 + H_2O + 2NO$	Fast	Products favored heavily
$HNO_3 + H_2O <=> NO_3^- + H_3O^+$	Fast	Products favored heavily

We deem the pathway presented by Miller to most closely reflect the situation under the conditions that concern us here. Other researchers have proposed more complex mechanisms. The complexity of these other mechanisms resides in their treatment of the gas-phase reactions. Near atmospheric pressure and at low NOx concentrations, as is the case here, gas-phase reactions become less important and Miller's proposed reaction scheme is acceptable. Figure 4.2 shows a schematic representation of the important reactions and mass-transfer components for the mechanism proposed by Miller (1987).

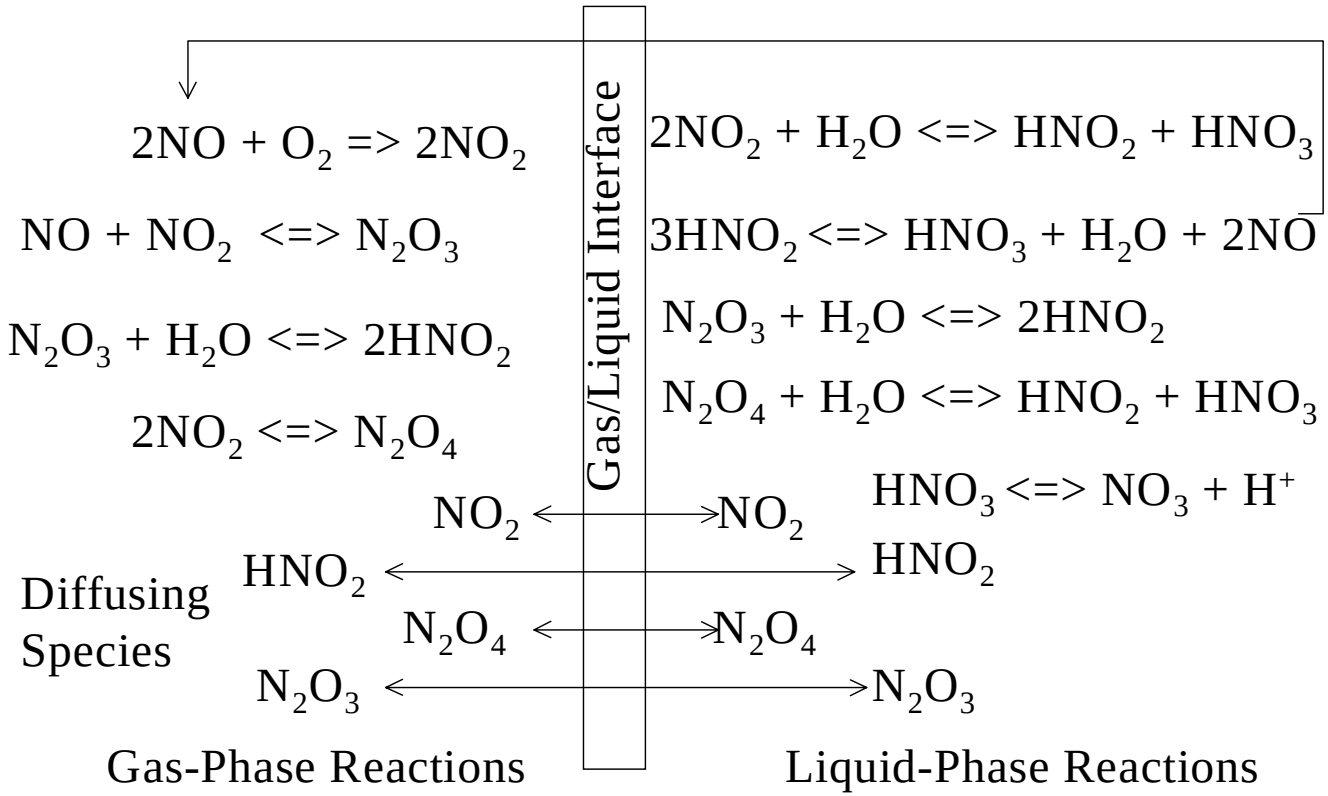

Figure 4.2. Full mechanism of NOx absorption in water for the mass transfer and reactions in the scrubber/absorber (Miller, 1987).

Even if we could develop a computer model that would account for all the pathways and different reactions shown in Figure 4.2, would we want to do this? As previously stated, we want the simplest, most theoretically sound model that can accurately predict the behavior of the system under conditions of interest. For us, these conditions are process variables and retrofit options that positively or negatively affect the system performance of the removal of NOx from fumes as they exist at RFAAP. We can neglect certain aspects of the overall mechanism as having inconsequential contributions to our conditions of interest in the process. However, we want to begin with a complete representation of the physical system, from which we can make logical assumptions to simplify the model to a manageable size. We want to eventually arrive at a reaction model that we can put to work for us.

4.1.5 Assumptions Made for the Equilibrium Model

4.1.5.1 Assumption I: Neglect Reaction (4.1)

I. The oxidation of NO to NO_2 remains a very important aspect of NOx chemistry. However, the forward rate of reaction (4.1) is very slow and "has been identified as a major rate limitation in the overall absorption mechanism" in cases where NO represents the major contributor to total NOx and NO_2 that must be produced from NO oxidation (Miller, 1987). Again, the oxidation reaction, (4.1) $2NO + O_2 \rightarrow 2NO_2$, eliminates NO and produces NO_2 in the presence of oxygen.

From reaction-rate data presented by Suchak and Joshi (1994), we perform calculus to show the time-dependent concentration of NO for the starting conditions of the fume feed to the bottom of the column. We present the results in Figure 4.3. Based on the total volume of the column, we calculate a residence time of 22 seconds for the gas flow rate of 4000 standard cubic feet per minute (SCFM) through the column. Obviously, the entire column volume is not available for gas flow. Therefore, the actual residence time depends on the void volume of the column and comes to even less than the 22 seconds assumed for Figure 4.3. Figure 4.4 shows the same calculations for different initial concentrations of NO. The data presented in Figure 4.3

represent the maximum NO that the system at RFAAP should have to deal with, but Figure 4.4 shows how the rate of NO consumption depends strongly on the NO concentration. Therefore, in the ammonia oxidation plant, reaction (4.1) would proceed much faster because of the higher concentration of NO and the higher column pressures. Therefore assumption I would not be valid for that case.

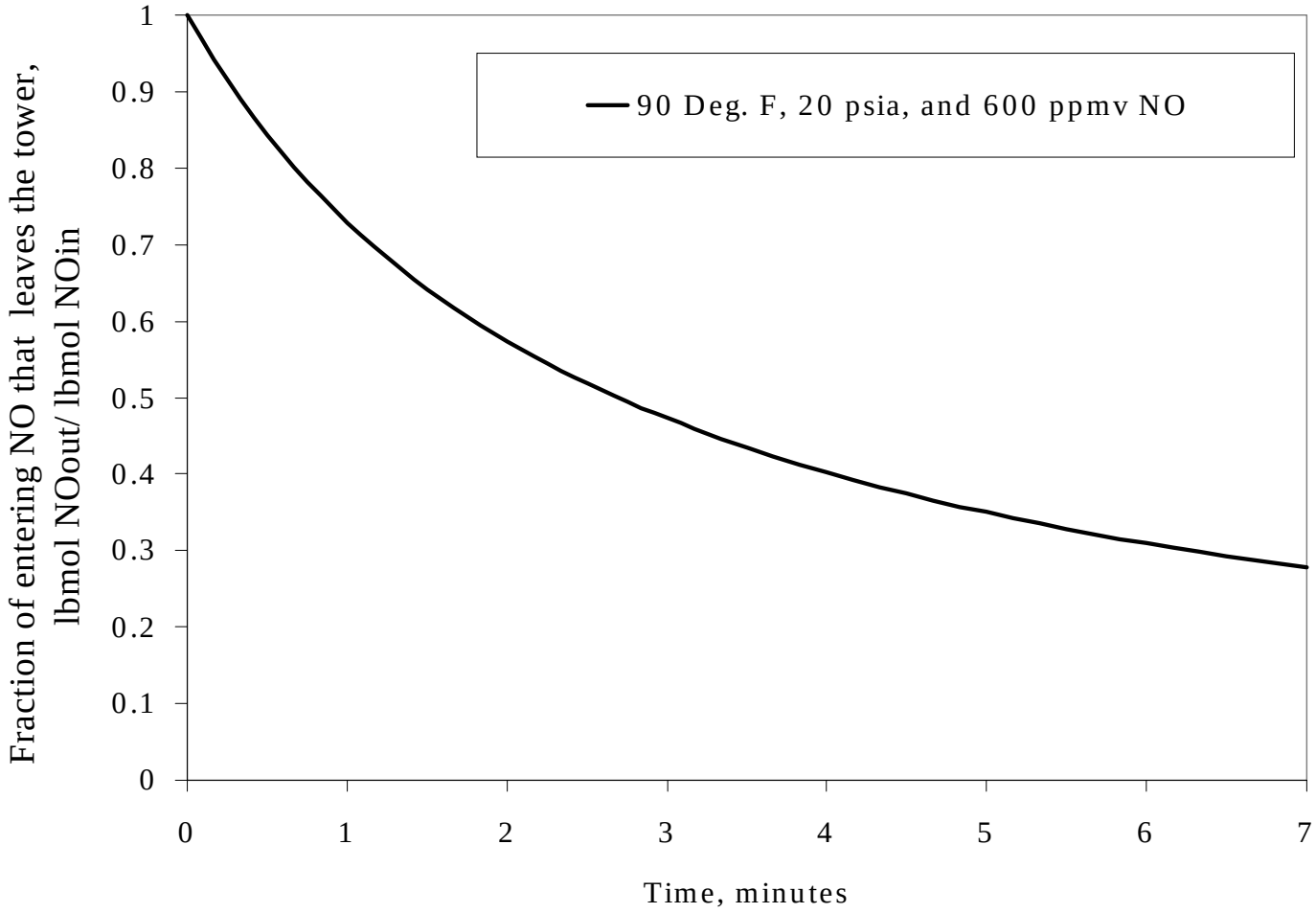

Figure 4.3. Time-dependent concentration of NO from reaction (4.1) for the conditions of the scrubber/absorber (Suchak and Joshi, 1994). Column residence time = 1/3 minute, less than 10% NO consumed. Initial partial pressure of NO = 0.062 kPa.

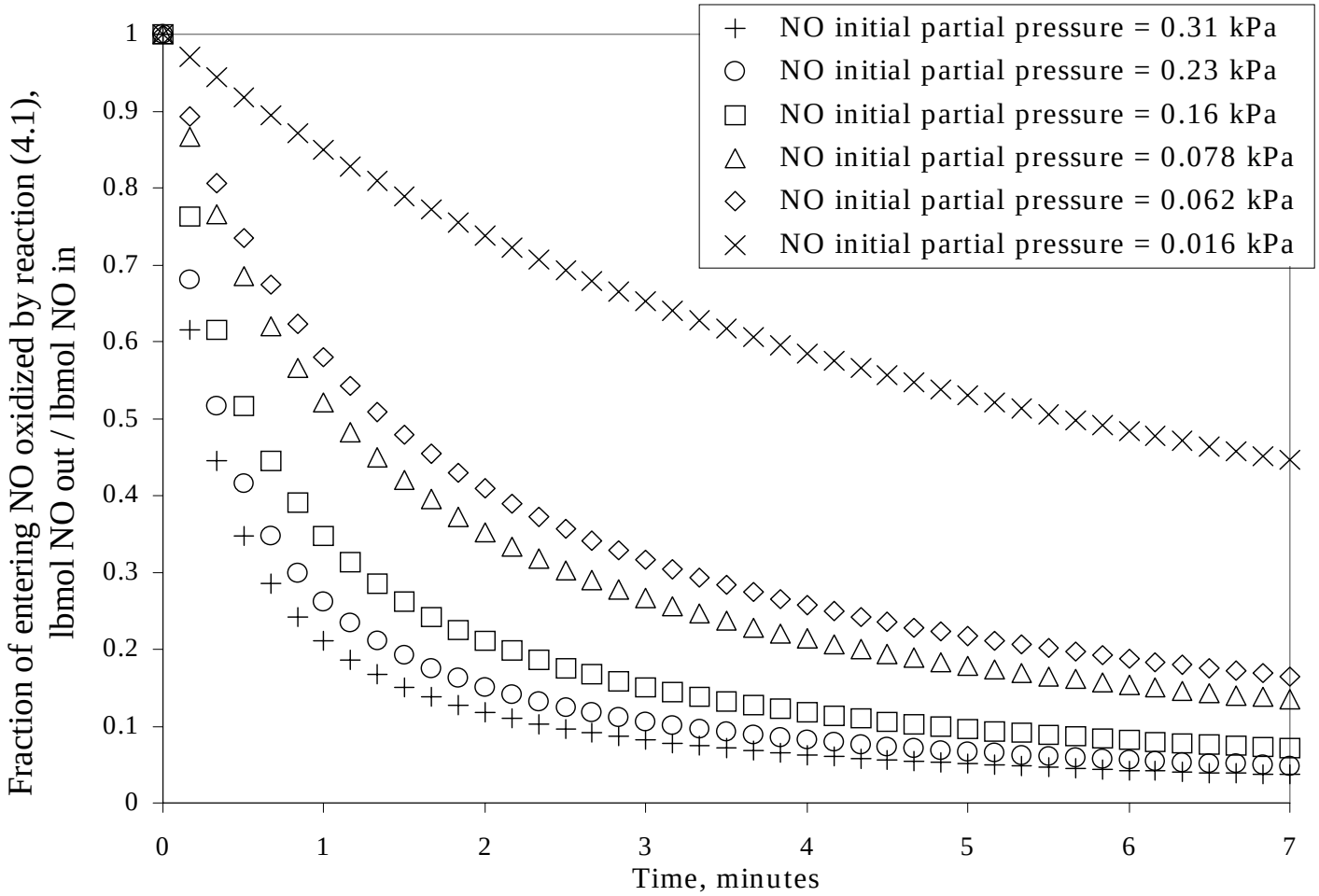

Figure 4.4. Plot of fraction of initial NO partial pressure vs. time for different starting partial pressures modeling reaction (4.1) within the scrubber/absorber. The NO partial pressure of the fumes entering the scrubber at RFAAP is approximately 0.062 kPa.

Figure 4.3 clearly shows that for the conditions and time scale of the scrubber/absorber, the amount of NO that oxidizes to NO_2 is very low. Therefore, because of the time-scale and concentration of NO and because NO_2 represents the major component of total NOx fed to the scrubber/absorber column, we neglect reaction (4.1).

4.1.5.2 Assumption II: Treat Reaction (4.2) as Being in Instantaneous Equilibrium

II. Reaction (4.2), (4.2) $2NO_2 \leftrightarrow N_2O_4$, proceeds very fast, is reversible, and equilibrates rapidly (Miller, 1987, Matasa and Tonca, 1973). This reaction typically achieves equilibrium in 10^{-4} seconds (Matasa and Tonca, 1973). Therefore, we can assume this reaction to be at equilibrium with respect to other time-dependent concentrations. In other words, in a dynamic environment, we assume that the ratio of products over reactants to be a constant (the equilibrium constant, K) for reaction (4.2). Put simply, we can calculate the concentration of N_2O_4 in the gas phase at any time if the concentration of NO_2 or the total (NO_2 + N_2O_4) is known.

4.1.5.3 Assumption III: Combine Reactions (4.4) and (4.5)

III. Reactions (4.4) and (4.5) are fast and complete in the liquid film, and researchers often represent them in a combined form (Miller, 1987), (4.4) $N_2O_{4(l)} + H_2O \leftrightarrow HNO_3 + HNO_2$, (4.5) $3HNO_2 \leftrightarrow HNO_3 + H_2O + 2NO_{(g)}$, Combining Reactions (4.4) and (4.5), we get (4.4,5) $3N_2O_{4(l)} + 2H_2O \leftrightarrow 4HNO_3 + 2NO_{(g)}$. Reactions (4.4) and (4.5) equilibrate rapidly. Therefore, we assume reaction (4,5) to be at equilibrium in the liquid phase.

4.1.5.4 Assumption IV: Neglect the N_2O_3 Pathway

IV. The association of NO and NO_2 molecules, reaction (4.6), is much slower than reaction (4.2), coming to equilibrium in 0.1 seconds (Matasa and Tonca, 1973), (4.6) $NO + NO_2 \leftrightarrow N_2O_3$. Also, N_2O_3 is much less stable and less soluble than N_2O_4. For these reasons, we

neglect the contribution to NOx removal from the N_2O_3 path in the equilibrium model. Figure 4.5 shows the equilibrium fraction of NO_2 that exists in dimer form as N_2O_4 as a function of gas temperature. We perform the calculations for the same conditions as for the gas stream entering the scrubber. The reader can see that at approximately 80 to 90 ^oF, there exists an appreciable amount of N_2O_4.

Figure 4.6 is similar to Figure 4.5, except that Figure 4.6 shows the equilibrium fraction of NO and NO_2 that exists as N_2O_3. The reader can see that within the relevant temperature range, there is roughly one-tenth the N_2O_3 available as N_2O_4. Given that N_2O_4 absorbs slightly faster per mole and also exists in higher concentrations, we neglect the effect of N_2O_3 absorption.

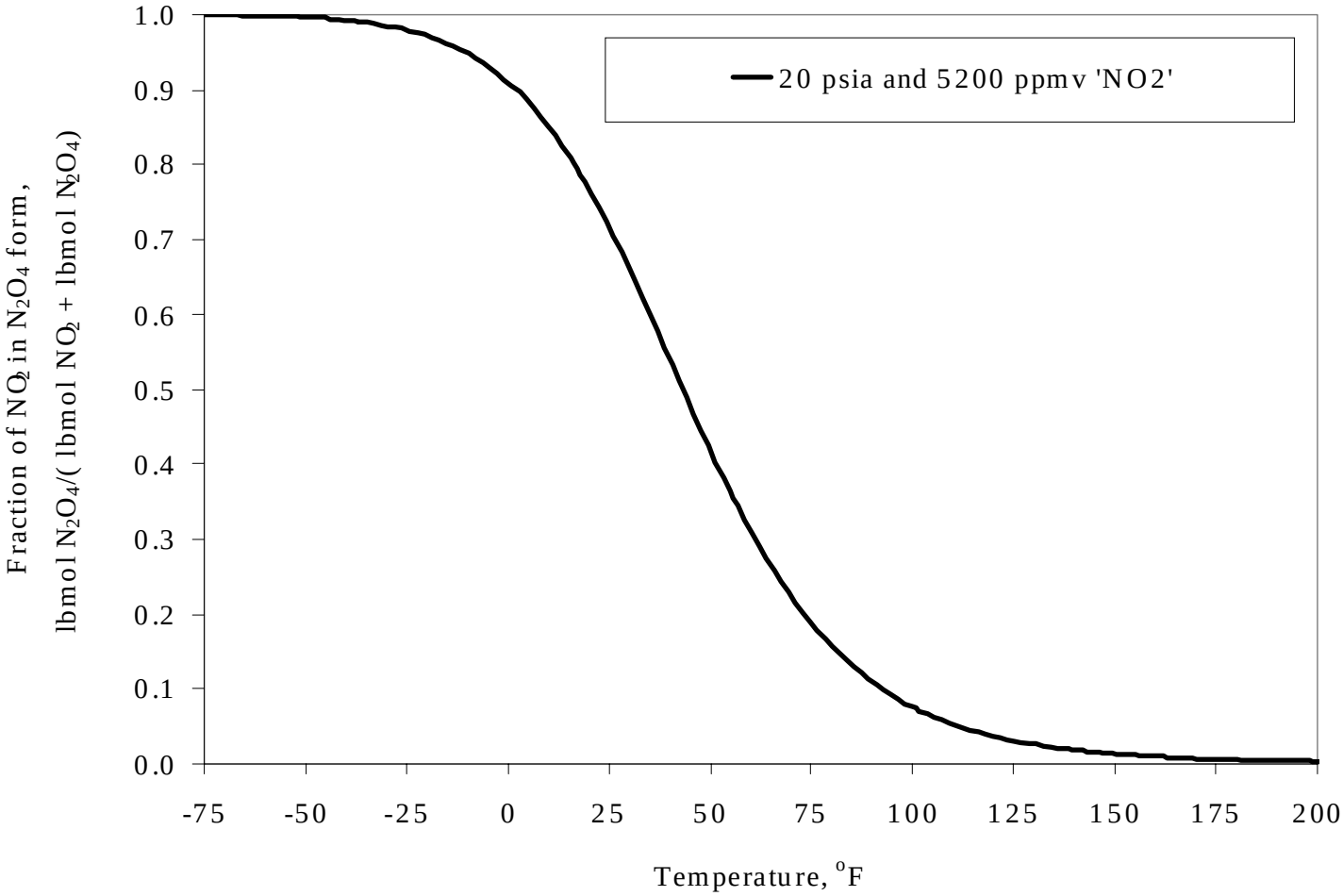

Figure 4.5. Plot of equilibrium N_2O_4 ratio vs temperature. Conditions of the stream are 20 psia and the same NOx concentration as that of the fumes entering the bottom of the scrubber/absorber.

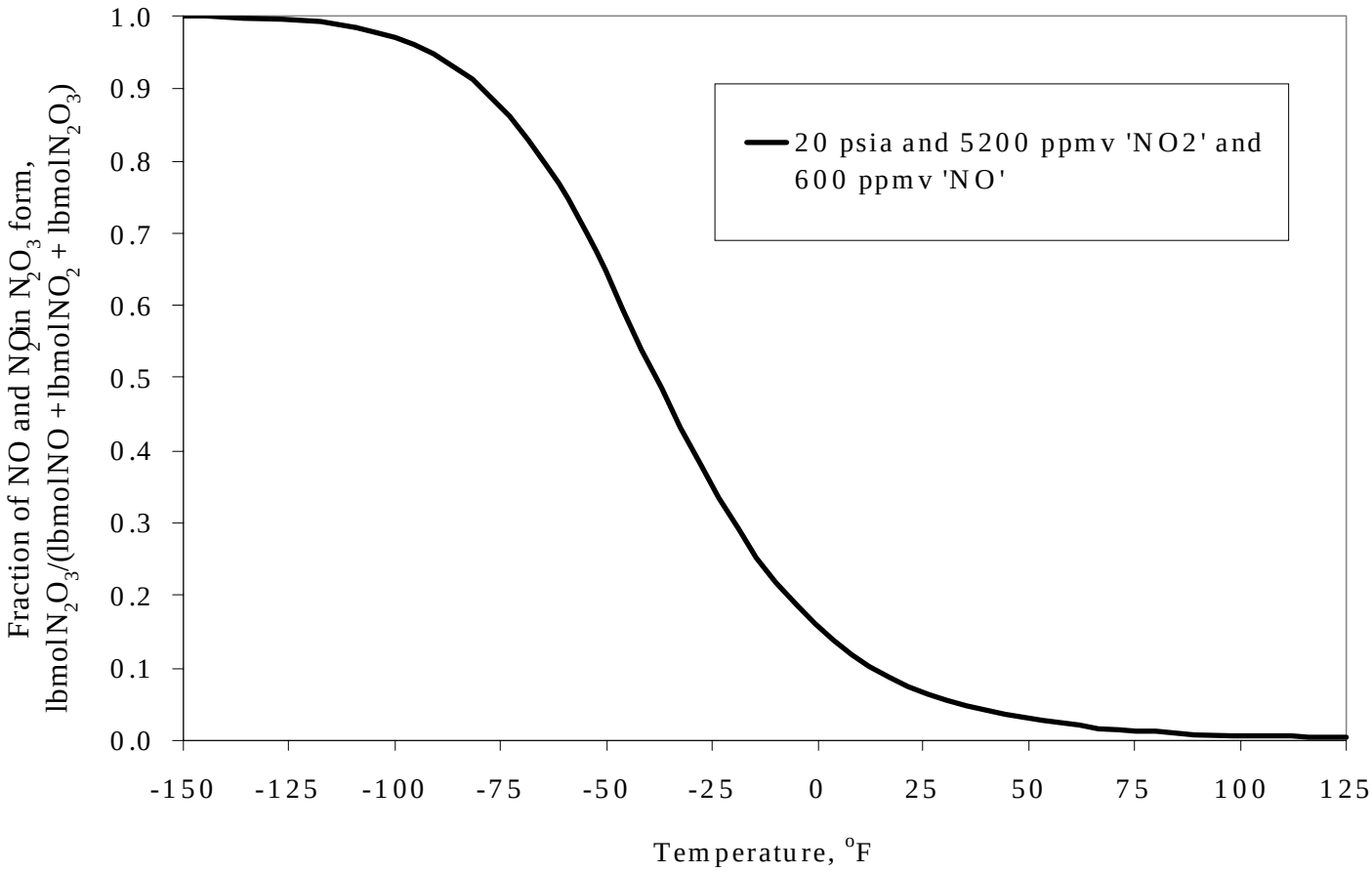

Figure 4.6. Plot of equilibrium N_2O_3 ratio vs temperature. Conditions of the stream are 20 psia and the same NOx concentration as that of the fumes entering the bottom of the scrubber/absorber.

4.1.5.5 Assumption V: Eliminate HNO_2

V. HNO_2 does not exist for extended periods because it is a very unstable compound. For this reason, it is customary to combine reactions (4.4) and (4.5) to eliminate the intermediate HNO_2 (Miller, 1987). Figure 4.7 shows the mathematical method by which we eliminate the intermediate HNO_2 from reactions (4.4) and (4.5). This pseudo-steady-state assumption implies that the concentration of HNO_2 remains very low and relatively constant at any time, because it reacts away by reaction (4.5) as quickly as it is produced by reaction (4.4).

Literature data for the liquid-phase oxidation of HNO_2, (4.9) $2HNO_2 + O_2 \leftrightarrow 2HNO_3$, remains unavailable (Miller, 1987). Also, liquid-phase concentration of O_2 is also very low. Therefore, we neglect the effect of HNO_2 oxidation in the liquid phase.

(4.4) $N_2O_4 + H_2O <=> HNO_2 + HNO_3$

(4.5) $3HNO_2 <=> HNO_3 + H_2O + 2NO$

multiply reaction (4.4) by 3, then add to reaction (4.5).

$$\begin{array}{rl} & \overset{2}{} \\ 3 \text{ x } (4.4) & 3N_2O_4 + 3H_2O <=> \cancel{3HNO_2} + 3HNO_3 \\ + \quad (4.5) & \cancel{3HNO_2} <=> HNO_3 + \cancel{H_2O} + 2NO \\ \hline & 3N_2O + 2H_2O <=> 4HNO_3 + 2NO \end{array}$$

Figure 4.7. Elimination of HNO_2 from the reaction mechanism by adding reaction (4.4) to reaction (4.5).

4.1.5.6 Assumption VI: Assume Vapor-Phase Acid Concentrations Are Negligible

VI. Researchers assume the vapor-phase production of nitric and nitrous acid to be negligible (Miller, 1987). Therefore, we neglect reactions (4.10) and (4.12).

$$2NO_2 + H_2O \leftrightarrow HNO_3 + HNO_2 \qquad (4.10)$$

$$HNO_{3(g)} \leftrightarrow HNO_{3(l)} \qquad (4.12)$$

4.1.5.7 Assumption VII: Neglect Reaction (4.13)

VII. The lower solubility and reactivity of NO_2 than that of N_2O_4 leads us to neglect reaction (4.13), $3NO_2 + H_2O \leftrightarrow 2HNO_3 + NO$. Suchak and Joshi state that "absorption of NO_2 as such is negligible" (Suchak and Joshi, 1994). Also, Miller says that "the NO_2 routes are slow relative to those involving the reactants N_2O_4 and N_2O_3 and can usually be neglected in evaluating nitric acid absorption performance" (Miller, 1987).

The research shows that NO_2 does not absorb on its own to any appreciable extent (at least for low partial pressures of NO_2). It must change its form chemically and enter the liquid phase as a dimer (N_2O_4), or in union with a NO molecule (N_2O_3). These forms absorb much faster than do NO and NO_2 individually, and the observed rate of NO_2 absorption is actually the rate of absorption of N_2O_4 and N_2O_3. Therefore, we neglect the absorption reactions of NO_2 through the NO_2 pathway of Table 4.1.

Figure 4.8 shows the mathematical representation of the effect of our assumptions on the mechanism we show in Figure 4.2. Figure 4.9 shows the resulting mathematical representation of NOx absorption. ASPEN automatically calculates the mass transfer associated with vapor-liquid equilibrium at each stage of the scrubber/absorber column. Therefore, all species can exist at various concentrations in the vapor or liquid; however, we greatly simplify the reactions in

which they participate. These assumptions leave us with a highly simplified model that Table 4.4 summarizes.

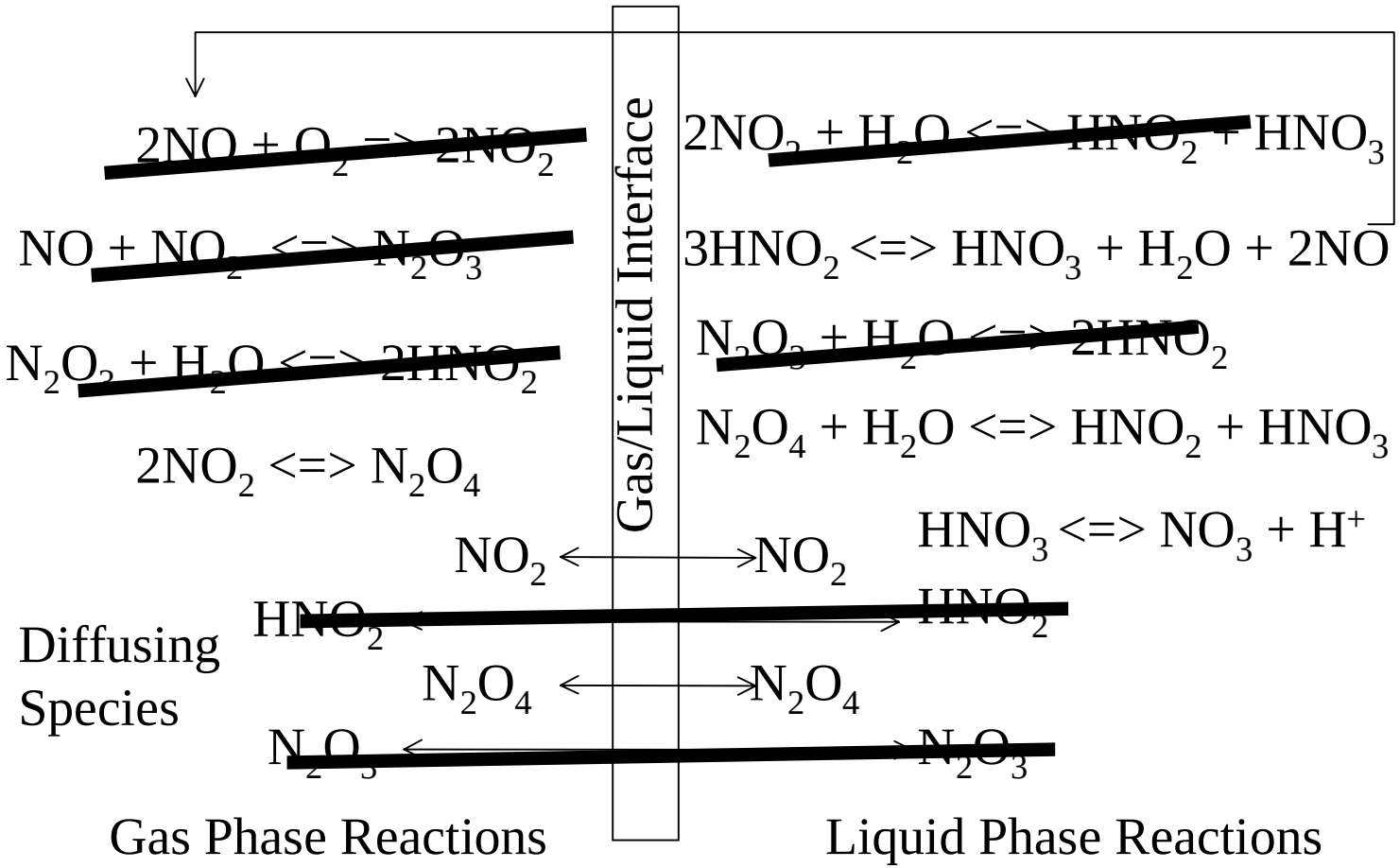

Figure 4.8. Elimination of reactions and species based on assumptions for the case of NOx absorption at RFAAP.

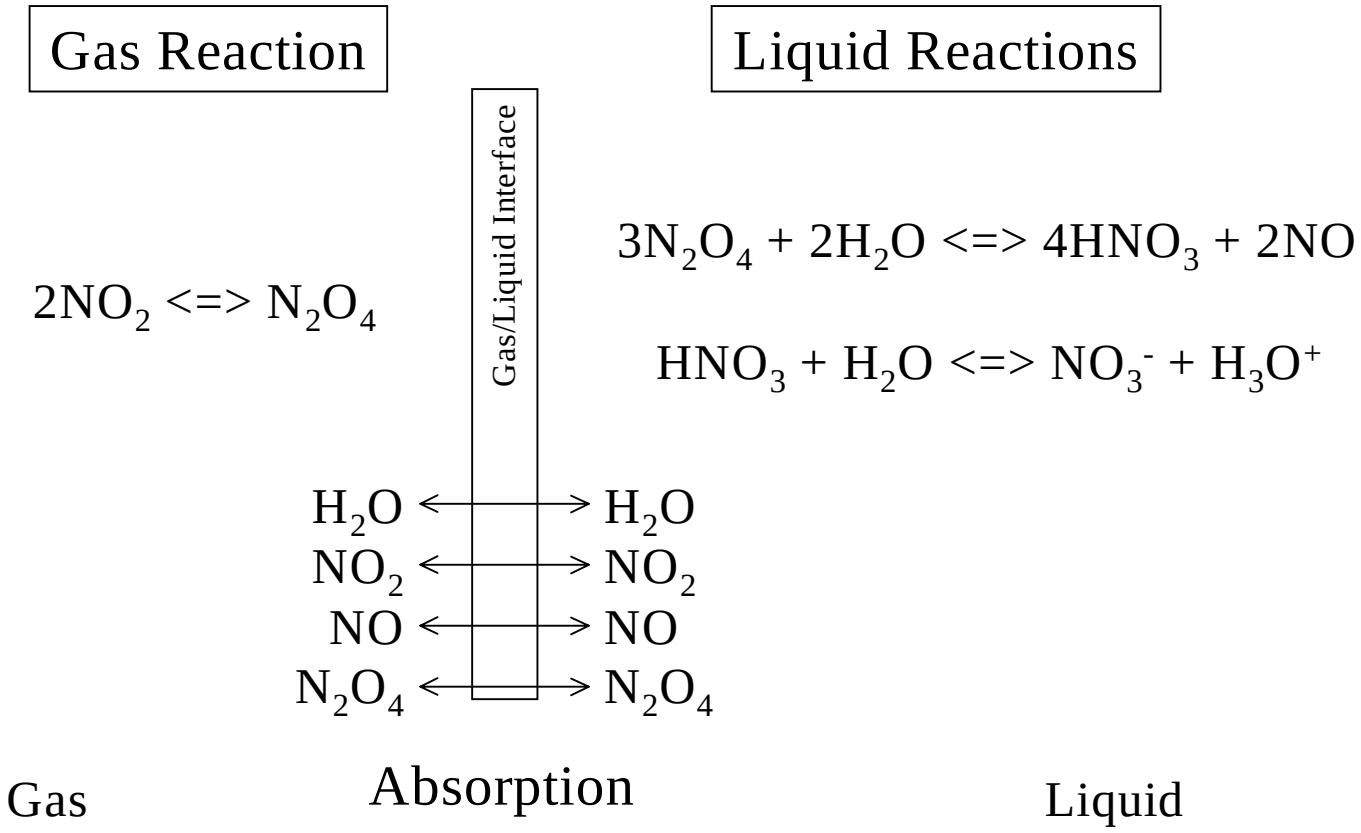

Figure 4.9. Final reaction and absorption mechanism after the application of assumptions I-VII. Note that ASPEN calculates vapor-liquid equilibrium in the scrubber /absorber column, so all species are capable of interfacial mass transport.

Table 4.4. Simplified reaction mechanism for NOx abatement.

Description	Reaction	
Gas-phase reaction:	$2NO_{2(g)} \leftrightarrow N_2O_{4(g)}$	(4.2)
Transport:	All species able to diffuse between phases	
Liquid-phase reaction:	$3N_2O_{4(l)} + 2H_2O_{(l)} \leftrightarrow 4HNO_{3(l)} + 2NO_{(g)}$	(4.4,5)
Dissociation of nitric acid:	$HNO_3 + H_2O \leftrightarrow NO_3^- + H_3O^+$	(2.5)

Note: (l) refers to liquid phase and (g) refers to gas phase

The whittling down of such a complex system to as simplified a model as we propose may raise some doubt in the mind of the reader. To calm these doubts, we restate the hypothesis that we consider these assumptions valid for the conditions relevant to the process we are modeling. Table 4.5 summarizes the conditions for which the model described in Table 4.4 applies. We do not contend that the same model would hold for the ammonia oxidation portion of the plant at RFAAP or for the flue-gas treatment of a gas-turbine power plant. However, we do state that from the same starting point of the full mechanism, applying the appropriate assumptions would arrive at an acceptable model for these processes as well. In the discussion of the first equilibrium model in Section 4.2, we present the model results that we hope justify, for the reader, the assumptions we make in this section.

Table 4.5. Limiting conditions of the assumptions made to arrive at Table 4.2.

Low Pressure
Low partial pressure of NOx
Low nitric acid concentration
Low NO partial pressure
Low NO_2 partial pressure
NO to NO_2 ratio of partial pressures or total NOx partial pressure low
Low temperature

4.1.6 Equilibrium Model of the SCR Unit

The use of an equilibrium model becomes somewhat more dubious when applied to the catalyst vessel. The reaction rates and the complex interaction with the heterogeneous catalyst bed represent the major resistance to reaction in the catalyst vessel. In fact, the required use of a very expensive catalyst bed underscores the extreme 'distance' from equilibrium of the reactions involved. This situation differs fundamentally from that of the scrubber/absorber. There, literature reports state that the reactions achieve equilibrium; however, mass transfer between the phases constitutes the limiting step in the overall consumption of NOx. The eventual failure of the equilibrium model to deal with the SCR becomes the impetus for the development of the kinetic model.

4.2 Discussion of the First Equilibrium Model

The first equilibrium model utilizes a reactive-distillation model to simulate the scrubber/absorber. ASPEN calculates each stage of this model for the vapor and the liquid in equilibrium with each other. We specify the set of reactions resulting from the mechanism simplification to occur on each stage of the column. ASPEN calculates the equilibrium for the reactions via a Gibbs free-energy minimization. Physical and chemical equilibria dictate the

behavior of the entire simulated tower. In an actual absorption column, a steady state of mass transfer between phases usually exists. Figure 4.10 gives a visual illustration of the vapor and liquid compositions of the key components during steady state. In a batch system at infinite time, the vapor and liquid phases eventually reach equilibrium. Equilibrium concentrations for the components are not equal between the vapor and the liquid. Chemical potentials dictate the amount of each component that resides in the vapor and the liquid. Figure 4.11 shows a notional view of how the system in Figure 4.10 would look if allowed to reach equilibrium. The system that Figure 4.11 shows is analogous to how ASPEN calculates the component concentrations on a stage in the scrubber/absorber under the equilibrium assumption.

The major physical differences between the conversion and equilibrium models reside in the scrubber/absorber and the catalyst-vessel units. The first equilibrium model simulates the scrubber/absorber as a single column, eliminating the separate scrubber drums and external conversion reactors. These changes are clearly visible by comparison of the two process flow diagrams. Compare Figure 3.18 with Figure 4.12, the block flow diagram for the first equilibrium model. Within the reactive-distillation model for the absorption column, we change the specification of the reactions from conversion to a Gibbs free-energy minimization calculation. ASPEN calculates reaction equilibria by minimizing the Gibbs free energy of the system. For the catalyst vessel, we replace the conversion reactor with an equilibrium model using the same Gibbs free-energy minimization technique. We include reactions (4.14) and (4.15) in the equilibrium model of the catalyst vessel.

$$4NH_3 + 4NO + O_2 \leftrightarrow 4N_2 + 6H_2O \qquad (4.14)$$

$$NO + NO_2 + 2NH_3 \leftrightarrow 2N_2 + 3H_2O \qquad (4.15)$$

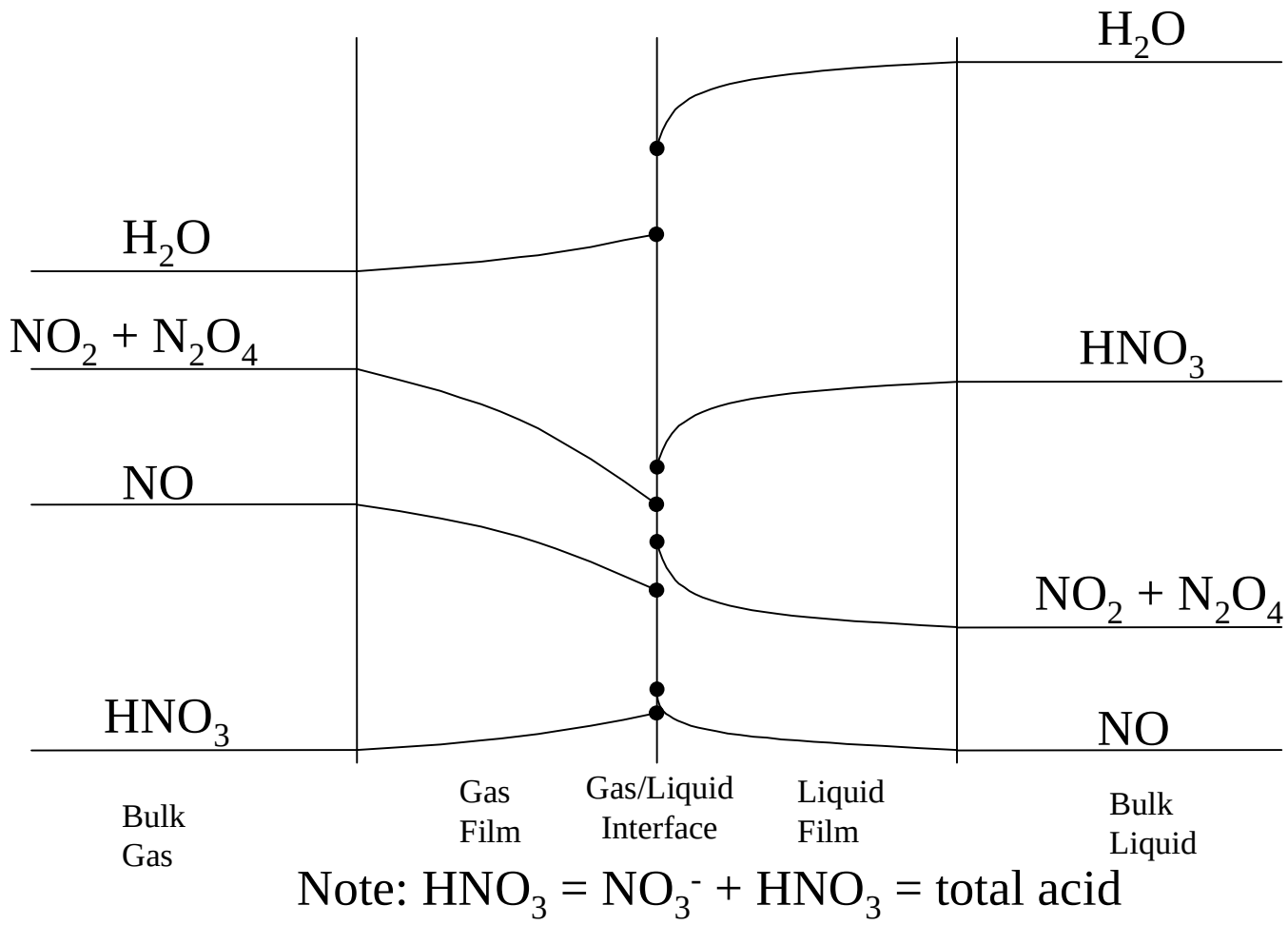

Figure 4.10. Qualitative representation of diffusing species composition profiles at steady-state.

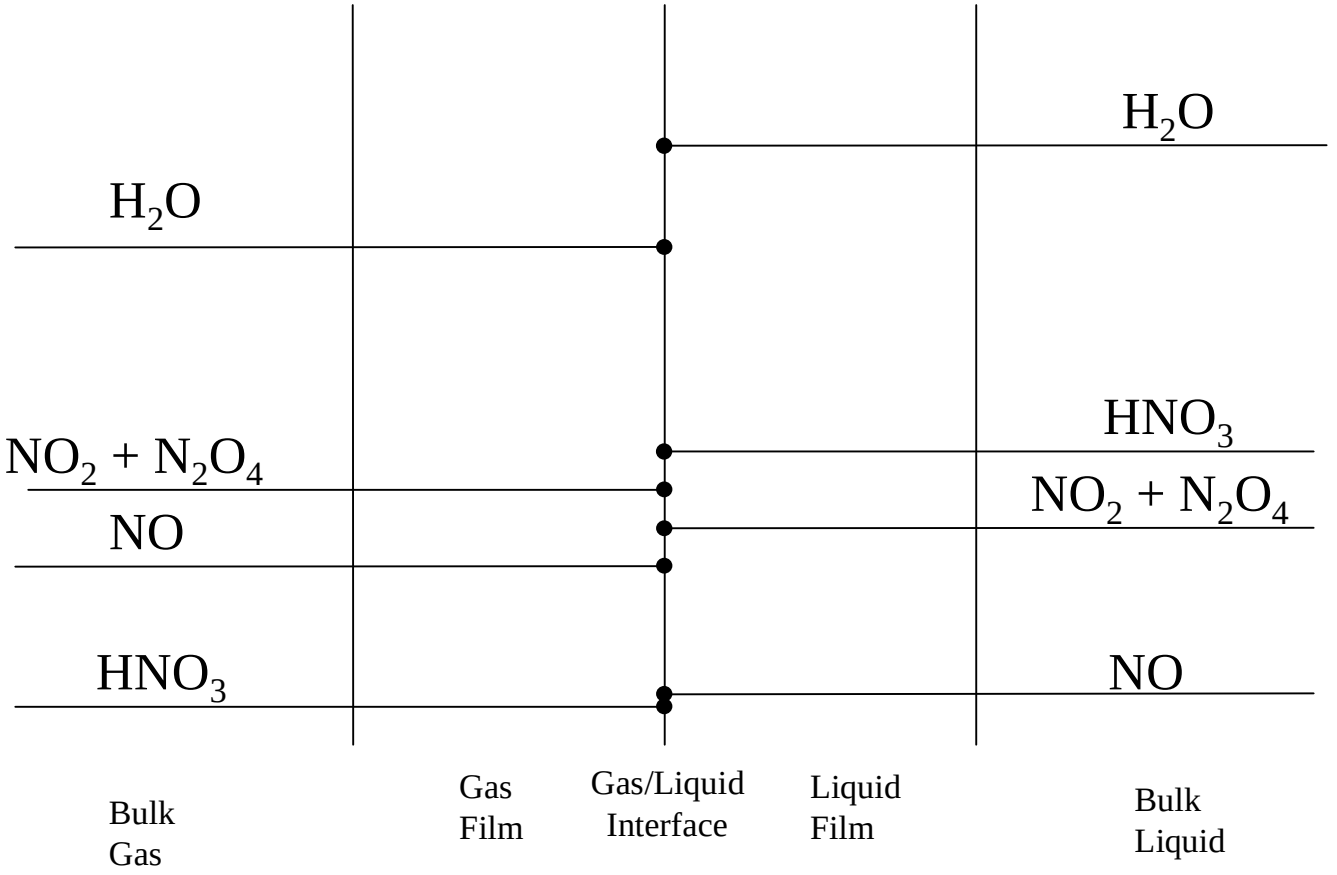

Note: $HNO_3 = NO_3^- + HNO_3$ = total acid

Figure 4.11. Qualitative representation of diffusing species composition profiles at equilibrium.

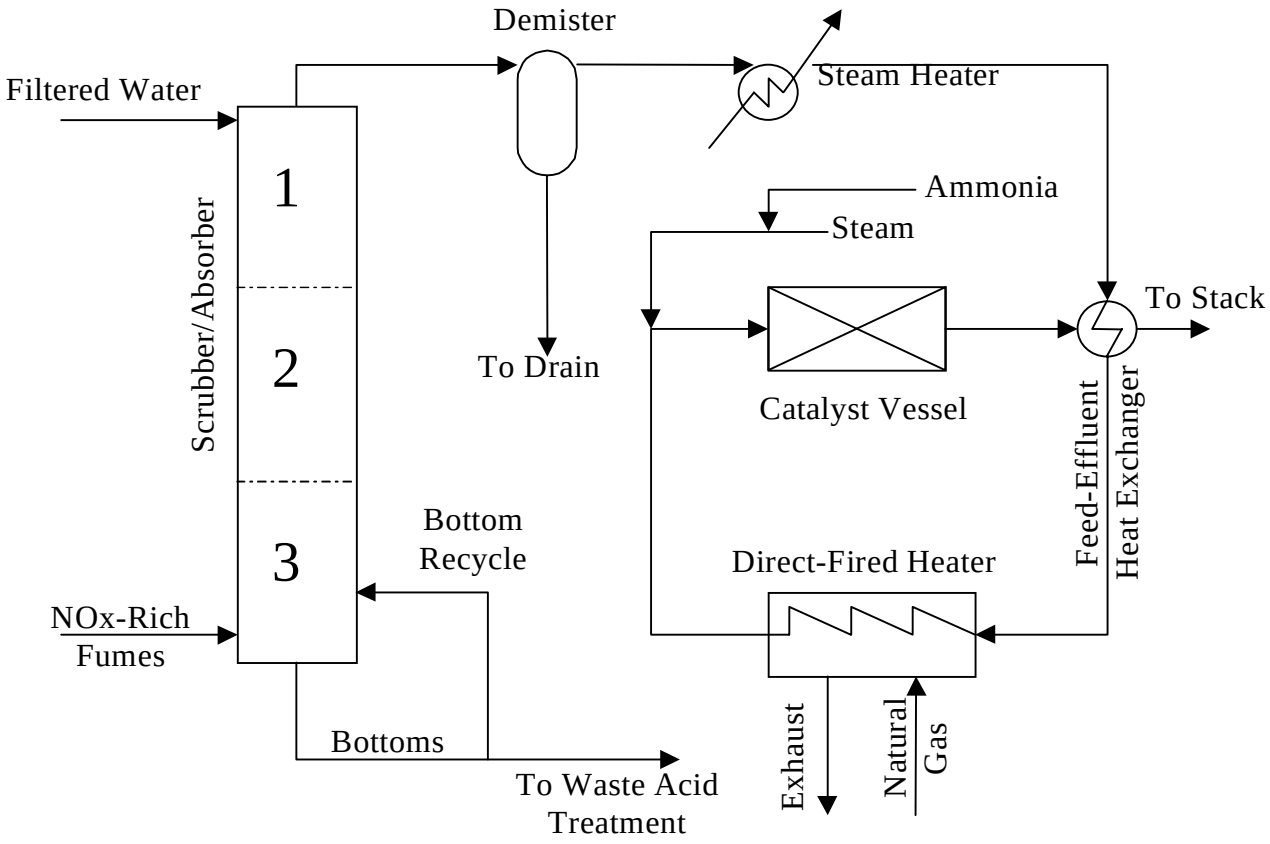

Figure 4.12. Block flow diagram of the NOx abatement system for the first equilibrium model.

4.2.1 Results of the First Equilibrium Model

In the first equilibrium model, we ignore the prospect of column inefficiency. Therefore, each stage provides a 100% efficient vapor-liquid equilibrium state. We change the number of theoretical stages in the absorber column until the outputs closely matches the proposed mass balance. A column of three equilibrium stages agree with the mass balance to a great degree. Figure 4.13 illustrates the flowsheet used in the computer model. Initially, we desire a close agreement from which we can observe the sensitivity of column and catalyst-vessel behavior versus process-parameter variations.

For the equilibrium model, we deem matching the mass balance exactly as less important than a close match with appropriate responses to operating conditions. However, the ASPEN Plus simulation results do agree with the mass balance provided by RFAAP surprisingly well. Table 4.6. shows the results of the base-case equilibrium model as compared to those for the conversion model and the proposed mass balance provided by RFAAP.

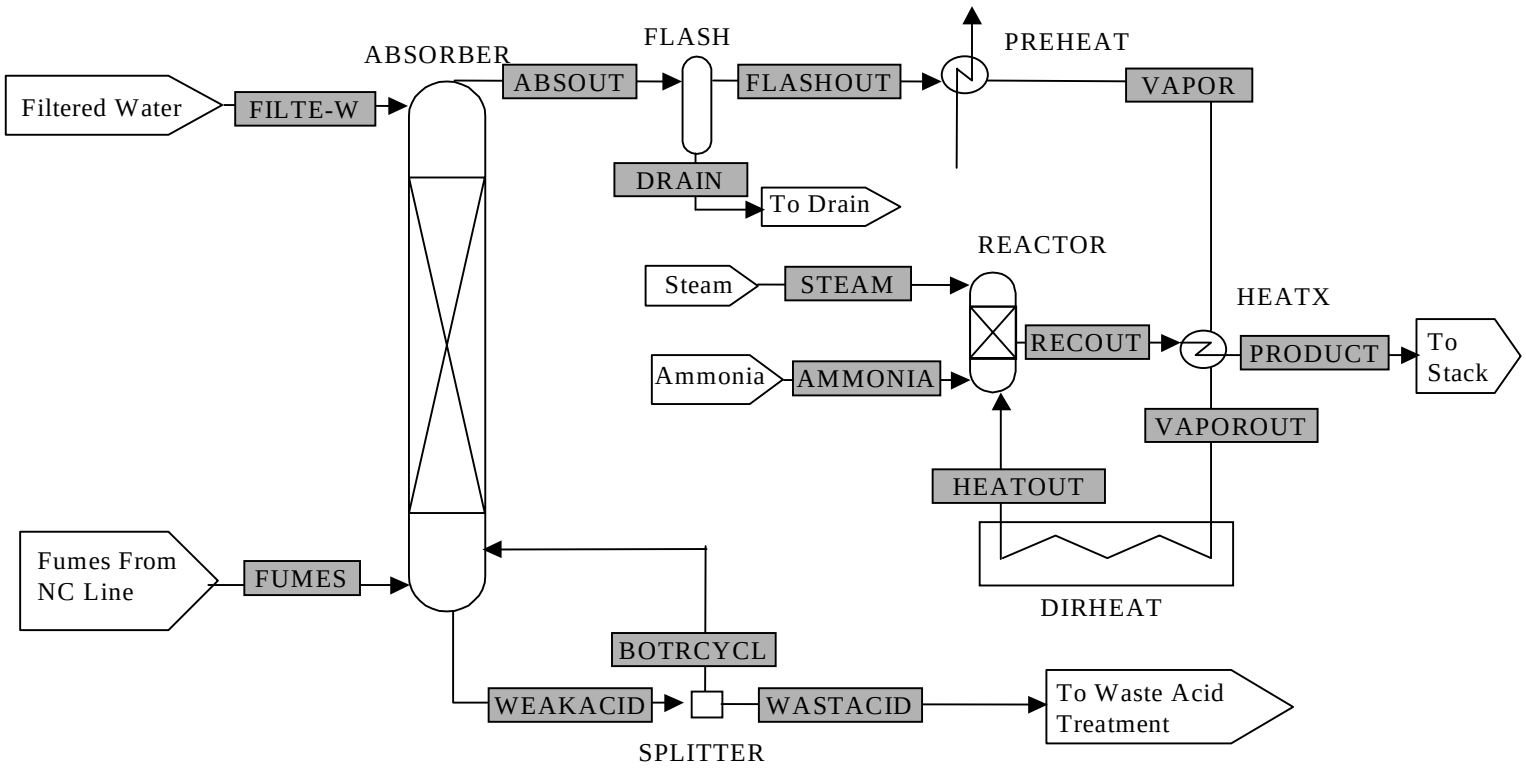

Figure 4.13. Equilibrium model flowsheet for the computer simulation.

Table 4.6. Output flows for the equilibrium model as compared to those for the conversion model as well as data supplied by RFAAP.

Stream:	Acid From Scrubber (RFAAP Data)	WASTACID (ASPEN) Conversion Model	WASTACID (ASPEN) Conversion Model	Gas to Vent Stack (RFAAP Data)	PRODUCT (ASPEN) Conversion Model	PRODUCT (ASPEN) Equilibrium Model
Mole Flow lbmol/hr						
NO		8.954E-3		0.06	0.0598	
NO_2		6.115E-3		trace	9.748E-3	
H_3N				trace	0	
O_2		1.650E-6		132.06	132.052	
N_2		1.748E-6		496.77	498.763	
H_2O	13.1	21.412		23.86	15.939	
H_2SO_4						
HNO_2						
HNO_3		2.091				
Total Flow lbmol/hr	20.8	25.618		654.75	646.824	
Total Flow lb/hr	376	556.292		18631	18486.98	
Total Flow cuft/hr		7.791			3.90328E5	
Temperature F	86	80.000		350	350.000	
Pressure psi	60	14.000		14.1	14.400	

The deviations between the models and the RFAAP data deserve some discussion at this point. The numbers for the conversion model agree almost exactly with the RFAAP data, whereas the values for the equilibrium model are close but not exact. The reader may ask why this is the case. This situation arises because we manipulate the conversion-model reactions to give exact matches to the RFAAP data. The only arbitrary manipulation of the equilibrium model is the selection of the three equilibrium stages. All the other input values are those given by RFAAP, except for the specification of the equilibrium-reaction model. The results are therefore more genuine, and we accept some deviation from the data provided by RFAAP.

The lack of sufficient meters, sensors, and indicators on the equipment at RFAAP limit the usefulness of the available plant data. Recall that the RFAAP mass-balance data originate from design data, and not actual operating data. ASPEN Plus equilibrium calculations result in close agreement with the data provided. In this light, the small deviations of the equilibrium model should appear less significant. In fact, the equilibrium model displays remarkable accuracy, considering the simplicity of the reaction mechanism used.

Figure 4.14 compares the results of the first equilibrium model to an example found in the literature. We reproduce data from Thomas and Vanderschuren (1996) the results for experiments on NOx absorption. We use the same nomenclature in Figure 4.14 as do the authors.

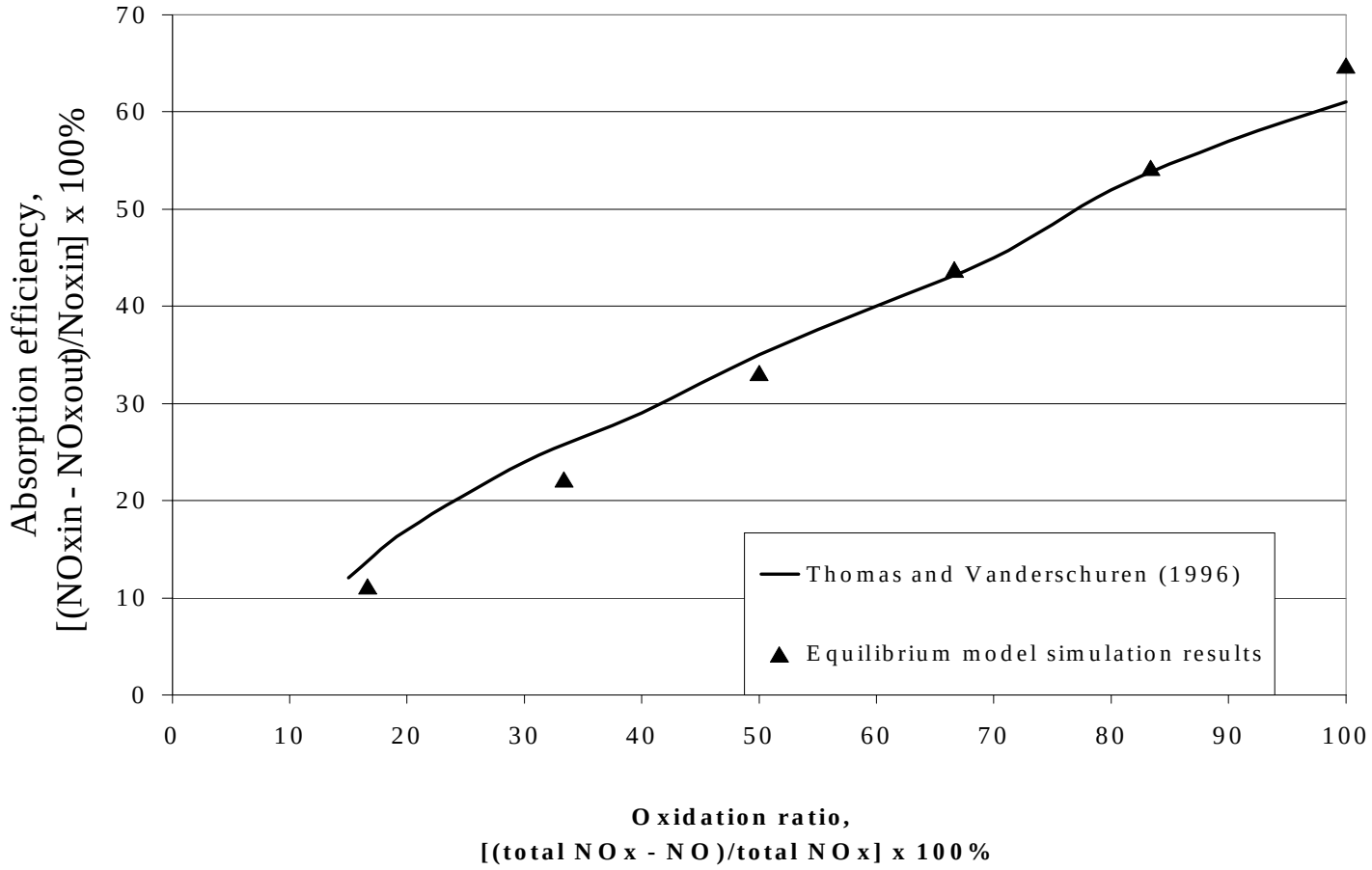

Figure 4.14. Comparison of absorption results to those of Thomas and Vanderschuren (1996). Absorption efficiency and oxidation ratio are terms used by these authors (see Figure 2.9). Absorption efficiency has the same definition as this thesis for overall NOx absorption ($NO + NO_2$). Thomas and Vanderschuren define the oxidation ratio as total NOx minus NO divided by total NOx.

The absorption efficiency represents the percentage of total NOx that is absorbed and is defined as $A \equiv ((p_{NOx})in - (p_{NOx})out)/(p_{NOx})in$. The oxidation ratio gives a measure of the ratio of NOx that is in the form of NO_2 or $N2O_4$. They define the oxidation ratio as $OR \equiv (p_{NOx} - p_{NO})in/(p_{NOx})in$.

Finding experimental data appropriate for comparison with the results we obtain from the equilibrium model presents a serious challenge. Very few sources of NOx absorption data concern themselves with a system similar to the one at RFAAP. Thomas and Vanderschuren present the closest match to our system. Figure 4.14 clearly shows a strong agreement between the equilibrium model results with those of Thomas and Vanderschuren.

4.2.2 Sensitivity Analyses for the First Equilibrium Model

We loosely categorize attempts at optimizing an existing NOx absorption unit into two strategies. First are measures aimed at positively affecting the rates and equilibrium constraints of the reactions; second are measures implemented to improve the mass-transfer efficiency of the column. In a system such as NOx absorption, these two factors are not only additive, but also multiplicative. For example, improving N_2O_4 absorption in the liquid and NO desorption on a stage pushes the equilibrium of the liquid reaction to produce higher HNO_3 concentrations. In other words, adding more reactants and removing the products of the reaction (4.4,5), $3N_2O_{4(l)} + 2H_2O_{(l)} \leftrightarrow 4HNO_{3(l)} + 2NO_{(g)}$, pushes the reaction to the right.

Reactions can also aid in absorption. The dimerized form of NO_2, N_2O_4 absorbs more readily than NO_2 as a monomer. Therefore, pushing the reaction $2NO_2 \leftrightarrow N_2O_4$ to products gives a form of NO_2 that absorbs much faster. The ultimate products of the absorption of NO_2 and N_2O_4 are the same (HNO_3 and NO), but absorption of N_2O_4 proceeds more rapidly. Also, the consumption of liquid phase N_2O_4 by reaction (4.4,5) decreases the concentration of N_2O_4 in the liquid film, increasing the driving force of absorption from the gas to the liquid.

Furthermore, we categorize the effects of process variable changes into two groups. The first group consists of effects that are seen in the results of the computer model. The second group encompasses the effects that are not manifested in the results of the computer model, but would be present in an experiment with the actual column. We can only conjecture at the second category because the computer model remains the only quantifiable information we have on our particular system.

Engineering experience and the literature give us qualitative predictions of how our system should react to some process changes. The sum total of the results revealed by our model and those that it does not show represent the reaction of the actual process to process adjustments. For example, temperature and pressure have profound effects on the NOx absorption system. We pose these questions. Can the equilibrium model, as it exists, account for temperature and pressure variations cited in the literature? If so, how do these variables affect the absorption column being studied? If the model cannot accurately simulate column behavior, what additions need to be made? Is it even possible to develop a model with the software available that can satisfactorily simulate the real situation? Where appropriate, we will make distinctions between results expected from the model and results expected from the actual system. Ideally, the two situations coincide; in reality, there may be wide variations. We will attempt to explain important or surprising results.

We must make one more explanation of the way results are presented in this section. As the previous section explains, the primary role of NOx absorption is to remove NO_2. Reduction of NO proceeds very slowly under these conditions and reduction of NO_2 by reaction (4.4,5) actually produces NO faster than it is removed. Therefore, unlike some literature sources, we present the reduction in NO_2 as opposed to the reduction of total NOx for the absorption column. The total NOx reduction is actually somewhat less than the reduction of NO_2 alone because of the production of NO. Also, in most of the plots regarding the column, *the symbol NO_2 refers to both NO_2 and N_2O_4.*

We take the opposite approach when analyzing the catalyst vessel because it is designed for the removal of NO. Therefore, we present the results for that unit as removal of NO instead of NO_2 or total NOx. Even though total NOx removal is the priority, the true gauge of effectiveness for the scrubber/absorber is NO_2 removal, while that of the catalyst vessel is NO removal.

Although presenting results for NO_2 and N_2O_4 as the sum of the two and labeling it NO_2 simplifies the digestion of the information we present for the reader, it is important to understand the role of N_2O_4 in the chemistry of our system. Most literature sources use the same approach to the nomenclature. Some distinguish between the molecule NO_2 and the sum of NO_2 and N_2O_4 by adding a star as NO_2* to the sum term. We neglect such nomenclature as we believe it adds to confusion.

4.2.2.1 Column-Tray Number

Overall stage number is one of the first topics engineers address when designing or retrofitting an existing column. Varying the number of trays is also analogous to varying the overall efficiency of the column. Obtaining an optimum vapor velocity in the column can achieve this effect. Due to capital costs, modification to the existing process at RFAAP remains at a lower priority than parameter adjustment. Therefore, column-tray number receives less emphasis than the other sensitivity tests presented here. Figure 4.15 shows the effect that increasing or decreasing overall column number has on the NO_2 exiting the column.

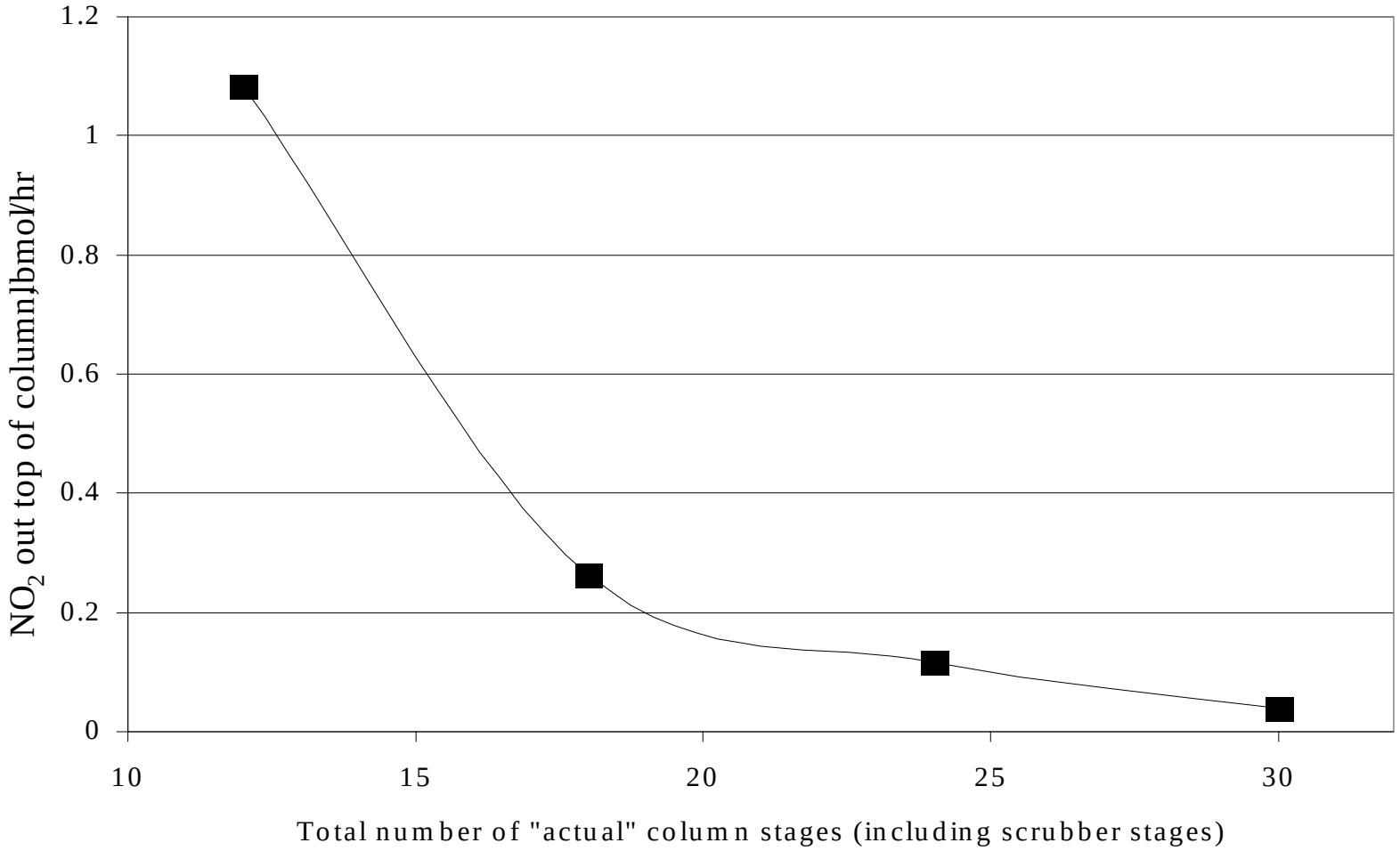

Figure 4.15. Plot of NO_2 out top of column vs total number of "actual" column stages. Assuming 3 stages for the base case is equivalent to 18 actual stages.

4.2.2.2 Column Cooling

The literature suggests temperature control as a means to improve NOx removal efficiency by scrubbing (Cheremisinoff and Young, 1977; Matasa and Tonca, 1973). We investigate several methods for cooling the column. These include: varying the fume-feed temperature, varying the filtered-water feed temperature, specifying a cooling-jacket duty, and cooling-tray duties. Temperature affects the equilibrium condition of the gas-phase and liquid-phase reactions. All the reactions involved in the model are exothermic, therefore generating heat and favoring products at low temperatures. Temperature also affects the vapor pressure of the components. Reduced temperature reduces component vapor pressures and favors absorption at atmospheric pressure.

Clearly, low temperature favors the absorption of NOx in our equilibrium model. We cannot determine directly from ASPEN how temperature affects the rate of the processes, nor are rate data readily available in the literature. This fact testifies to how widely researchers treat the reactions as equilibrium bound. Suffice it to say that most reaction rates increase with increased temperature, though this does not affect NOx absorption negatively because the important reactions are in instantaneous equilibrium. Therefore, we hypothesize that any reduction in the rates of these other reactions due to decrease in temperature is negligible.

Curiously, NO oxidation increases with a decrease in temperature. Again, we ignore this reaction in the equilibrium model altogether. However, it is interesting that the only reaction that is not assumed to be at equilibrium still improves our cause with a lowering of temperature. It is important to mention as well that increased fraction of NOx in the N_2O_3 and N_2O_4 form at lower temperatures, as Figures 4.5 and 4.6 illustrate, promote absorption at reduced temperatures.

Decreased vapor pressures and improved equilibrium provide NOx components with greater driving forces for absorption and therefore should also increase the rate of absorption.

Very little evidence in the literature suggests any drawback to cooling. Therefore, we study the effect of removing heat energy from the NOx absorption system by a number of different methods. Figure 4.16 represents the direct approach to column cooling. We start with the base-case results for NO_2 leaving the top of the column in stream ABSOUT. In the base case, we specify the column to be adiabatic, that is, no heat lost or gained from the surroundings other than the inputs and outputs. Figure 4.16 also shows what happens when we remove heat from the column. The heat removed from each of the three stages remains constant and equal. Therefore, the heat removed from each stage is exactly one-third of the value show in Figure 4.16 for the whole column.

We see that the removal of heat from the column increases NO_2 removal considerably in the beginning. Between 100,000 and 150,000 Btu/hr, diminishing returns set in. However, a heat removal of approximately 500,000 Btu/hr reduces NO_2 escaping the column essentially to zero.

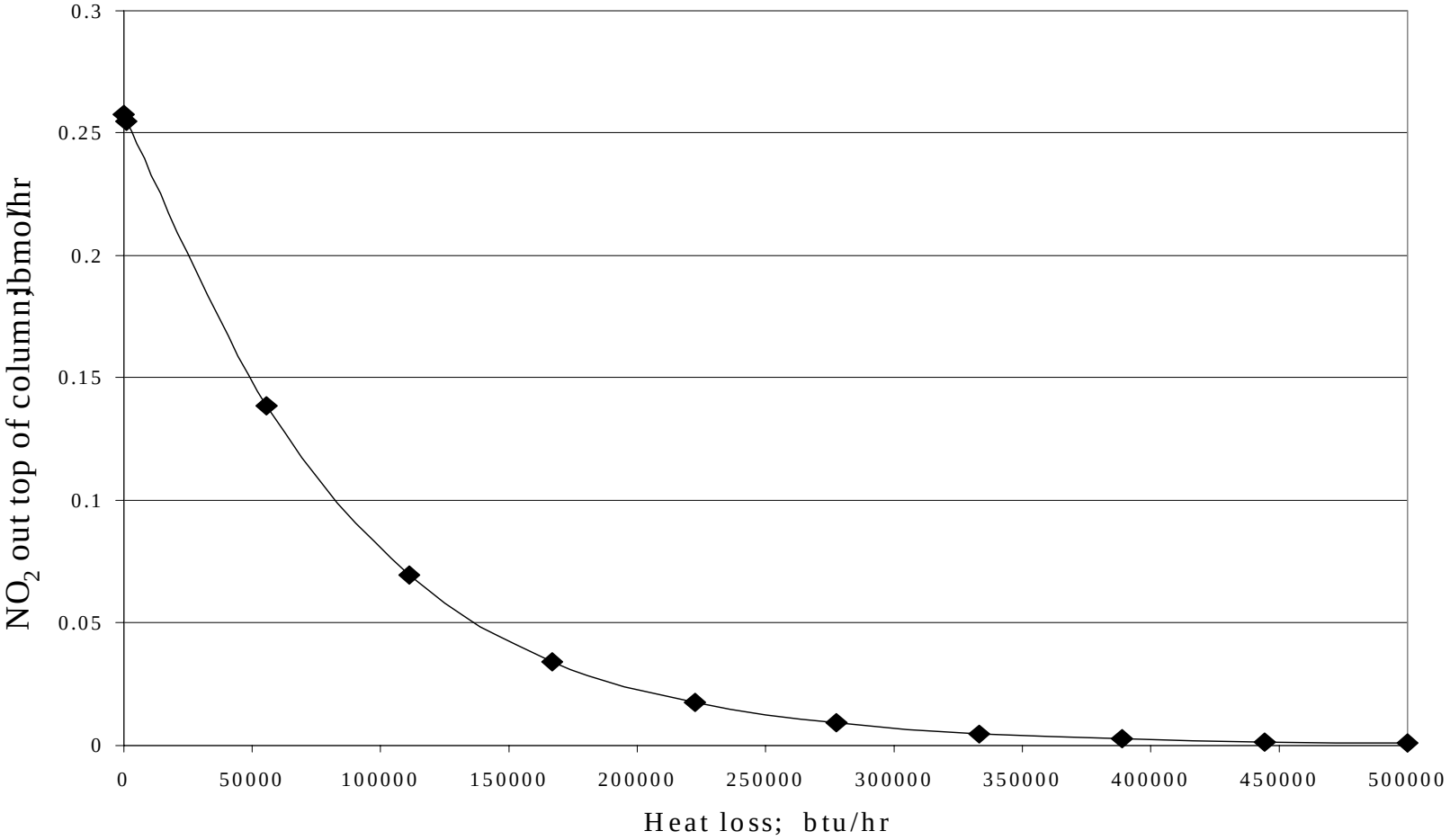

Figure 4.16. Plot of NO_2 out the top of the column vs. heat removed from column (heat loss). Simulates a cooling jacket or cooling trays. A heat loss of 0.0 btu/hr corresponds to the base-case model simulation.

4.2.2.3 Fume-Feed Temperature

We vary the simulation temperature of the fumes from the nitrocellulose line prior to feeding it into the top of the column. Figure 4.17 illustrates the results of cooling the fume stream. Comparison of Figure 4.17 with Figure 4.16 shows both to be analogous and comparable. However, we include Figure 4.18, which uses the same axis units as Figure 4.16, for direct comparison. Cooling the fume stream represents a viable and effective method of column cooling for improved NO_2 removal. Diminishing returns set in at a fume-feed temperature of 65 ^{o}F. This value represents a cooling of 25 ^{o}F from the initial temperature of 90 ^{o}F. A heat exchanger using chilled water would suffice for such an operation. We discuss this option in Chapter 6.

It appears that cooling the fume stream gives better results than assuming an overall heat loss from the column itself. We summarize this by saying that removing all the heat from the fume stream in the beginning before it is fed to the column is preferable to removing the heat one-third at a time on each stage. The approach of cooling the fumes initially allows the fully cooled fumes to contact three equilibrium stages. Cooling the column as a whole, as in Figure 4.16, cools each stage one-third of the way. Therefore, the top stage is the only one where the streams are cooled to their lowest temperature.

Figure 4.19 displays the effect that cooling the fume feed has on the acid weight fraction leaving the bottom of the column. Again, due to restrictions imposed by the acid-recovery group at RFAAP, we require a minimum nitric acid weight fraction of 0.30 for viable acid recovery. Here, we experience our first drawback to column cooling. The more we cool the column, the lower the concentration of acid in the waste-acid stream (WASTACID). We also discuss remedies for this effect in Chapter 6.

Due to conservation of mass, if column cooling causes increased NO_2 absorption and greater production of nitric acid, then the mass of acid leaving must be greater. Nitric acid does

not leave with the gas stream in ABSOUT to any appreciable extent, so it must be leaving in the waste acid stream. How can this be and still have dilute acid? Figure 4.20 shows that the overall mass flow rate of the waste-acid stream indeed increases as we lower the temperature. The answer is that decreasing the temperature also increases the amount of water that enters with the waste-acid stream. Without cooling, we observe a pseudo-distillation effect where all the acid leaves the bottom of the column, whereas some of the water that enters in the filtered water stream (FILTE-W) and the water vapor in the fume (FUMES) stream flows out the top in ABSOUT. Cooling the column causes this water to condense and flow out with the acid. Column cooling increases the absorption of all components including, unfortunately, water.

The simulation results do not account for the effect that cooling has on reaction (4.1), the oxidation of NO, because we assume that reaction to be negligible. However, we know that reducing the temperature of the gas has a positive effect on the rate of reaction (4.1), even though the computer simulation results do not show it. Again, increasing the conversion of NO to NO_2 increases NOx absorption by providing more soluble and reactive NOx species, namely NO_2 and N_2O_4. Figure 4.21 shows the effect that gas temperature has on the conversion of NO to NO_2.

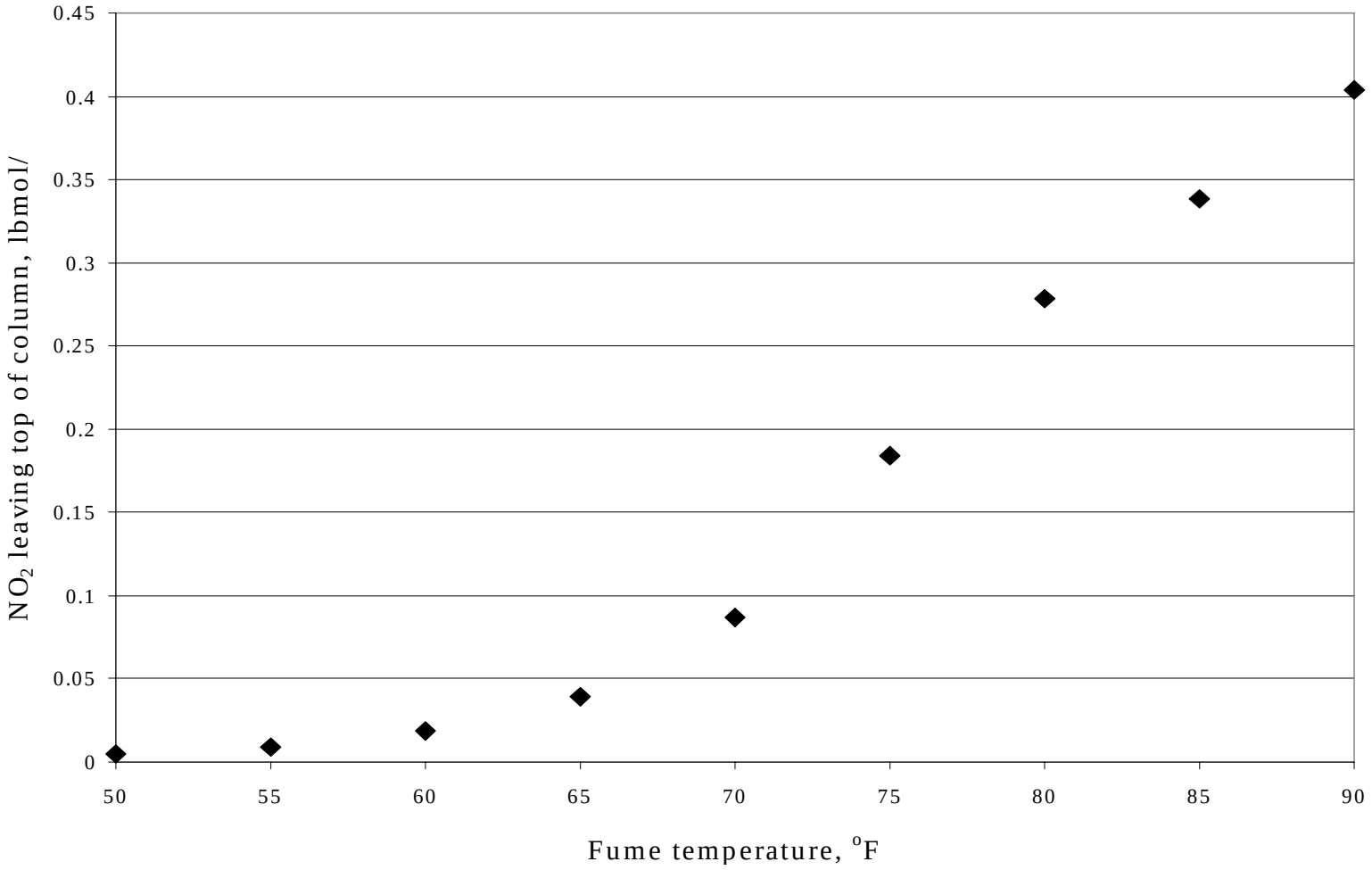

Figure 4.17. Plot of NO_2 escaping the top of the column vs. fume inlet temperature.

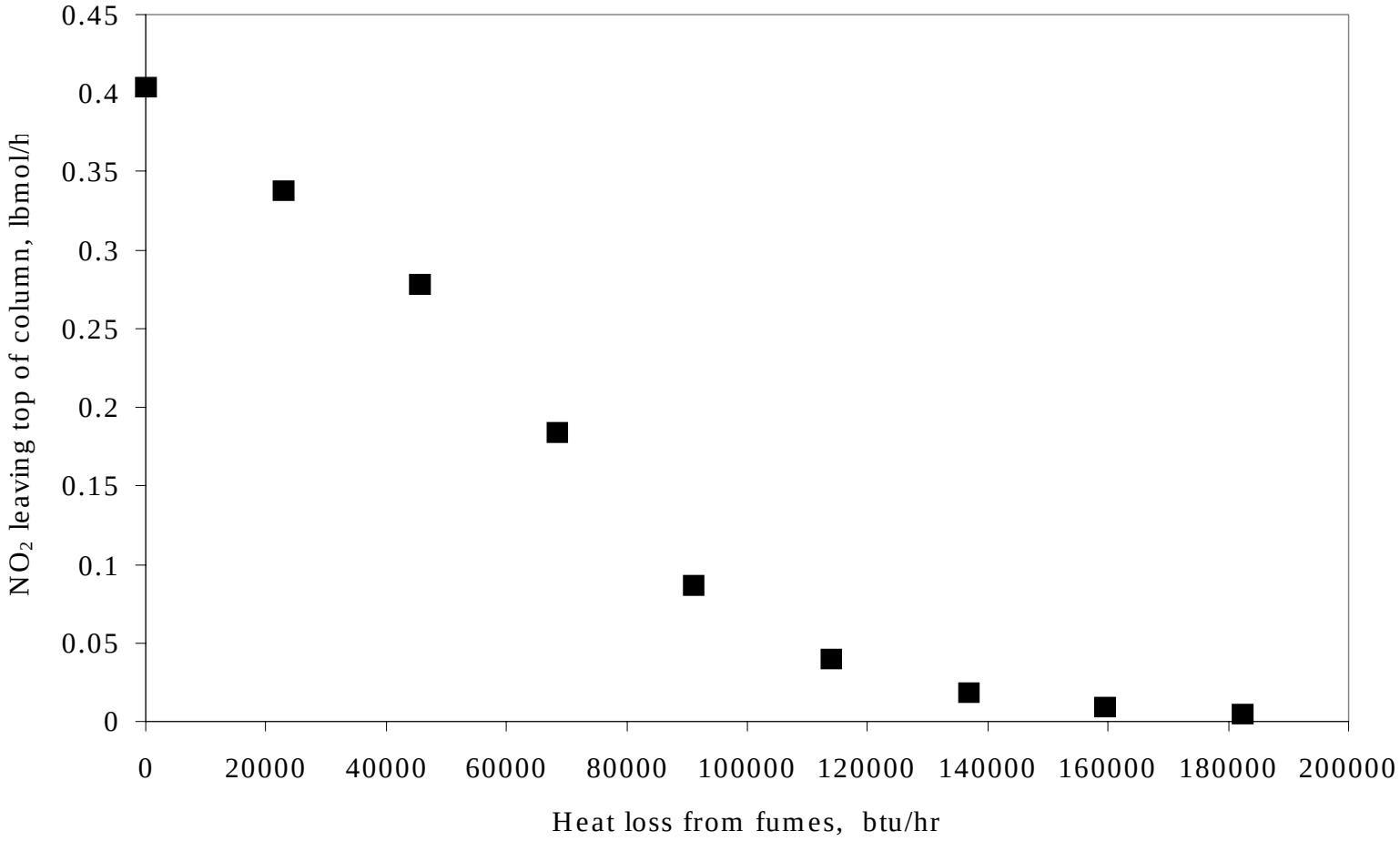

Figure 4.18. Plot of NO_2 escaping the top of the column vs. heat lost from the fume stream.

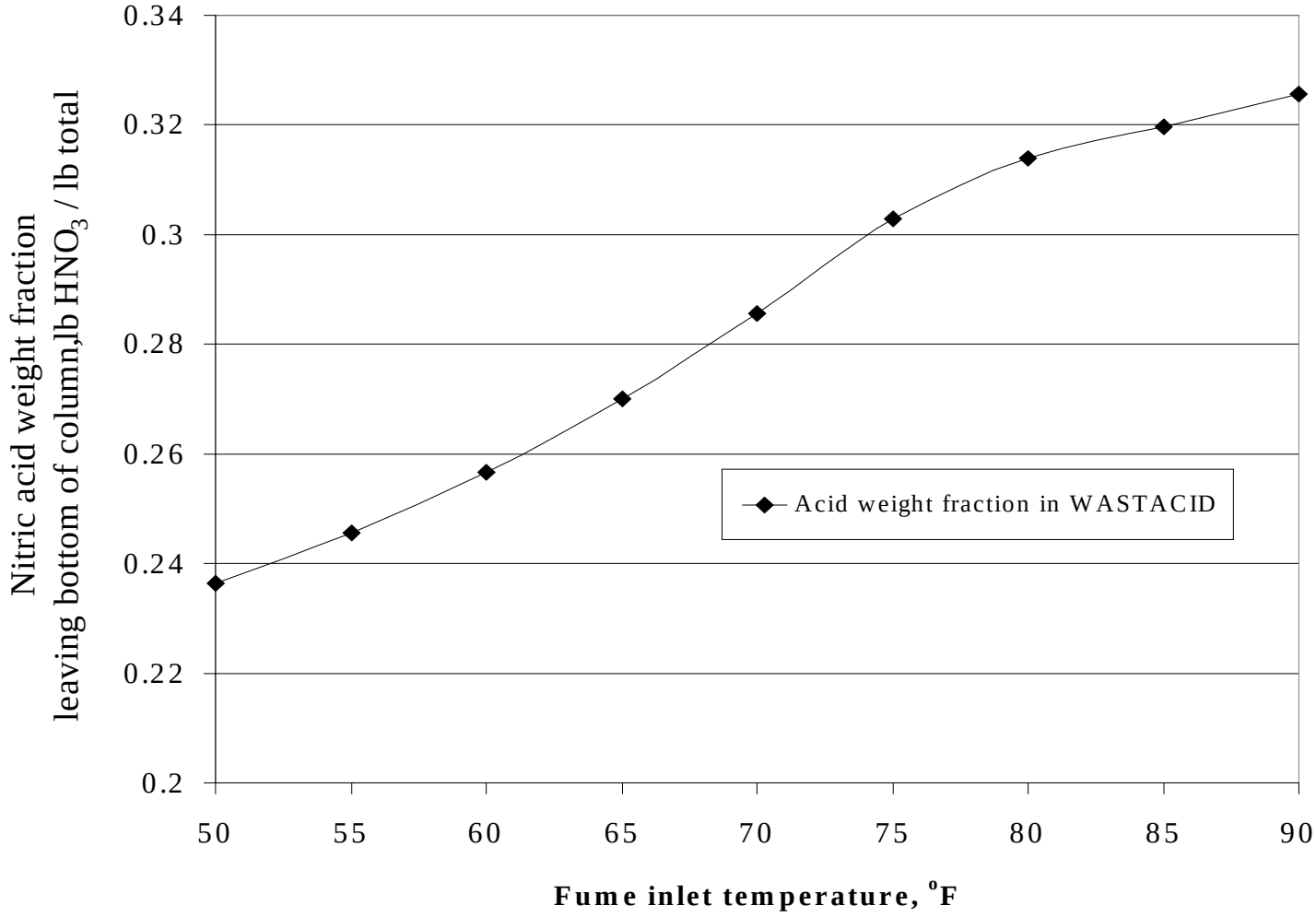

Figure 4.19. Plot of weight fraction of nitric acid leaving the column in the WASTACID stream for varying fume-feed temperature. An acid weight fraction of 0.3 represents the minimum value for which acid recovery is viable.

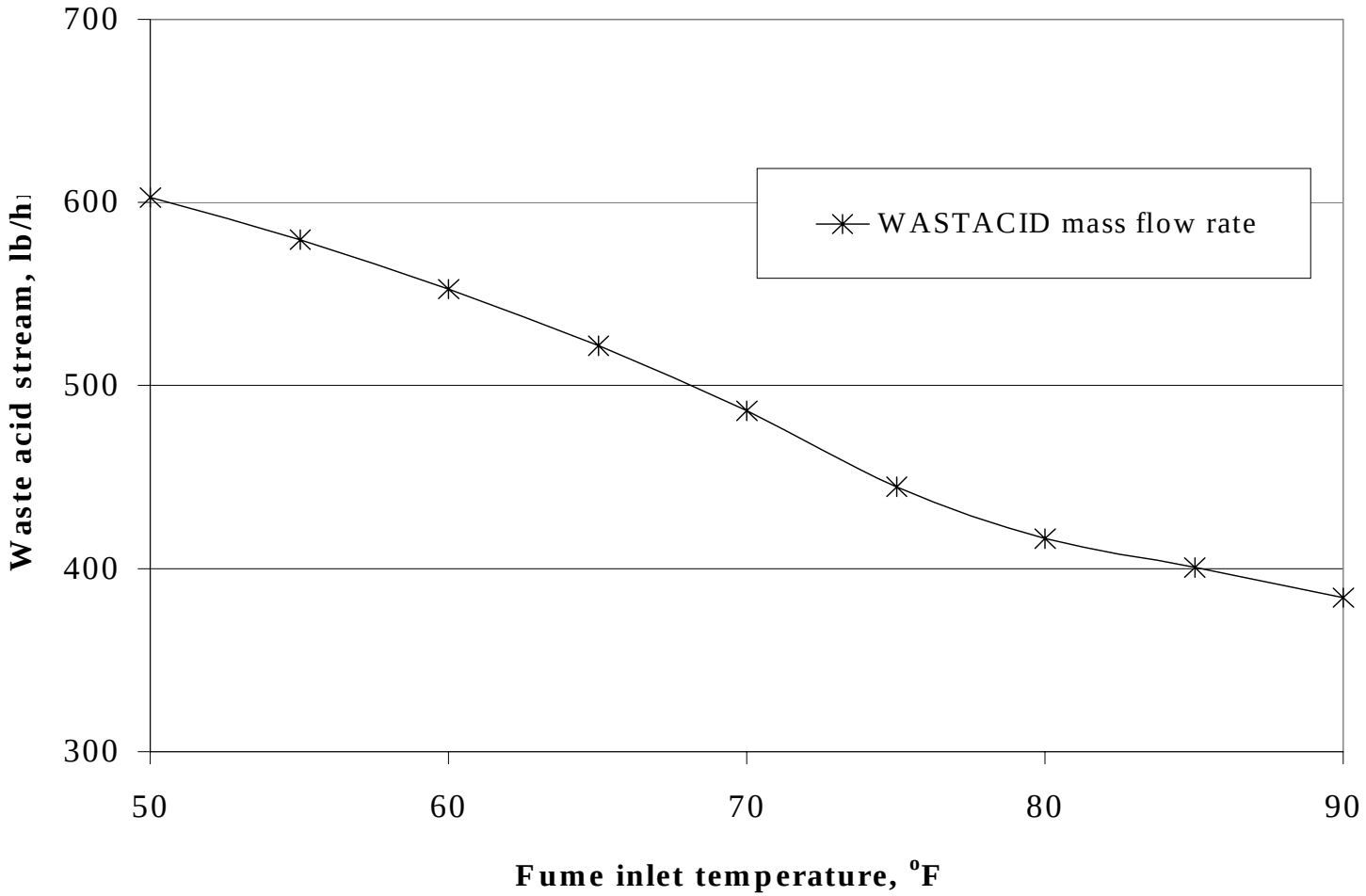

Figure 4.20. Total mass flow rate of liquid stream leaving the bottom of the column in WASTACID. Both acid and water flow rate increses as temperature of the fume stream is decreased. The increase in water flow rate dilutes the potential acid product.

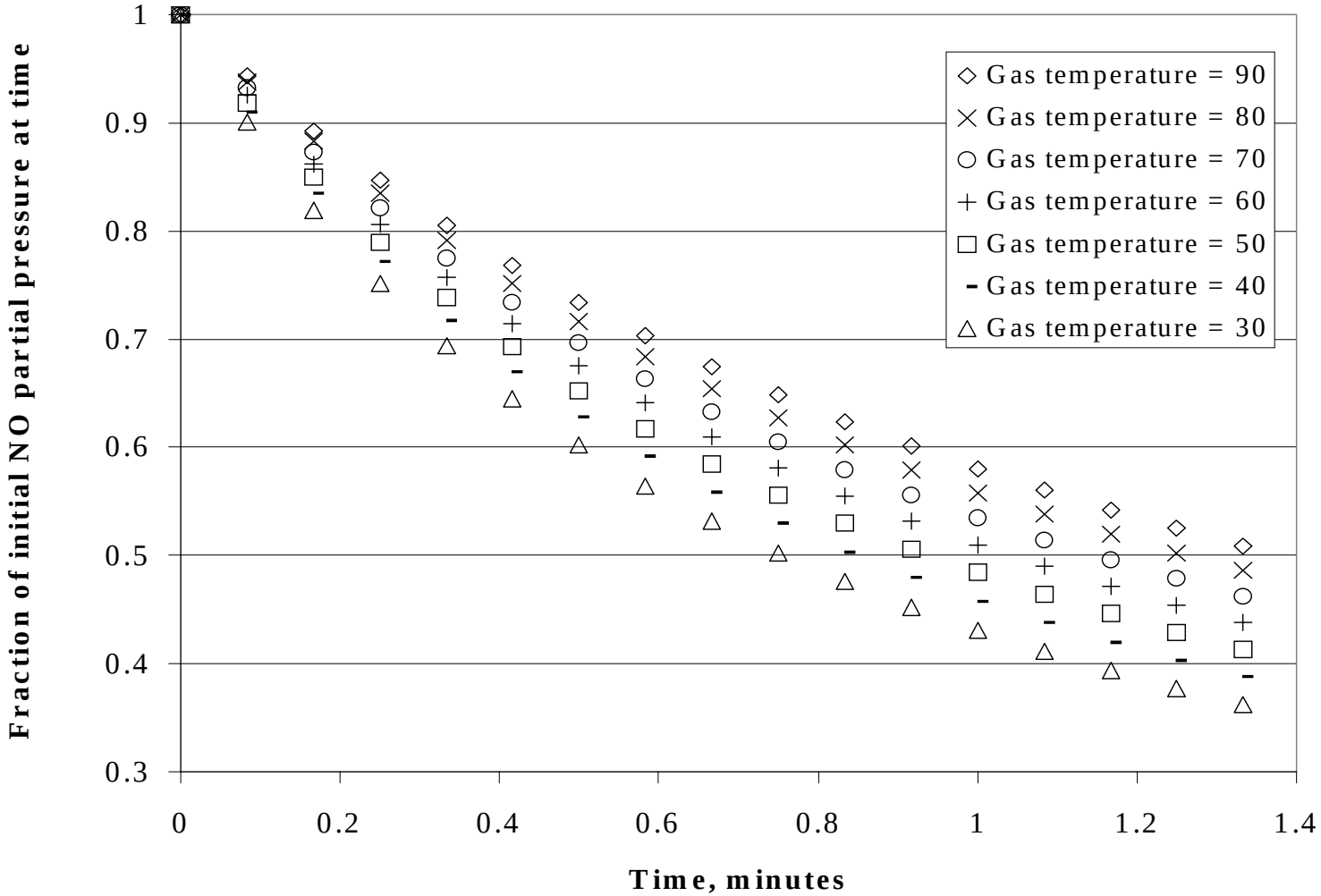

Figure 4.21. Effect of gas temperature on the time-dependent concentration of NO. Gas temperatures in ^{o}F. Gas pressure = 15 psi, NO flow rate = 0.5 lbmol/hr, total gas flow rate = 648 lbmol/hr.

4.2.2.4 Filtered-Water Feed Temperature

We vary the filtered water temperature prior to feeding into the top of the column. The flow rate of water in the filtered water stream is 22.2 lbmol/hr as compared to the 648 lbmol/hr flow rate of the fume stream. Clearly, cooling the fume stream offers greater overall heat removal per degree of temperature that stream is cooled. However, due to the higher heat-transfer rate of water compared to air, it seems reasonable to explore the option of cooling the water stream.

Figure 4.22 shows a clear improvement in NO_2 removal with cooling of the filtered water. However, comparing the results of filtered water cooling to those of cooling the fumes, the benefit of cooling the filtered water stream is disappointing just as we predict. Adding interstage liquid coolers to the column would increase the amount of heat exchange from the system. Interstage cooling simply requires a series of pumps and heat exchangers between stages. By cooling the liquid between stages, we increase the overall cooling of the gas as well. This option may offer an acceptable alternative to adding a heat exchanger to the fume stream or a cooling jacket for the column.

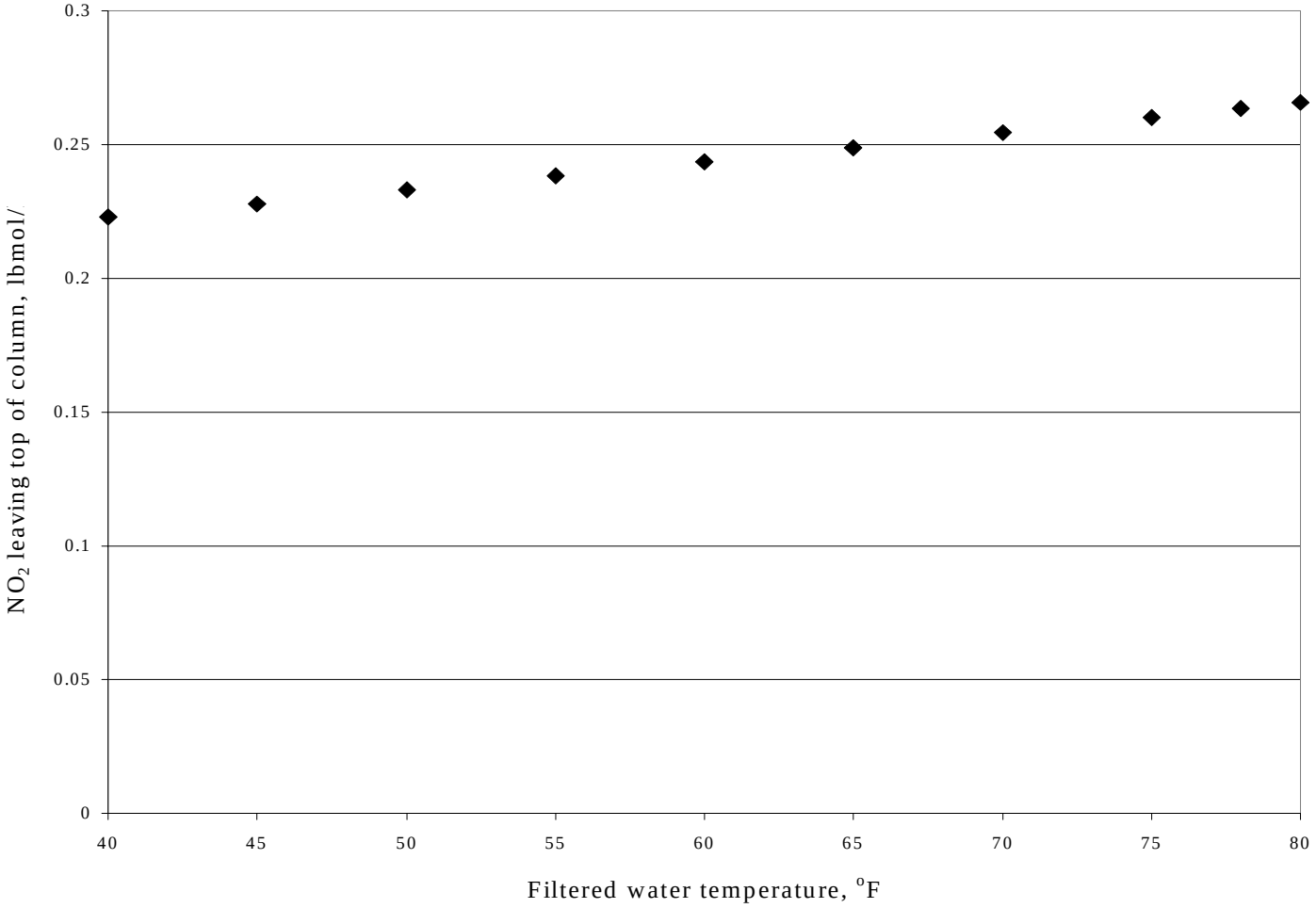

Figure 4.22. Plot of NO_2 leaving top of column vs. filtered-water inlet temperature.

4.2.2.5 Cooling-Jacket Duty

We specify a cooling jacket around the column with a constant heat-transfer rate for the column. We accomplish this by specifying a heat loss for the column similar to that presented in Figure 4.16. The overall heat lost divided by the number of stages gives the amount of heat lost from each stage. We simulate heat loss as equal quantities for each stage. Figure 4.23 plots the amount of NO_2 escaping the top of the column vs. the cooling-jacket duty for four different NO_2 feed rates (3.37, 4.0, 5.0, and 6.0 lbmol/hr). We keep the remainder of the components in the FUMES stream at constant feed rates corresponding to the base-case input specifications.

The reader can approach the information in this figure in several different ways. The most obvious one is to select a point on the x-axis for cooling-jacket duty. The vertical line from that value intersects the lines for the different feed rates of NO_2. The corresponding y-value gives the amount of NO_2 that will escape the top of the column at the corresponding feed rate of NO_2 and that cooling-jacket duty. Obviously, the base case has a cooling-jacket duty of 0 BTU/hr, so the y-axis for Figure 4.23 contains the same information as the NO_2-feed-rate sensitivity test for no column cooling. Values can be interpolated for NO_2 feed rates not explicitly shown in Figure 4.23.

Another way to approach the figure is to determine the maximum amount of NO_2 desired to escape the column in ABSOUT. This maximum value corresponds to a point on the y-axis. The horizontal line from there intersects the different NO_2-flow-rate lines with an x-value that corresponds to the required cooling rate of the column to achieve the desired value of NO_2 in ABSOUT. This information could be used to design a control system for a cooling unit for the column. Increases in NO_2 feeding to the column would trigger an increase in the cooling duty, increasing the removal efficiency and keeping the effluent NO_2 below the critical level. Low NO_2 rates would reduce the cooling duty, conserving energy.

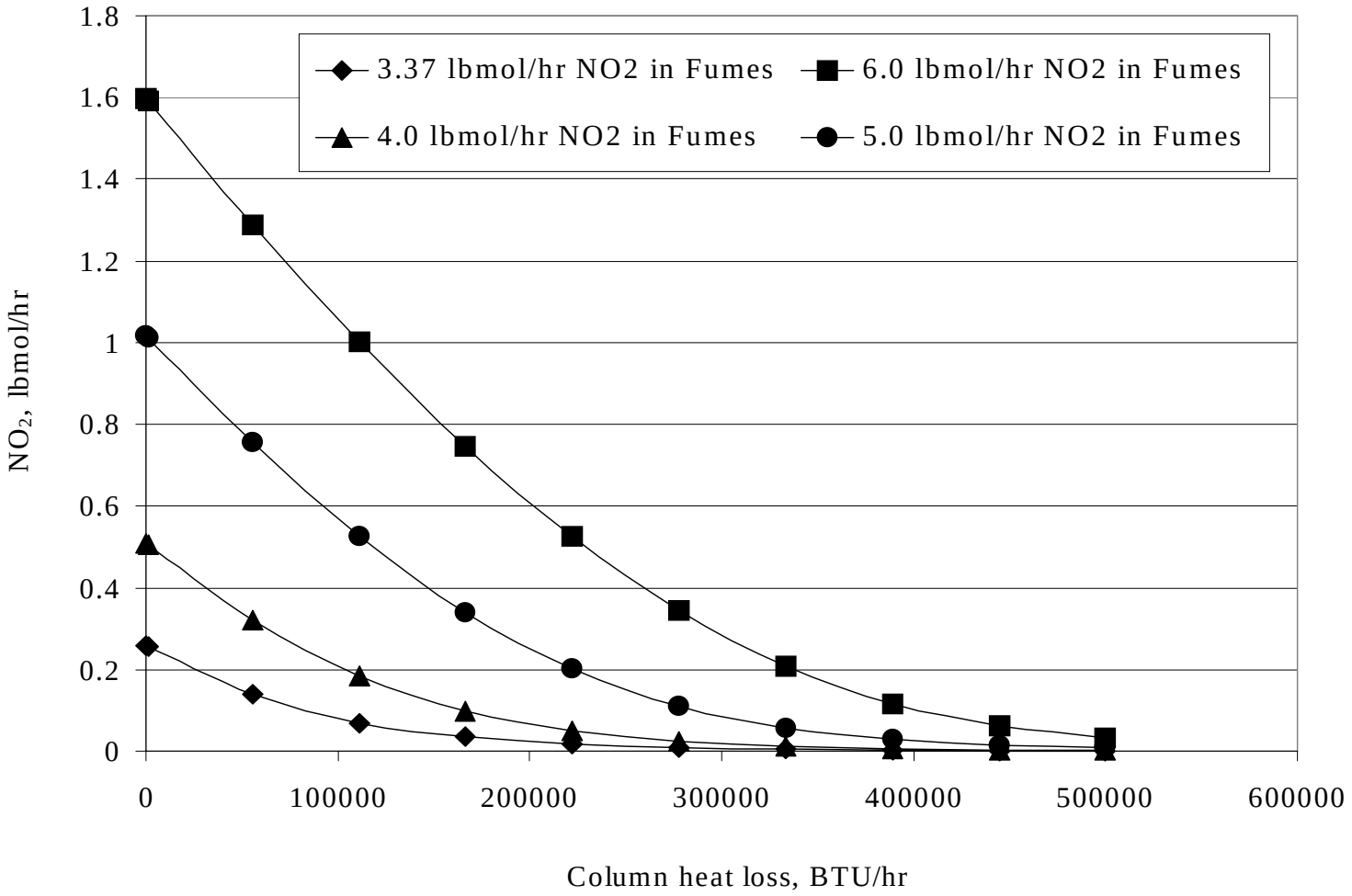

Figure 4.23. Plot of NO_2 out the top of the column in ABSOUT vs. BTU/hr of heat loss from column (simulating a cooling jacket) comparison of 3.37, 4.0, 5.0 and 6.0 lbmol/hr NO_2 in fumes

4.2.2.6 Column Pressure

Just like temperature, column pressure affects NOx removal in the column in a number of ways. First, pressure promotes the reactions in the gas phase. Most importantly for the current model, high pressure pushes the equilibrium of reaction (4.2), $2NO_2 \leftrightarrow N_2O_4$, to products. High pressure also promotes absorption of NOx gases. Therefore, increased pressure indirectly enhances the liquid-phase reactions by increasing the concentration of the reactants in the liquid. At high NO partial pressures and high nitric acid concentrations, high pressure potentially reduces NOx absorption by increasing the liquid concentration of NO for the reverse reaction of reaction (4.4,5) $3N_2O_{4(l)} + 2H_2O \leftrightarrow 4HNO_3 + 2NO_{(g)}$. Figure 4.24 shows the effect that column top-stage pressure has on the NO_2 and nitric acid flow rates leaving the column. Figure 4.25 shows the negative effect that increasing pressure exhibits on the nitric-acid effluent weight percent. Figure 4.26 shows that the reason for this negative influence is that the water that leaves as a liquid increases with increasing pressure.

Thankfully, the highest nitric acid concentration occurs at the bottom of the column, and the highest NO partial pressure occurs at the top of the column. Therefore, for the relevant set of conditions, this hindrance to the equilibrium of NO_2 absorption does not present a problem in the equilibrium model. Also it deserves restating that as Section 2.4.5 on current research discusses, evidence suggests that this situation may in fact be beneficial. High nitric acid concentration can improve the removal of NO, improving the reduction of total NOx. Again, the equilibrium model does not take this effect into account.

High pressure increases the forward rate of reaction (4.1), $2NO + O_2 \rightarrow 2NO_2$. Our equilibrium model neglects this reaction also. The low residence time in the column, as we discuss in Section 4.1, makes this effect small. However, the reaction rate varies with the cube of total pressure so the effect quickly becomes significant at elevated pressures. Figure 4.27 shows how pressure positively affects the oxidation of NO. Another advantage of higher pressure is that it reduces the vapor volumetric flow rate and thus the gas mass velocity.

Reduction of vapor velocity positively affects stage efficiency by increasing vapor-liquid contact time and vapor residence time. The equilibrium model ignores these effects also. Figure 4.28 illustrates the increase in residence time for increases in column pressure.

The predicted effect for our model for changes in pressure is not as dramatic as we should see in practice. This is partly because we neglect reaction (4.1) from our model. Also, the reduction in vapor velocity and the improved rates of absorption are kinetic effects. Our equilibrium model ignores kinetic effects. High pressure does, however, affect the equilibrium of reaction (4.2) and the equilibrium absorption of key NOx gases. Increased absorption of NOx gases likewise improves the liquid-phase production of nitric acid.

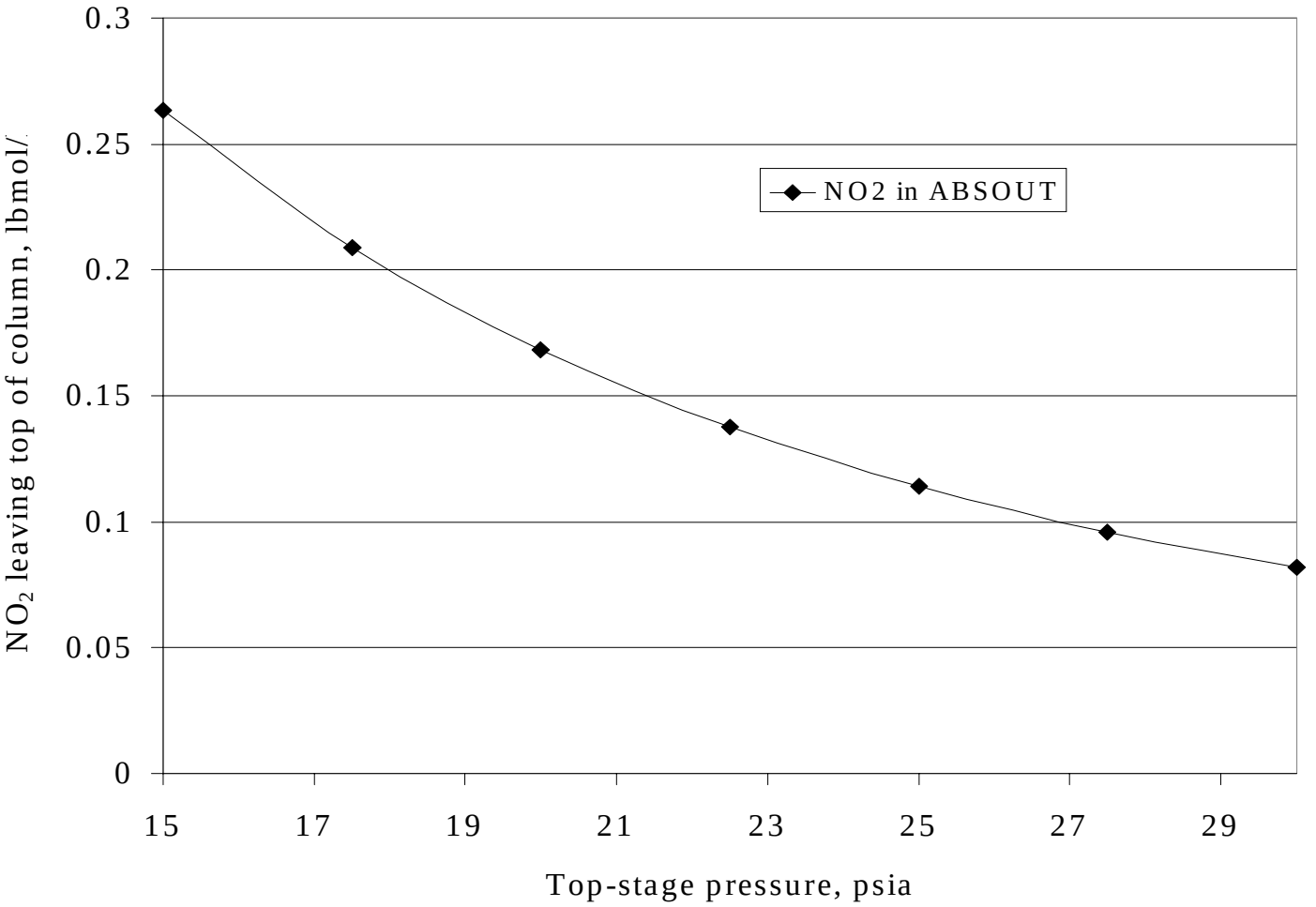

Figure 4.24. Plot of NO_2 in ABSOUT, HNO_3 in WASTACID, vs. top- stage column pressure. Rest of column has 5 psi pressure drop.

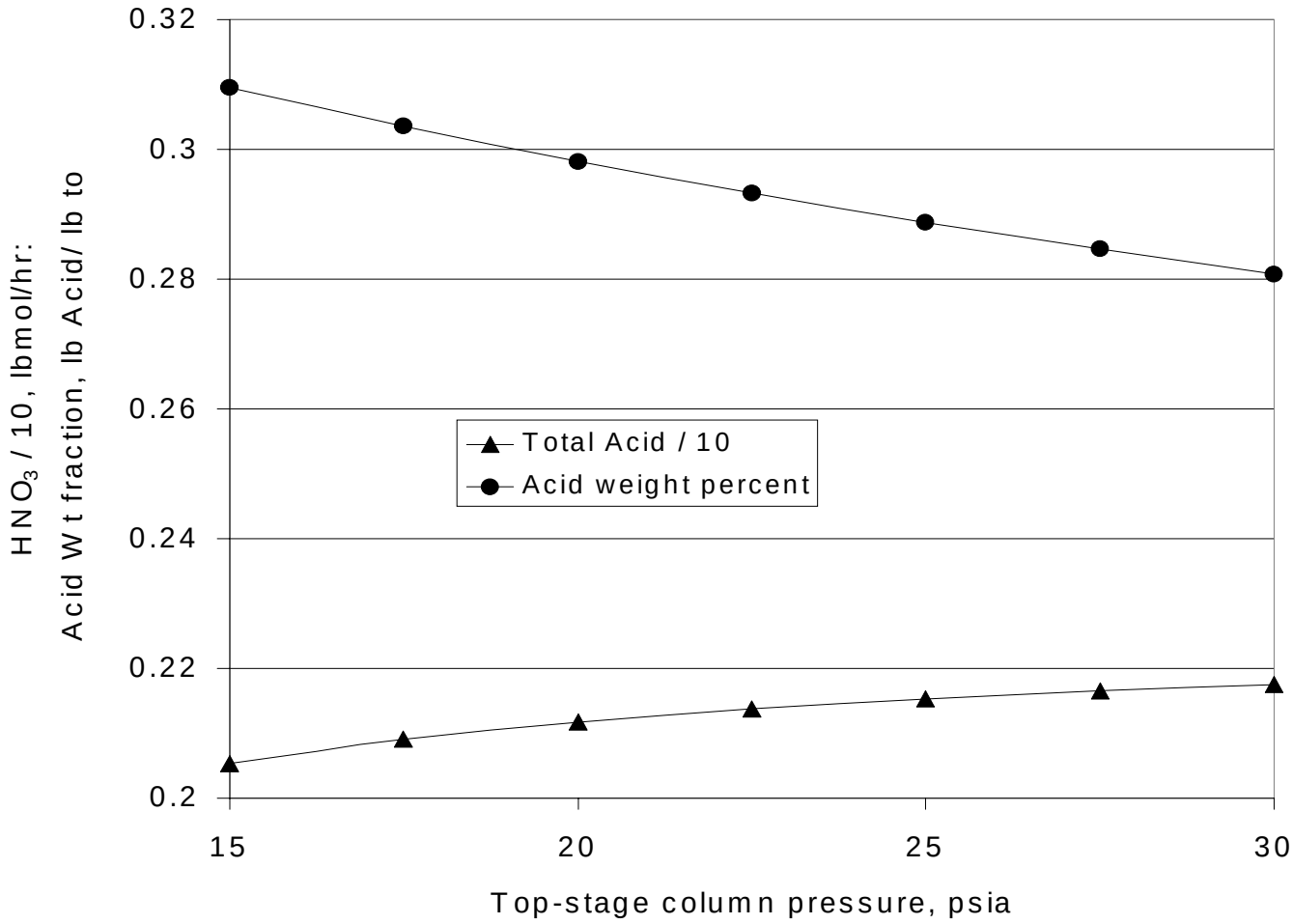

Figure 4.25. Plot of acid Wt.% in WASTACID, HNO_3 in WASTACID, vs. top-stage column pressure.

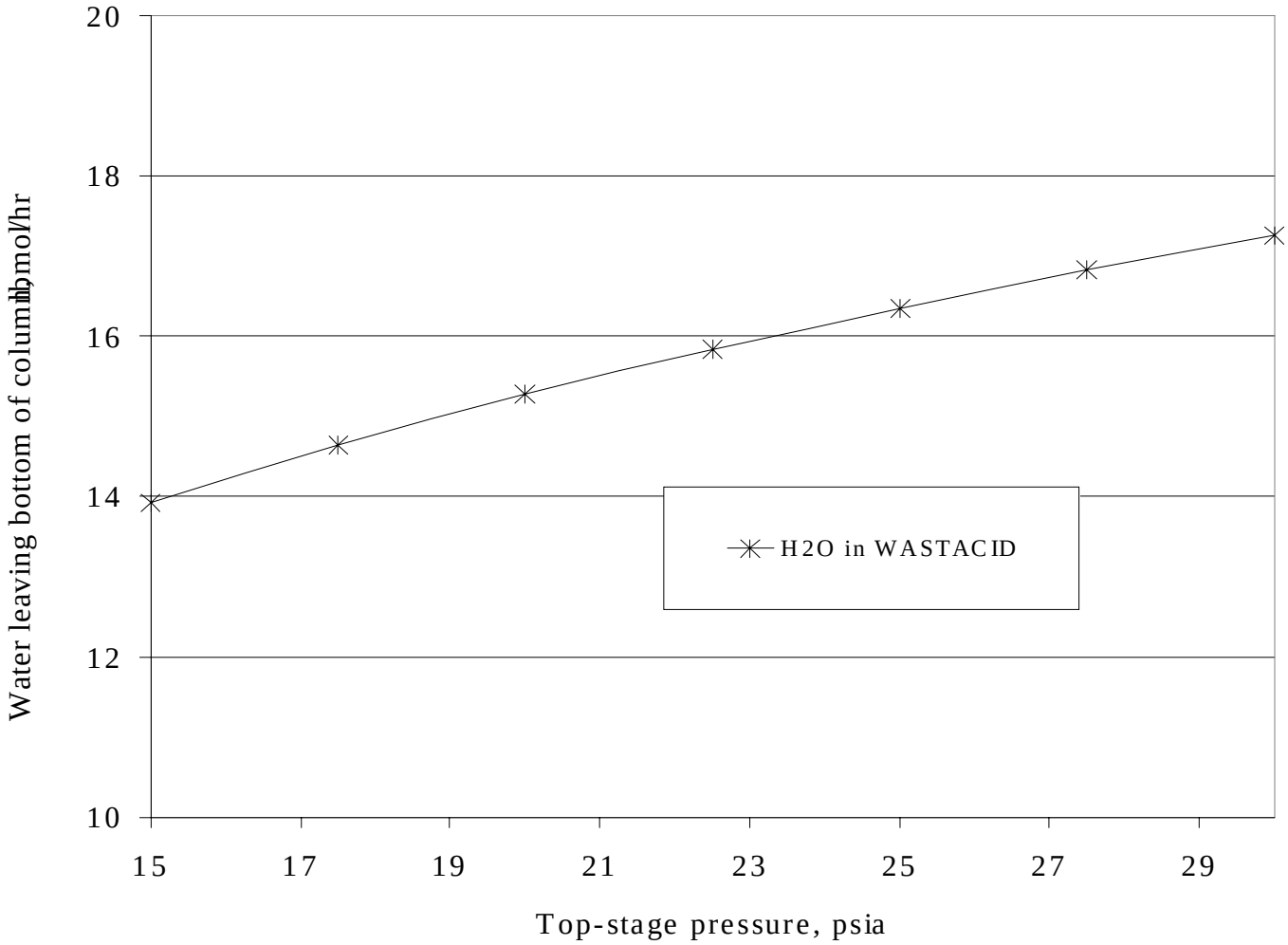

Figure 4.26. Plot of water in WASTACID vs. top -stage column pressure.

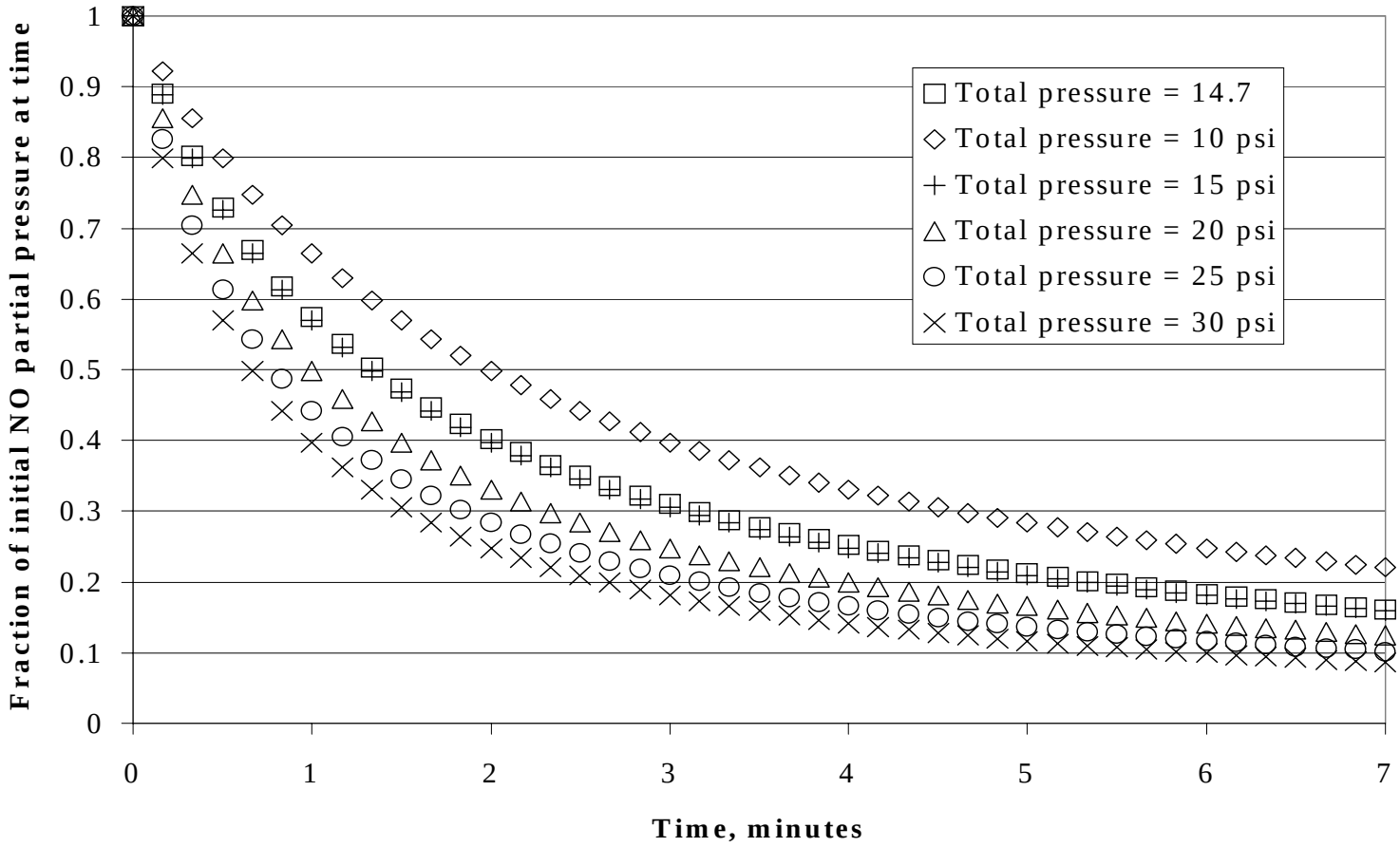

Figure 4.27. The effect of total column pressure on the time-dependent concentration of NO. Temperature = 85 ^{o}F, column height is 73.5 ft., column diameter = 5 ft., void-volume fraction of column = 0.8. The residence time of the column depends on total pressure (see Figure 4.25), NO flow in fumes = 0.5 lbmol/hr.

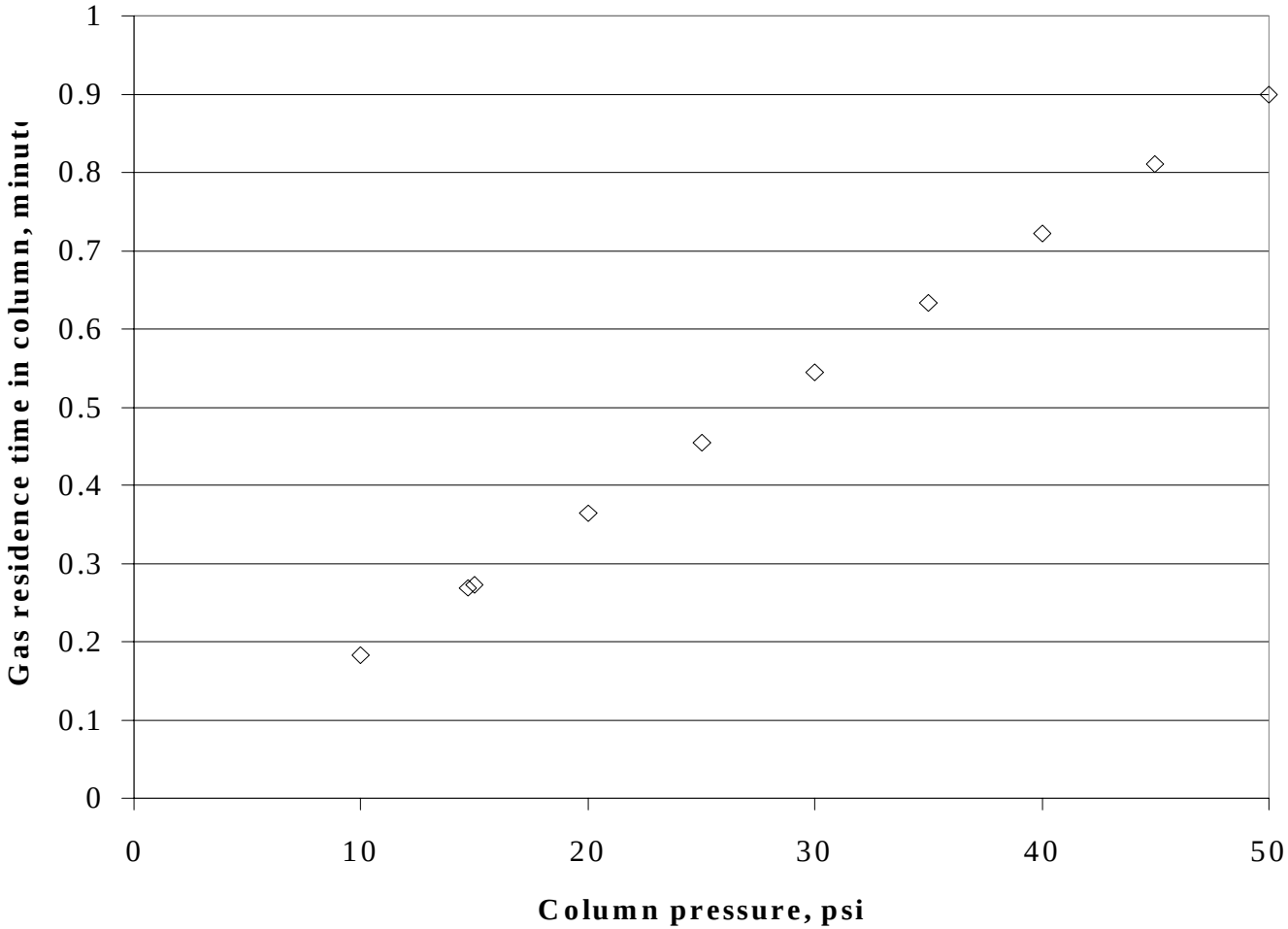

Figure 4.28. Effect of column on residence time for the fumes fed to the scrubber/absorber. Temperature = 85 °F, column height is 73.5 ft., column diameter = 5 ft., void-volume fraction of column = 0.8

4.2.2.7 NO Feed Rate to the Scrubber/Absorber

We predict that increasing the NO feed to our column will have a generally negative effect on column performance. Absorbed NO reacts with nitric acid to produce NO_2 according to our model. The two possible fates of the NO_2 produced in this manner escape to the top of the column, or react in water to produce nitric acid and regenerate NO. The equilibrium model takes no account of the proposed catalytic effect of nitric acid on NO removal. Also, the first equilibrium model neglects the presence of N_2O_3, and thus the contribution of that pathway to NOx removal. Therefore, we predict that the equilibrium model responds even more negatively to increases in NO than does the actual column. The lack of accounting for NO and N_2O_3 represents a shortcoming of the equilibrium model. However, we stand by our assumptions that for the case of NOx abatement under the conditions observed at RFAAP, the contribution from these components is minimal. Figure 4.29 shows the results of this test.

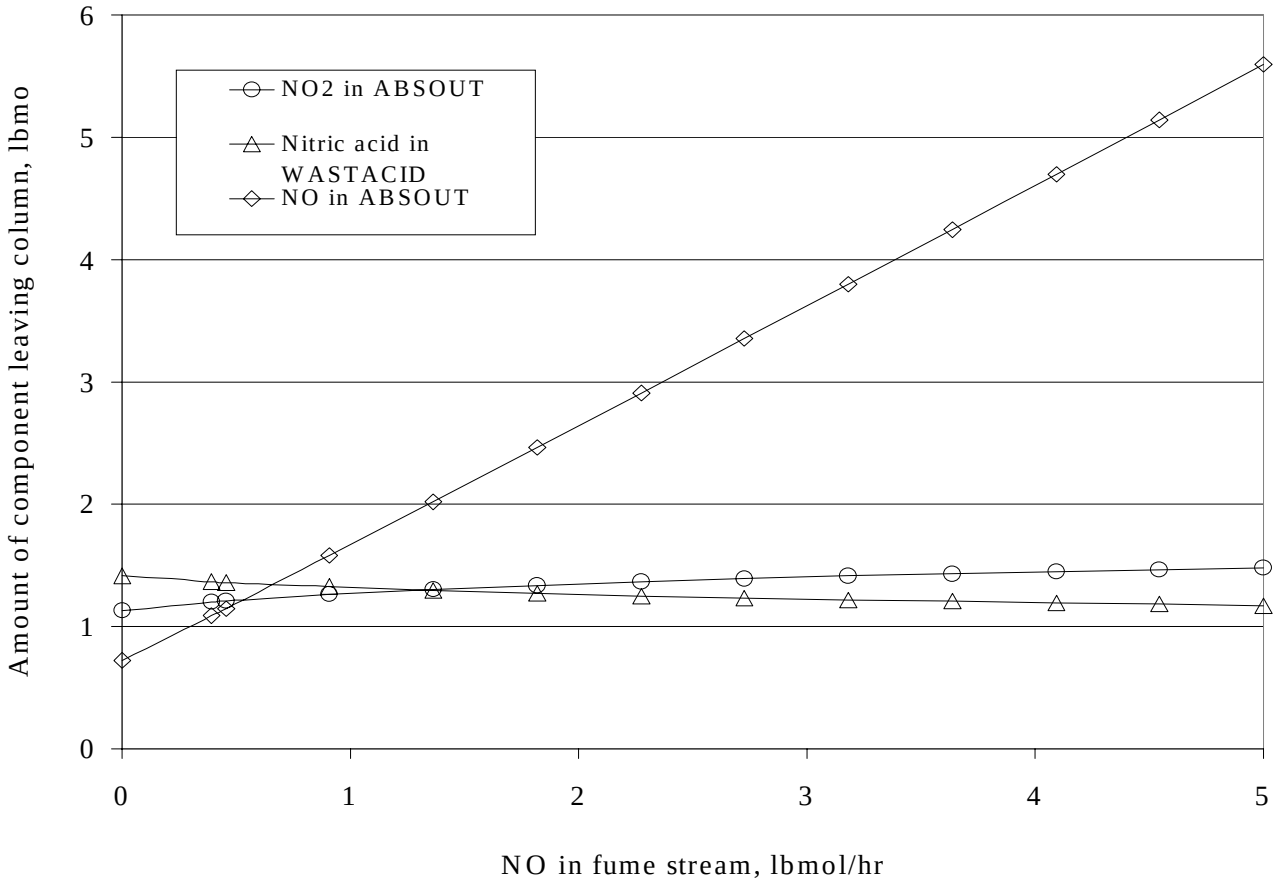

Figure 4.29. Plot of NO_2 leaving the top of the column in ABSOUT and nitric acid leaving in WASTACID versus the NO feed flow rate at a constant fume flow rate of approximately 650 lb-mol/hr.

4.2.2.8 NO_2 Feed Rate to the Scrubber/Absorber

Literature reports contend that NO_2 feed rate positively affects the percentage of the NO_2 removed. In a typical absorption system, increasing the amount fed would increase the amount absorbed, but not necessarily the percentage. This distinction follows from the dependence that NOx absorption has on reactions, and therefore, on the concentration of the key NOx gases participating in the reactions. Since air constitutes the bulk of the gases fed to the column, doubling the NO_2 feed rate has little effect on the overall gas flow.

We predict that our model will show similar sensitivity to NO_2 feed rate as that of the literature. The conclusion of this analysis should not be to feed more NO_2 by feeding a larger volume of fumes. On the contrary, we make the point to keep the NO_2 as concentrated as possible by minimizing the air that dilutes it before feeding it to the scrubber/absorber. Implementing such a strategy would require changing processes in the nitrocellulose line upstream, because there is no convenient method for concentrating NOx gases once they have been diluted in air.

We present the results for NO_2 feed flow rate in a number of ways to ensure understanding. Figure 4.30 shows the results for molar flow rate of NO_2 and nitric acid leaving the top and bottom of the column, respectively, versus the molar flow rate into the bottom of the column.

Figure 4.31 displays the results for total NOx removal efficiency versus inlet NOx concentration in ppmv. The NO inlet rate remains constant at 600 ppmv, while the NO_2 inlet rate varies between 0.0 ppmv and 23,150 ppmv.

Figure 4.32 gives a reaction profile for the three-stage equilibrium model for four different NO_2 inlet rates displayed in Figures 4.30 and 4.31. We connect the data points with a line only for ease of visualization. Each data point represents the amount of NO_2, in lbmol/hr,

that absorption/reaction remove on each stage. The terms reaction, absorption, and removal are synonymous for this plot. The negative values for the y-axis denote that NO_2 is in fact consumed.

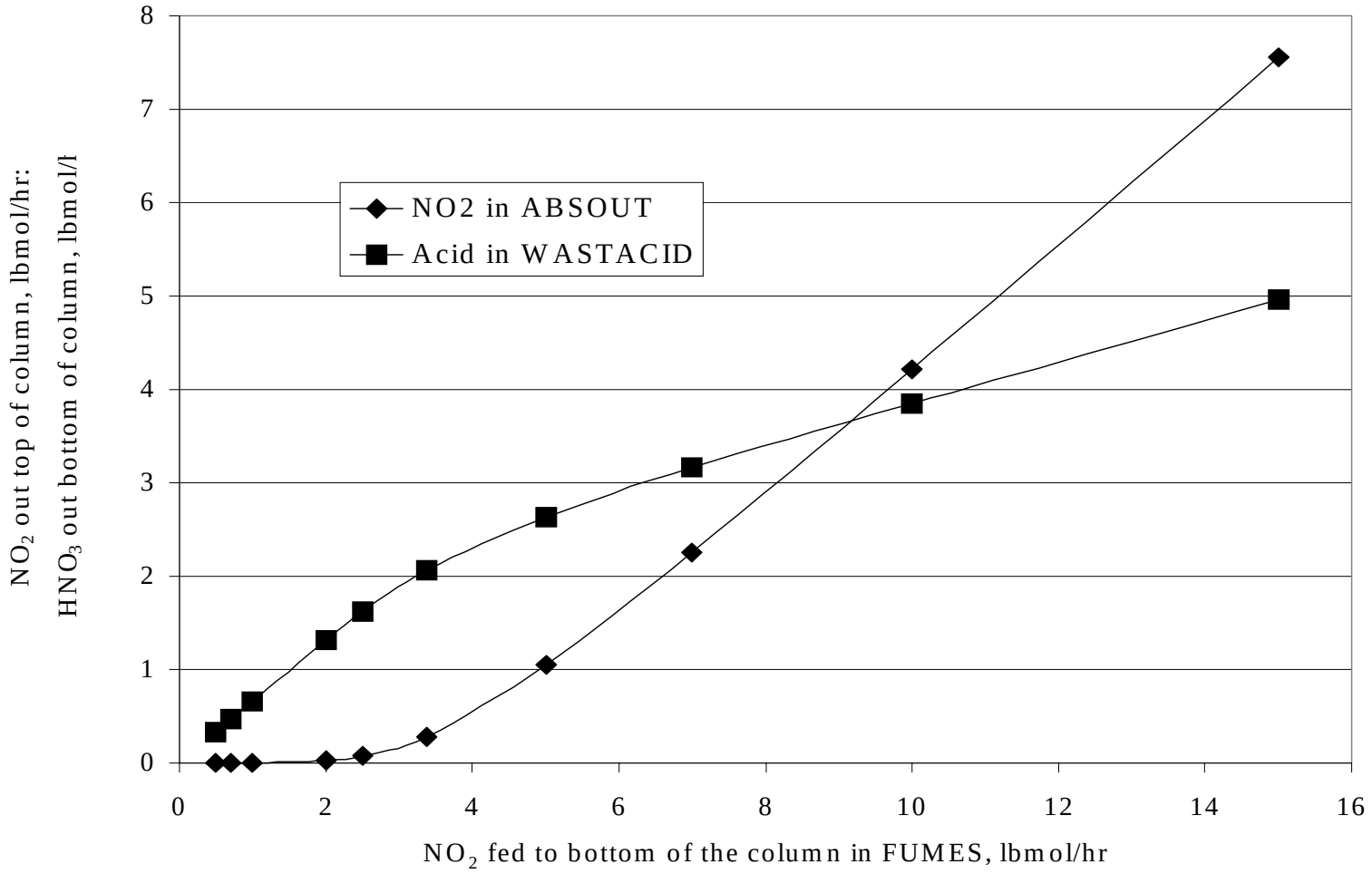

Figure 4.30. Plot of NO_2 leaving the top of the column in ABSOUT and nitric acid leaving in WASTACID versus the NO_2 feed flow rate at constant fume flow rate of approximately 650 lb-mol/hr.

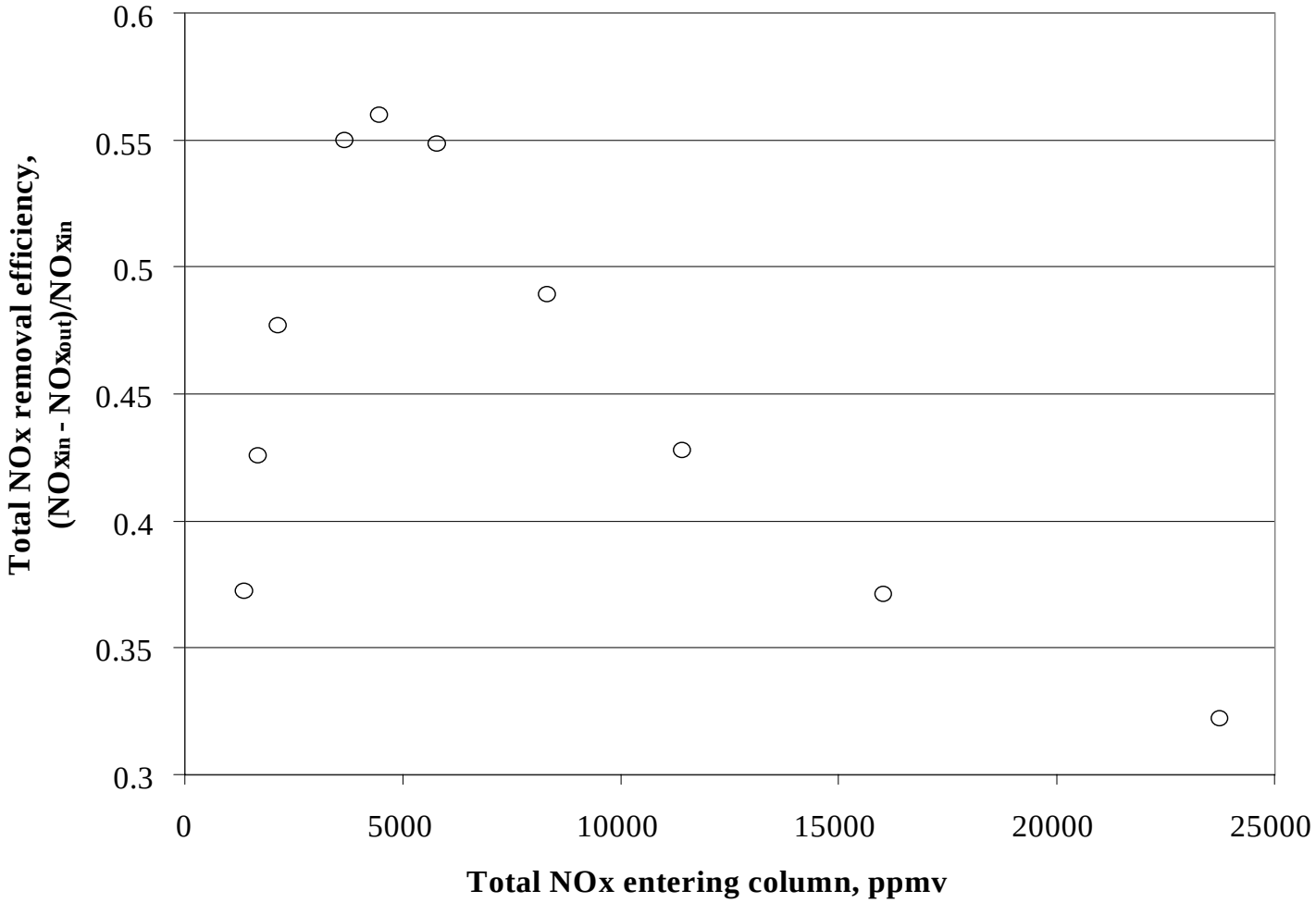

Figure 4.31. Plot of NOx removal efficiency vs. total NOx fed to the column. A constant NO feed rate of 0.39 lbmol/hr (600 ppmv) is fed while we vary the NO_2 rate.

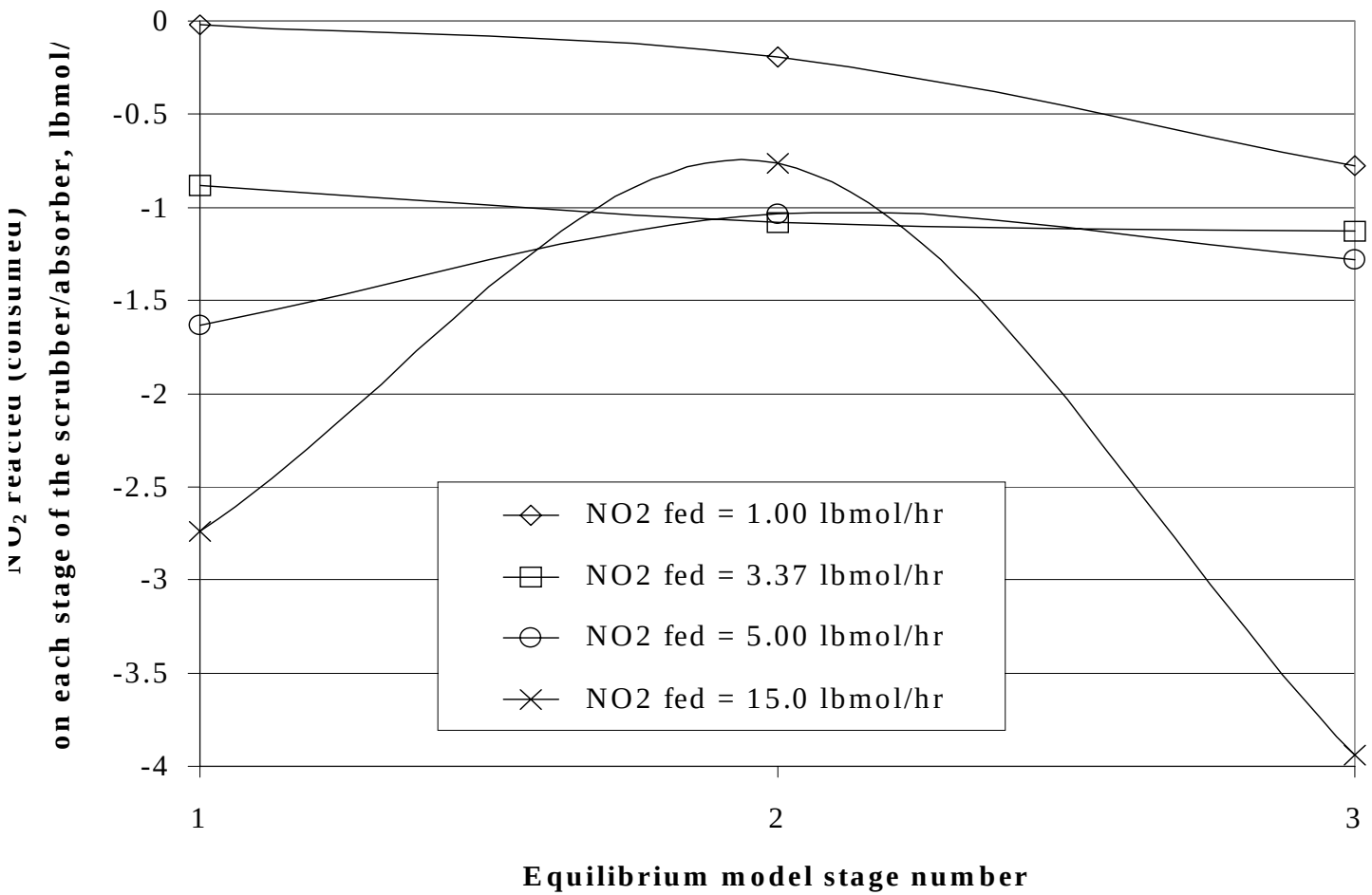

Figure 4.32. Plot of NO_2 reacted on each stage for 3-stage equilibrium model for varying feed flow rates of NO_2 in feed.

Figure 4.30 shows the effect of NO_2 inlet rate on the outlet rate of NO_2 and HNO_3. The NO_2 exiting the top of the column remains very low, and the nitric acid flow rate increases quickly until a feed rate of 3 lbmol/hr of NO_2. Not until a feed rate of 5 lbmol/hr does the effluent NO_2 rate exceed 1.0 lbmol/hr. However, above an inlet rate of approximately 4 lbmol/hr, the outlet NO_2 rate increases linearly with the inlet rate. The slope of this increase is approximately 0.63 (lbmol/hr $NO_{2,out}$)/lbmol/hr $NO_{2,in}$. The increasing nitric-acid effluent flow rate with respect to inlet NO_2 also becomes less dramatic. This result proves that merely increasing the total inlet rate of NO_2 at constant air rate does not improve the rate of absorption after a certain point. Above an inlet rate of NO_2 of 4 lbmol/hr, only 0.37 lbmol/hr NO_2 is absorbed for each extra lbmol/hr fed.

Figure 4.31 shows a clear maximum in the results for NOx removal efficiency versus total NOx inlet rate. The results in the region of inlet NOx less than the maximum value agree with literature results of Cheremisinoff and Young and others (Cheremisinoff and Young, 1977) that increasing NOx concentration increases removal efficiency. After the maximum, we observe the opposite effect. The maximum itself is not a gradual leveling off, but a sharp curve. We reason that the maximum occurs in the vicinity of a critical value of the filtered-water flow rate. More specifically, this critical value has to do with the nitric acid concentration allowable by equilibrium in the water effluent.

We refer the reader now to Figure 4.32. This figure shows where within our three-stage equilibrium model of the scrubber/absorber, the removal actually of NO_2 takes place. At low inlet rates of NO_2, the majority of the removal is in the bottom section (stage 3). This section corresponds to the bottom bubble-cap trays, as well as the scrubber section in the real column. However, recall that the computer model makes no distinction between a bubble-cap absorber tray and a scrubber stage. For higher inlet NO_2 concentrations, we see that the amount of NO_2 consumed at the top of the column (stage 1) increases dramatically and that of the middle of the column (stage 2) actually decreases.

What is physically happening in Figures 4.30, 4.31, and 4.32? The fumes rich in NO_2 enter the bottom of the column and contact the scrubbing water. At low NO_2 rates, this scrubbing liquid has a very low nitric acid concentration, so it can accept a large amount of absorbed NO_2 at equilibrium. The majority of the NO_2 removal takes place at this point and flows out the bottom of the column as nitric acid. As the fumes rise up the remainder of the column, little NO_2 remains to be removed. Therefore, very little reaction occurs from the middle to the top of the column.

At very high NO_2 inlet rates, the scrubbing liquid it contacts in the bottom of the column is high in nitric acid. Therefore, equilibrium dictates that the scrubbing liquid cannot accept a as much absorbed NO_2. However, because the NO_2 the concentration is so high in the gas, the equilibrium "pushes" that NO_2 into the liquid. This reduces the NO_2 concentration in the gas somewhat. As the gas proceeds to the middle of the column, the scrubbing liquid still has a high nitric acid content. Because the gas has less NO_2, there is not the driving force to push the NO_2 into the liquid. Therefore, very little reaction occurs in the middle of the column. Then, at the top of the column, the gas contacts a pure water feed. The pure water obviously has a large capacity for NO_2 and nitric acid absorption, and, thus, it absorbs a great quantity of these compounds. This process increases the nitric acid concentration in the scrubbing liquid as it goes down the column.

Interesting things happen in the regime between very high and very low NO_2 feed rates. Figure 4.32 shows that between the NO_2 flow rate of 3.37 lbmol/hr and 5.00 lbmol/hr, a transition takes place where the majority of the reaction conversion switches from the bottom (3.37 lbmol/hr) to the top (5.00 lbmol/hr). By the 15.0 lbmol/hr flow rate, the majority of reaction is again at the bottom, but the reaction remains high at the top, though the activity of middle has dropped sharply.

How would the rate-dependant factors affect the real column under the conditions of this graph? We, of course, attempt to take the distance from equilibrium of the column by using three-stages to simulate the actual tower (16 bubble-cap absorber trays and 2 scrubber sections).

This expedient is not perfect, however. First, the efficiency of the column is higher at points in the column where the driving force, or distance from equilibrium, is greatest. Therefore, the driving force, and thus the absorption rate and stage efficiencies, would be greater for the 15.0 lbmol/hr feed rate of NO_2 than for the lesser values. Also, we do not know whether bubble-cap absorber trays and the scrubber sections have the same absorption efficiencies. If they are not the same, we do not know which one is greater and by how much.

We assume that the scrubber sections have higher efficiencies in the actual column, because they occupy a larger volume of the column than the individual absorber trays. This fact, along with the driving force issue, suggest that the reaction conversion in the bottom of the column would be higher in the actual column. However, we lack sufficient information to estimate the degree to which this is the case.

4.2.2.9 Filtered-Water Flow Rate to Top of Column

We expect the result of increasing the filtered-water feed rate to be an increase in NOx absorption. Increasing water flow decreases the acid concentration and allows a greater driving force for absorption of NOx and production of acid. This greater driving force should also increase the rate of absorption, and thus positively affect the tray efficiency.

We vary the filtered-water flow rate to the top of the absorber in Figure 4.33 between 5 and 20 lbmol/hr. The figure shows the NO_2 escaping the top of the column and the weight percent of acid produced. Increasing the water flow rate both decreases the NO_2 in ABSOUT and dilutes the acid in WASTACID. However, the shape of the curves shows a point of diminishing returns. At this point, nearly all the NO_2 absorption has occurred. Therefore no more will be absorbed even as we add more water.

To judge if this phenomenon is representative, we present Figure 4.34. We display the data for this figure somewhat differently than that for Figure 4.33, although the shape of the curves should be familiar. Figure 4.35 shows the results of several simulations varying the NO_2

inlet rate as well as the filtered-water flow rate. This chart is reminiscent of Figure 4.23 for the heat loss from the column.

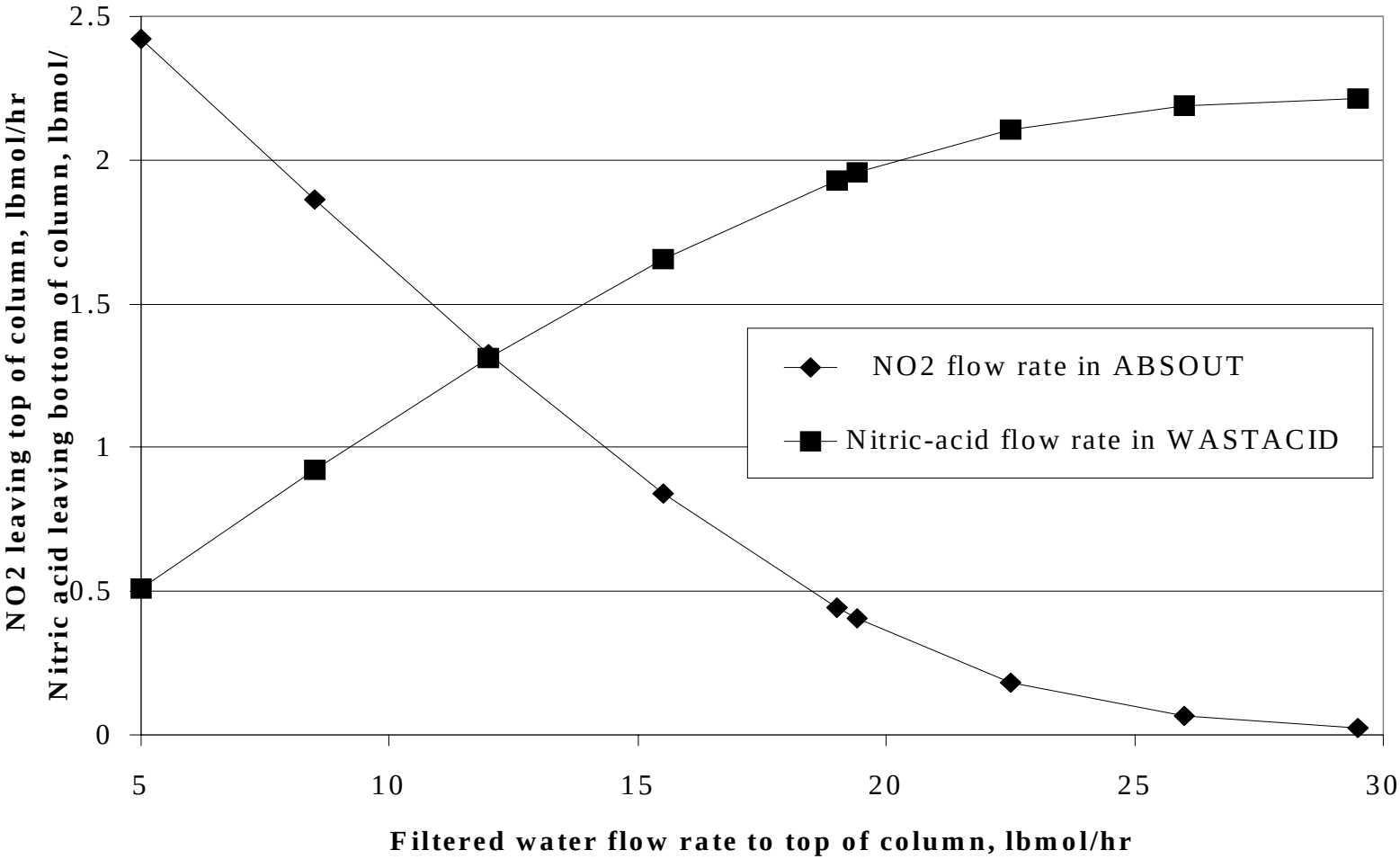

Figure 4.33. Plot of NO_2 out top of column and nitric acid wt% in WASTACID vs. filtered-water flow rate for NO_2 inlet rate of 3.37 lbmol/hr (5200 ppmv) and a total NOx inlet rate of 3.37 lbmol/hr (5800 ppmv) where the balance is NO.

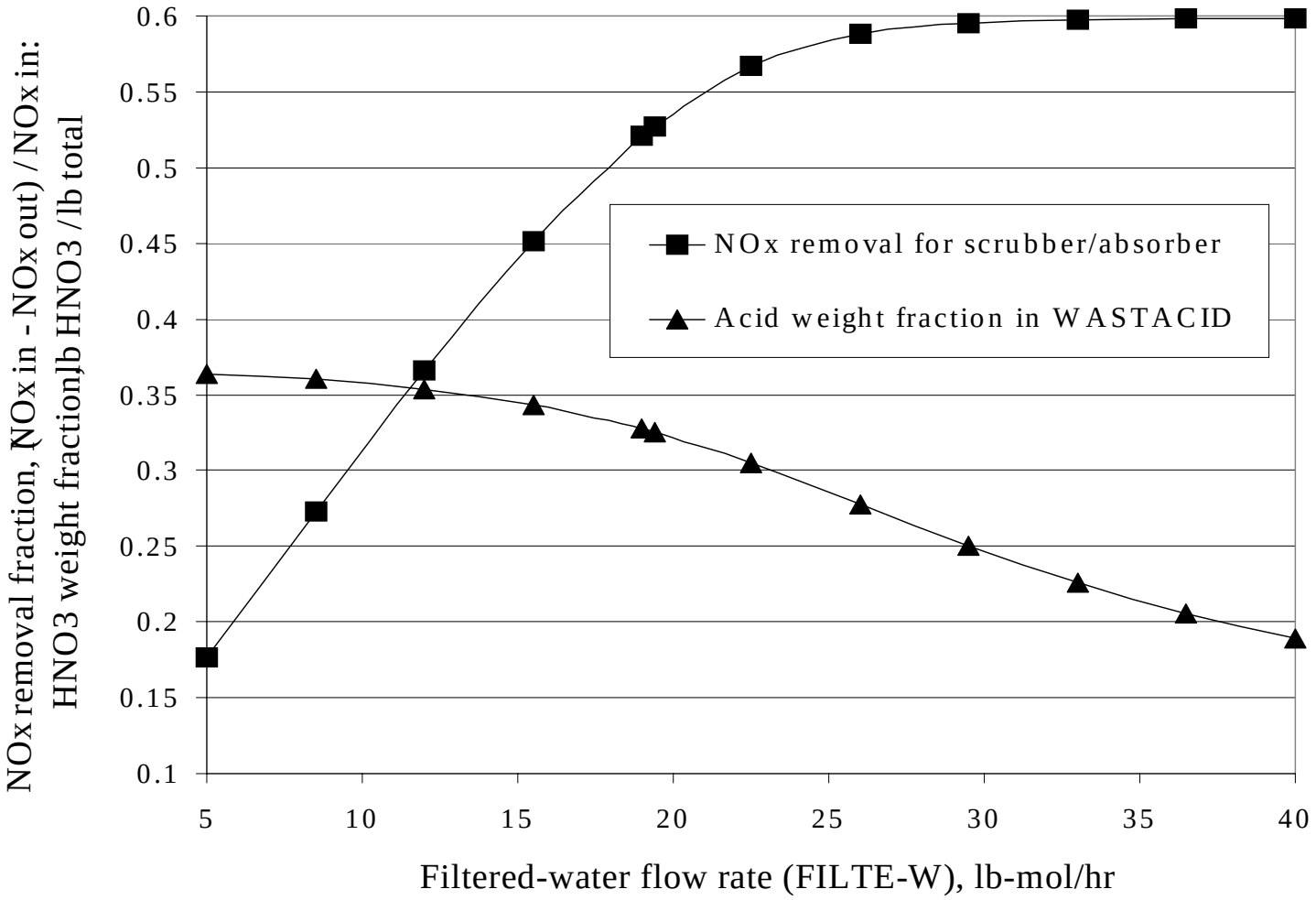

Figure 4.34. Plot of NOx removal % and acid wt% in WASTACID vs filtered-water flow rate. Total NOx feed = 3.76 lbmol/hr, fume temperature = 90 Deg F.

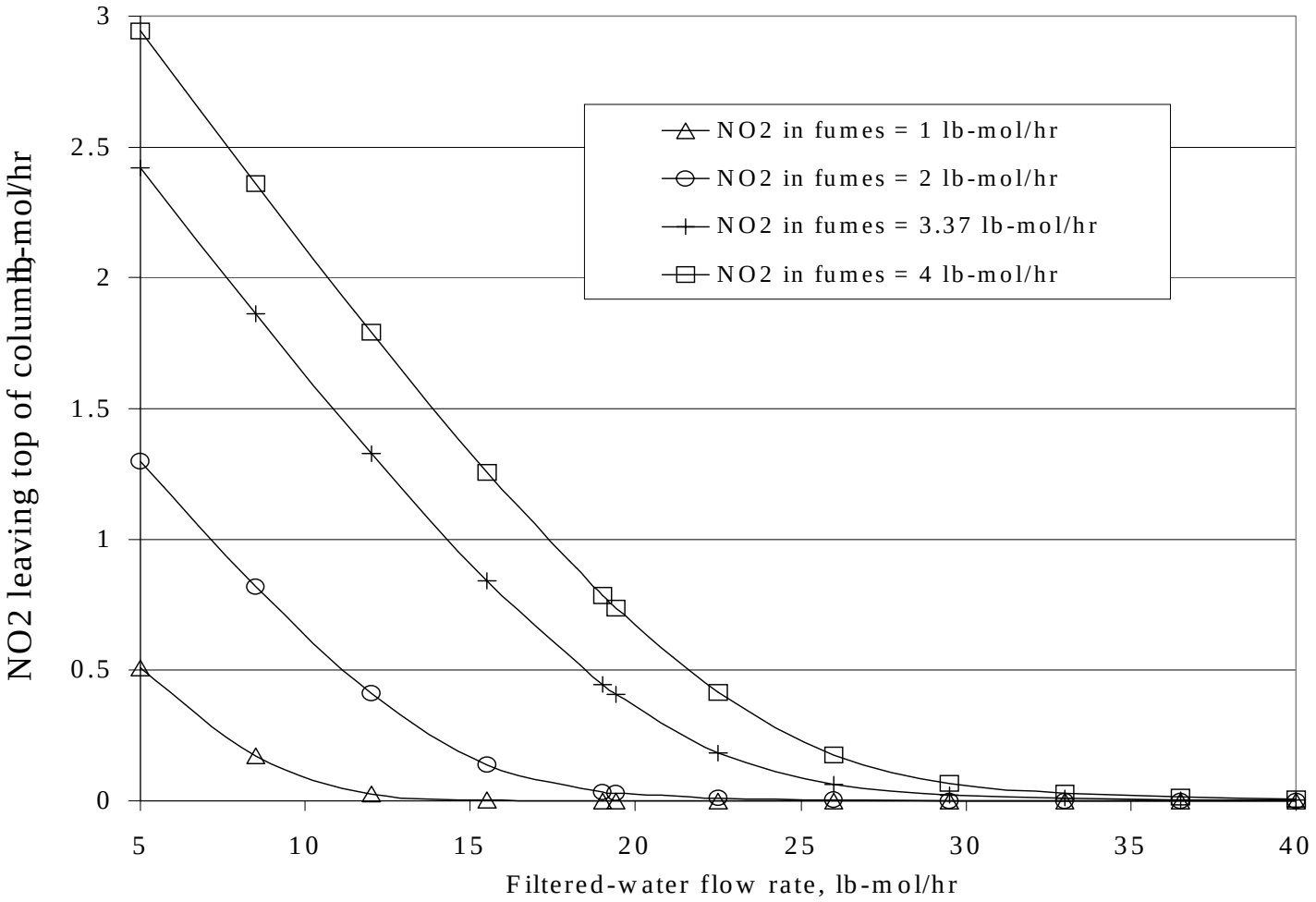

Figure 4.35. Plot of NO_2 escaping in ABSOUT versus filtered-water flow rate (FILTE-W).

Figure 4.33 shows the expected decrease in NO_2 and increase in nitric acid effluent rates with increasing water feed rate. The relationships are approximately linear in the beginning. Diminishing returns set in between 20 and 25 lbmol/hr of filtered water feed. However, after approximately 30 lbmol/hr flow of water, the NO_2 leaving the top of the column becomes virtually zero.

Figure 4.34 shows the same trend as Figure 4.33, though in the more conventional axis labels seen in the literature. The maximum NOx removal barrier clearly manifests itself in this figure. Again, the barrier theory states that no more than 66% of the feed NOx removal can take place. The percentage decreases as the fraction of feed that is NO increases. The 66% value for total NOx removal corresponds to a feed of all NO_2 where it removes all the NO_2 and converts one-third to NO. In this figure, the feeds are 3.37 lbmol/hr of NO_2 and 0.39 lbmol/hr NO. The theoretical maximum removal fraction percentage then is 0.597. Figure 4.34 agrees with this value quite well.

Figure 4.35 shows that for any NO_2 input, we can achieve the desired NO_2 output by adjusting the water flow rate just as we could by adjusting column-cooling duty in Figure 4.23. Here, the engineer or the automated control system can specify the water-feed rate depending on the flow of NO_2 to the column.

At this point, the reader should notice the familiarity of the trends displayed in the plots of parameters that improve NOx absorption. Initial gains level off after the process consumes a certain percentage of the NOx (NO_2 specifically). The three most effective factors for improving NOx absorption (cooling, pressure, and filtered-water flow rate) all dilute the nitric acid effluent, reducing its recovery value.

The diminishing returns seen at low NO_2 rates mean that NOx removal below these levels requires greater effort by cooling, pressurizing, or inputting water, which in turn dilute the acid

effluent beyond the point of recoverability. Therefore, it is important to determine the maximum allowable NOx emission and target the removal to it with tight process control.

The equilibrium model does not account for the catalytic effect of nitric acid. Therefore, the predicted effect of increasing the nitric acid present in the column is promoting consumption of nitric acid and the production of NO_2. We desire to avoid this situation, because it effectively reverses any positive gains made for NO_2 removal in the column. Unfortunately, we cannot glean from the simulation results what variables maximize the catalytic effect of HNO_3, while minimizing the reverse of reaction (4.4,5). Also, we predict that the equilibrium model overestimates the effect of nitric acid. This is because the NO_2 concentration in the gas and the nitric acid concentration in the liquid, as the initial reactant and the ultimate product, respectively, in a complex chain-reaction sequence, control the equilibrium of the system. Increasing the concentration of nitric acid pushes the reactions back to the reactants. Because the true process never actually reaches equilibrium, we predict the effect on the column at RFAAP to be less dramatic.

4.2.2.10 NO Feed Rate to the Catalyst Vessel

We now switch our focus from the scrubber/absorber to the catalyst vessel for selective catalytic reduction. Researchers developed selective catalytic reduction primarily for the removal of NO, although it does have some limited NO_2 removal capability. However, we prefer to remove NO_2 in the scrubber/absorber because that process proves quite effective for that role, as well as the removal of NO_2 by absorption concentrates NO in the gas stream. In this vain, the results presented for the catalyst vessel emphasize NO removal.

We vary the amount of NO fed to the catalyst vessel keeping all other variables constant, including ammonia flow rate. We predict that the NO escaping the catalyst vessel will increase as we increase the NO feed. However, because the catalyst vessel is an equilibrium model, we predict that it should not be perfectly linear nor should it be a one-to-one ratio unless all the ammonia is consumed. Figure 4.36 shows these results.

As expected, the NO effluent increases directly with NO feed rate. Interestingly, ASPEN calculates that the ammonia is completely consumed for all values of NO. Apparently, the equilibrium lies strongly to products; however, it is unlikely that a total consumption of ammonia occurs in the actual process. The equilibrium model appears flawed for the reactions in the catalyst vessel.

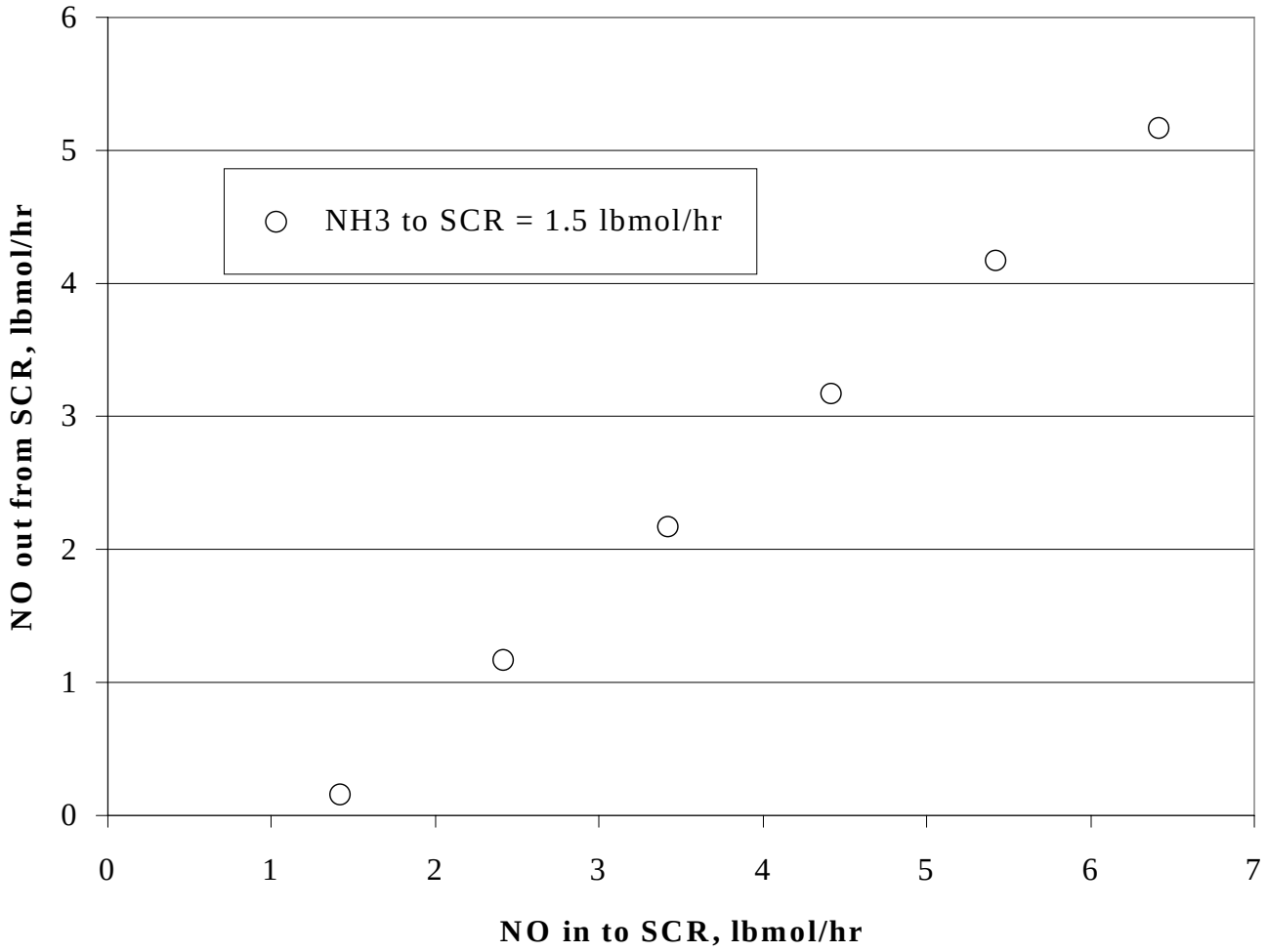

Figure 4.36. Plot of the amount of NO exiting the SCR vs the amount of NO fed to the SCR for an ammonia flow rate of 1.5 lbmol/hr.

4.2.2.11 Ammonia Feed Rate to the Catalyst Vessel

We predict that increased ammonia feed rate results in increased NO removal from the catalyst vessel and increased ammonia escaping the catalyst vessel, also known as the ammonia slip. Figure 4.37 shows the amount of NO that leaves the catalyst vessel versus the amount of NH_3 fed for several different NO feed rates to the reactor.

Figure 4.37 shows no clear trend in the data for the dependence on ammonia. Essentially, the ammonia reacts completely for every NO flow rate. From literature data for experiments on similar reactors, we know this cannot be the case. Even for the equilibrium assumption of infinite residence time, there should not be a complete consumption of ammonia. ASPEN apparently experiences a mathematical limit of some kind for this calculation.

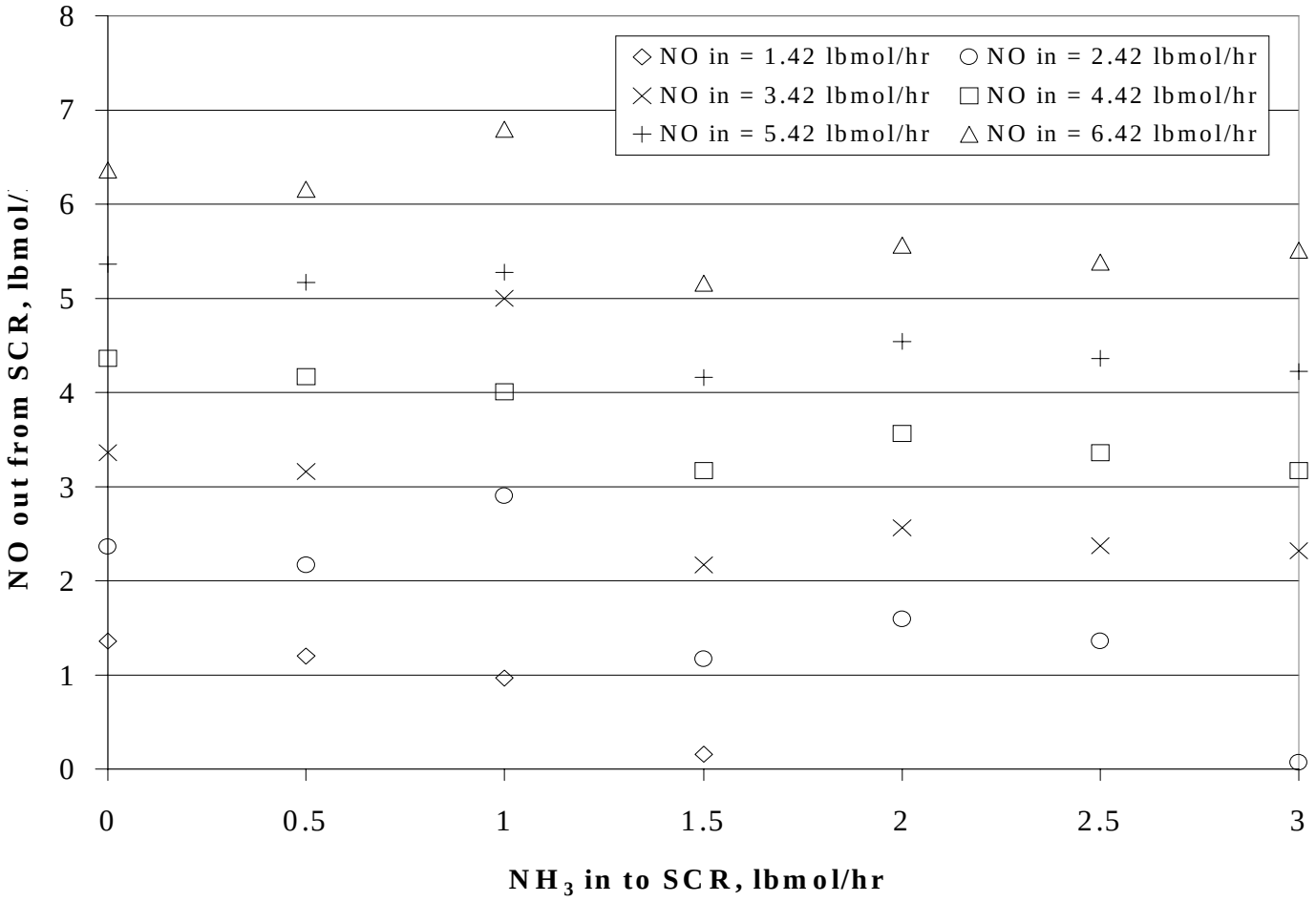

Figure 4.37. Equilibrium model results for the amount of NO leaving the column vs. ammonia feed rate for several different NO inlet rates.

4.2.2.12 Steam Feed Rate to the Catalyst Vessel

RFAAP utilizes steam to safely vaporize the ammonia that is stored as a liquid in pressurized tanks. This approach is not unusual for chemical plants requiring the feed of vaporized ammonia to processes. However, the fact that steam is a product of the SCR reactions does make this approach interesting in this case. As we know, feeding products to a reactor pushes the reaction equilibrium back to reactants by increasing the rate of the reverse reaction through mass action.

We predict from principles of chemistry that increasing the steam flow rate will decrease the conversion of NOx. Recall that the ultimate products of the SCR reactions are N_2 and H_2O. Nitrogen already comprises approximately 76% of the gas to the catalyst vessel. Adding more H_2O should react with this excess nitrogen on the catalyst surface yielding NO and NO_2. We predict this outcome for the real process.

However, given the dose of reality afforded by the previous two figures for the catalyst vessel, we predict that the model simulation results will continue the trend and will show that all the ammonia is consumed by reaction with NO and the extra steam does not affect the results.

Figure 4.38 shows the results of the model for steam flow rate. The results surprise us in that the model, at least qualitatively, for once agrees with the theory. Too skeptical for such a simple result, we extend the test to higher steam rates. Figure 4.39 shows this result. The model surprises us again, proving both predictions to be correct and wrong at the same time. We present no explanation for this result other than an unpredictable mathematical anomaly created by the extreme equilibria in the catalyst vessel.

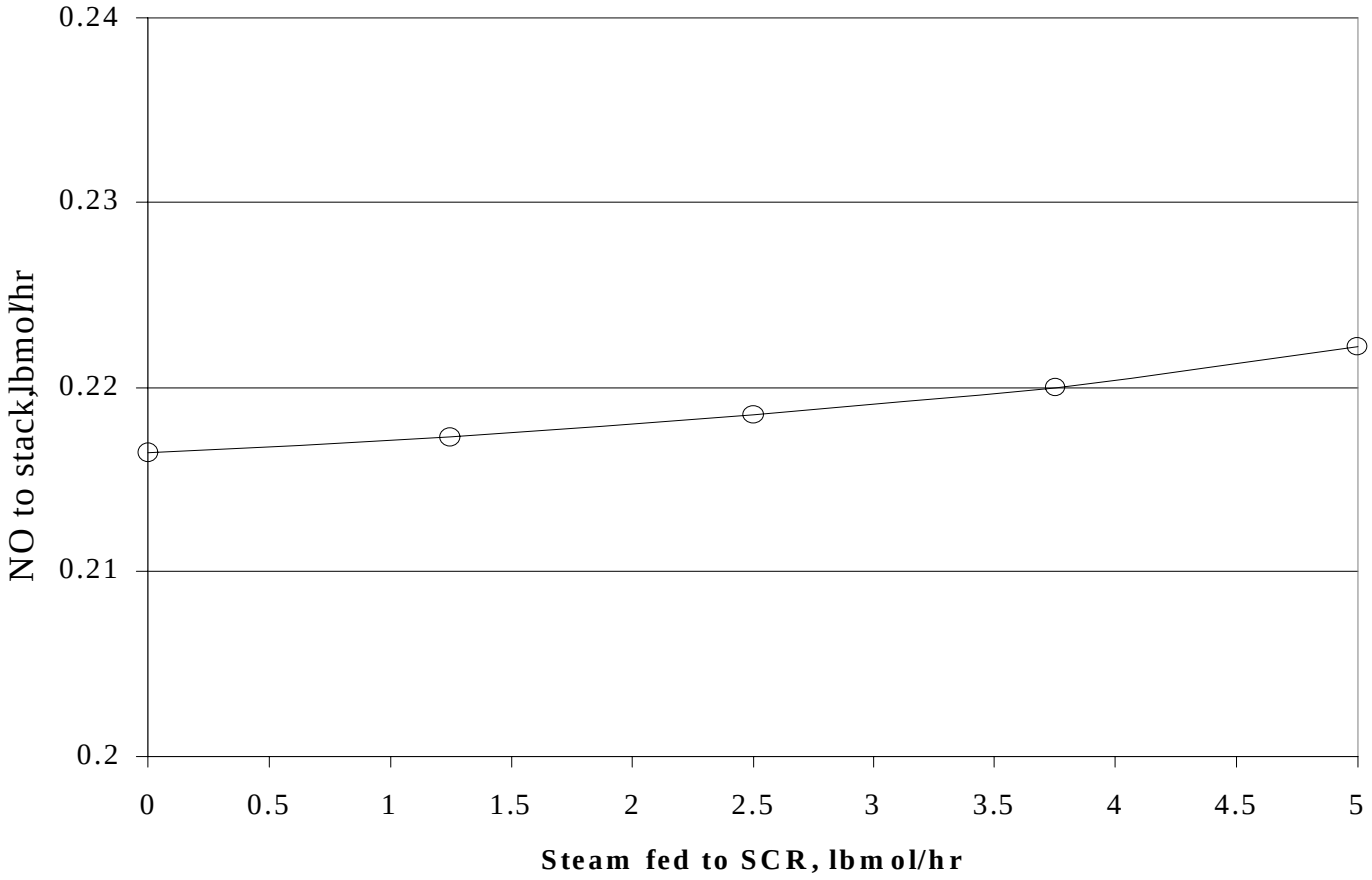

Figure 4.38. Plot of NO exiting the SCR vs. the steam flow rate fed with ammonia to the SCR.

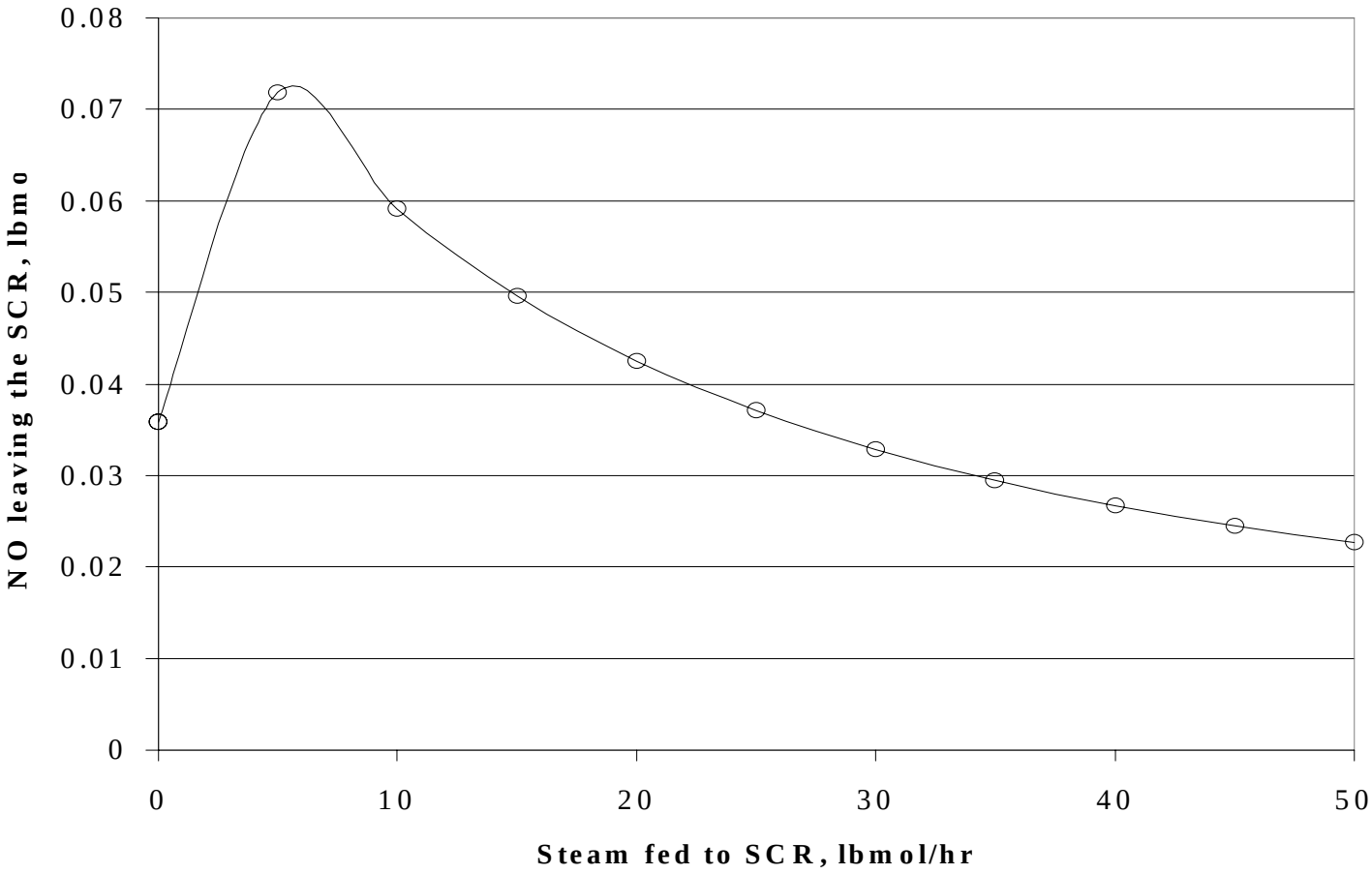

Figure 4.39. Plot of the NO that leaves the SCR unit unreacted versus the amount of steam fed to the SCR. RFAAP uses steam to vaporize the ammonia feed to the catalyst vessel.

4.2.3 Advantages of the First Equilibrium Model

The first equilibrium model gives clear advantages over the conversion model. Ease of use constitutes its most obvious advantage. The single reactive-distillation tower of the equilibrium model houses all the specifications and calculations that require seven separate blocks in the conversion model (ABSORBER, SCRUBTOP, SCRUBBOT, ABSREACT, SCRREACT, BOTREACT, and FLASHBOT). Also, the equilibrium model eliminates the need for all the material streams required to connect those seven blocks.

The improved results and response to sensitivity tests represent the most important advantage of the equilibrium model. This chapter shows that the equilibrium model matches the expected results supplied by RFAAP, but the scrubber/absorber model also matches experimental results from literature. We now have confidence in the response the model gives to sensitivity variables. We can draw conclusions as to how these variables affect the real process based on how they analogously affect the simulation results.

4.2.4 Disadvantages of the First Equilibrium Model

The main problem with the treatment of all reactions in the NOx abatement system at RFAAP as equilibrium reactions is the instability of the SCR under this method. Equilibrium so heavily favors the products for these reactions that ASPEN cannot cope with the calculations for the equilibrium constant. The problem is so complete with this unit that the sensitivity tests for the system of adding excess products or reactants give completely different results than those predicted. However, in most cases, ASPEN returned erroneous results. Clearly, the equilibrium assumption is faulty for this unit.

The second problem with the first equilibrium model is unrealistic representation of the column as a total of three stages. For general results regarding inputs and outputs, this problem is indeed secondary. However, we want to know certain aspects of the system behavior on a

stage-by-stage basis. A three-stage model can only give us an idea of this behavior. The three-stage arrangement arises from the assumption of equilibrium for the mass transfer and the reactions. As discussed, we feel justified in this assumption for the important reactions in this system. However, the residence time required for the mass transfer to bring the gas and liquid into equilibrium is extremely long. The first equilibrium model contains no answer for mass-transfer efficiency.

4.3 The Second Equilibrium Model

4.3.1 Motivation for a Second Equilibrium Model

The first equilibrium model displeases us in its unrealistic physical representation. Having only three stages, it is a hypothetical model of what a column with 100% mass-transfer efficiency would have to look like to give equivalent results as those provided in the mass balance. Ideally, we would like to simulate a real 18-stage column with an 18-stage model. A more consistent model would allow us to analyze the stage-by-stage behavior of the column to pinpoint any bottlenecks and other areas for optimization.

4.3.2 Vaporization Efficiencies

Unit operations involving equilibrium-staged separations, by definition, utilize well-characterized equilibrium states for the components involved. Such models assume that each stage is allowed to proceed completely to equilibrium. This assumption is rarely true in any case and is especially flawed in the case of NOx absorption. Rate considerations constitute the main drawback of this assumption. Different systems require different periods of time to reach equilibrium. Some systems, especially those involving chemical reaction, never approach equilibrium closely.

Somewhat counter-intuitively, systems with the largest driving force for separation and absorption represent the most “inefficient” equilibrium operations. That is, the change they

undergo on a stage, relative to the change they would undergo were they to reach equilibrium on that stage, is very small. Such systems require large residence times because of the great changes in component concentration.

Mass requires time to transfer between phases. Diffusional factors represent the resistance to the system achieving equilibrium. Also, as absorption proceeds, proximity to equilibrium begins to reduce the driving force for further mass transfer. Therefore, as a system approaches equilibrium, the rate at which it proceeds further decreases rapidly. Mathematically, we can see this concept from the fact that we define equilibrium as a state where there is no change in any variables, X, with respect to time, $dX/dt = 0$. As a system approaches equilibrium, the rate of change of process variables (concentrations, temperatures, extents of reaction, etc.) approaches zero. Achieving total equilibrium would require a residence time of infinity and likewise infinite-sized vessels.

Systems consisting of many different processes complicate the issue further. Depending on the rate of progress of each process and the distance to equilibrium, different processes can have vastly different efficiencies. For example, as stated previously, reaction (4.1) $2NO + O_2 \leftrightarrow 2NO_2$ remains far from equilibrium, whereas we assume that reaction (2.5), $HNO_3 + H_2O \leftrightarrow NO_3^- + H_3O^+$, achieves equilibrium in a very short period of time.

The special case of NOx absorption has several factors working against its efficiency, and thus the assumption of equilibrium. First, the dependence on reaction and the stability of the final product (nitric acid) in water set up a huge driving force. However, the rate of absorption of NO_2 and N_2O_4 are agonizingly slow. Despite the fact that the reactions involving these components in the system achieve equilibrium almost immediately, the rate-limiting factor in the process is the absorption and diffusion of the reactants and products. The very low solubility of NOx species in water causes this fact. Although water can ultimately absorb large quantities of NO_2 and N_2O_4, remember that the conversion to nitric acid must consume them. The solubilities of the components themselves are low and their partial pressures are extremely high. Therefore, the large y_i/x_i value at the interface hinders the rate of mass transfer.

In modeling unit operations, an efficiency factor typically represents the degree to which a unit operation achieves equilibrium. For the reasons given above, these factors differ for every system and also are complex functions of the specific parameters of the processing equipment, including packing and tray design, liquid- and vapor-flow characteristics, inerts in the system, etc. Engineers typically use the Murphree efficiency to estimate equilibrium stage efficiencies in tray columns.

The Murphree tray efficiency is defined as $E_M \equiv (y_n - y_{n-1})/(y_n^o - y_{n-1})$. The equation constitutes a ratio between the change in vapor phase of component y_n between the vapor feed to a stage and the vapor leaving that stage over the change that would take place if it reaches the equilibrium value. A Murphree of 1.0 means that it attains an equilibrium condition. A Murphree of 0 would signify no transfer of component y_n to, or from, the vapor phase. Murphree stage efficiencies are always between 0 and 1.0; however, flow and concentration gradients across plates can result in Murphree stage efficiencies greater than 1.0. In non-reactive stage operations, Kx_{eq} can typically replace y_n^o. That is because we define K as $K \equiv y_{eq}/x_{eq}$.

In NOx absorption, the value of the vapor composition of NO_2 in equilibrium with the liquid composition of NO_2 depends on several factors aside from just the value of K. Because of reaction, NO_2 remains in chemical equilibrium with other species in the vapor and liquid. Even in absorption systems without chemical reaction, determination of stage efficiencies requires a complex empirical function or extensive experimental data on the system (Peters and Timmerhaus, 1991, pp. 661-667). Due to the highly empirical nature of stage efficiencies and their dependence on a vast array of process and design variables, there exists no satisfactory or reliable method for predicting NOx absorption tray efficiencies a priori.

Vaporization efficiencies represent another method for estimating the distance of a system from equilibrium. We define the vaporization efficiency as $E_V \equiv y_i/(Kx_i)$. Again, we define $K \equiv y_{eq}/x_{eq}$. Therefore, we apply vaporization efficiencies to equilibrium calculations as follows: $E_V * K = E_V * y_{eq}/x_{eq} = y_i/x_i$. Thus, a value of E_V greater than one gives a ratio of y_i/x_i

greater than y_{eq}/x_{eq}. This corresponds to a greater vapor fraction or lower liquid fraction of component i than is normally present if the stage achieves equilibrium. A value of E_v less than one gives a ratio of y_i/x_I less than y_{eq}/x_{eq}. This corresponds to a lesser vapor fraction or greater liquid fraction of component i than is normally present if this stage achieves equilibrium.

The use of vaporization efficiencies gives a couple of advantages and some disadvantages. We can force a component to one phase or the other, depending on whether we specify E_v as greater than or less than one. We can define vaporization efficiencies per stage and per component. Selection of these parameters may depend on the overall direction of mass transfer. For example, on stages where NO is consumed due to high HNO_3 concentration, the main direction of mass transfer proceeds from the vapor to the liquid. On stages where NO_2 absorption results in NO production, the overall direction of mass transfer is from the liquid to the vapor for NO and from the vapor to liquid for NO_2. We can modulate the vaporization on each stage to reflect the resistance to phase interchange differently for each component. However, the Murphree efficiency usually presents a more flexible method than vaporization efficiencies. For Murphree efficiency, a single efficiency value can estimate the resistance to transfer to and from either phase for all components.

As a result, we decide to use component vaporization efficiencies on each stage for consistency and due to the lack of a solid theoretical basis to do otherwise. We specify the vaporization efficiency of 2.5 for NO, NO_2, and N_2O_4. The mere assignment of $E_V = 2.5$ for these species increase the number of stages required for the separation from 3 in the first equilibrium model to 18 in the second equilibrium model. In reality, we select the value of 2.5 so that the model stages would equal the actual stages used in the tower at the RFAAP site. Figure 4.40 illustrates the way the second equilibrium model looks in order to compare it to previous models.

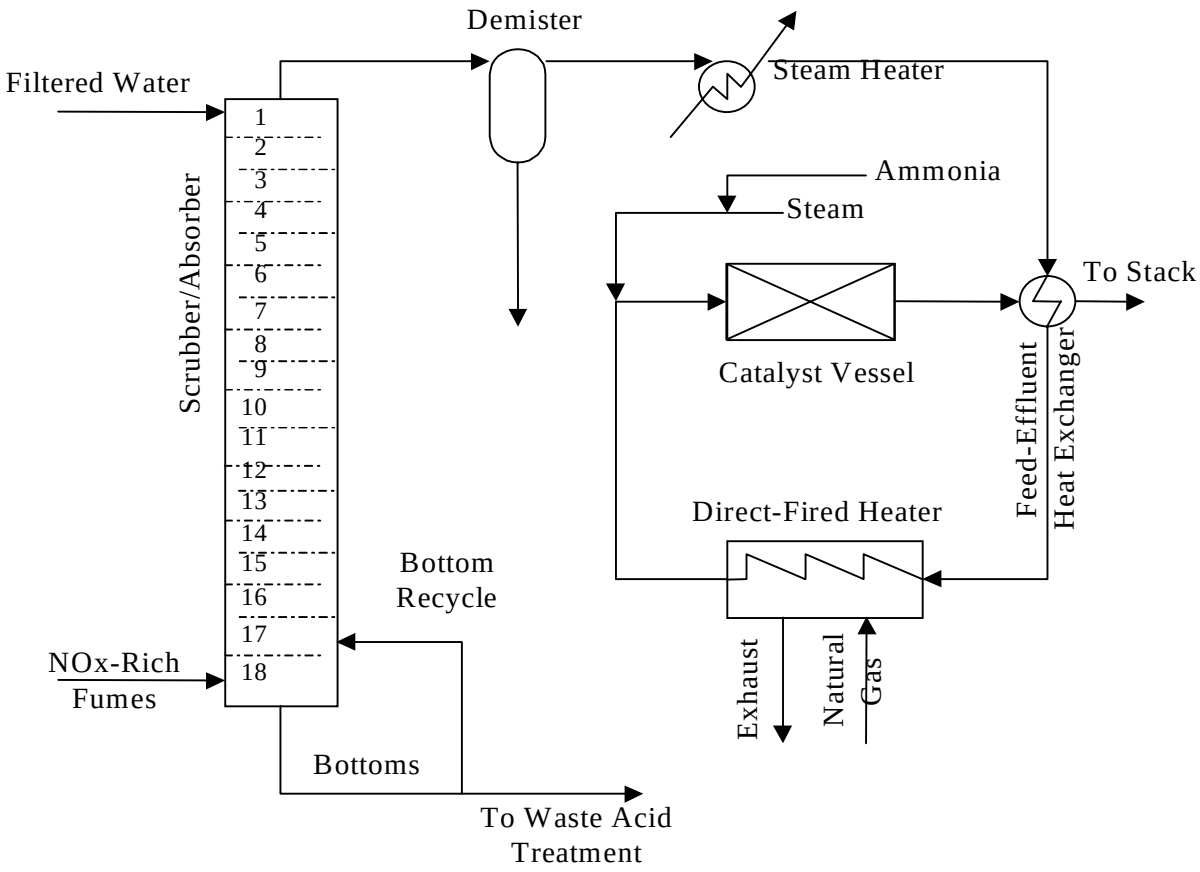

Figure 4.40. Block flow diagram of NOx abatement system for second equilibrium model.

As we showed for the first equilibrium model, the ratio of the equilibrium stages to the actual stage, also known as the overall column efficiency, for this particular system came to be 17%. Engineers typically use 40% as a rule of thumb for absorption-column stage efficiencies. From this, we see that NOx absorption achieves less than half of the efficiency of typical absorption systems that do not depend on chemical reactions. The reader should realize that although we define the vaporization efficiency as $E_V \equiv y_i/(Kx_i)$, its effects are far more reaching than just on the vapor and liquid compositions. Recall that reaction equilibrium depends on partial pressure in the vapor phase and concentration in the liquid phase. These values arise from functions of y_i and x_i. Therefore, vaporization efficiencies affect vapor-liquid equilibrium directly and affect reaction equilibrium indirectly, although profoundly.

4.3.3 Results of the Second Equilibrium Model

The results for the second equilibrium model do not differ greatly with those for the first equilibrium model. They do provide more information as to the physical process of stage wise NOx absorption. Table 4.7 gives the important stream results as compared to the RFAAP data. Figure 4.41 shows the column profile in temperature for the 18-stage simulation results. Figures 4.42 and 4.43 show the vapor and liquid component composition profiles, respectively, for the important species.

Table 4.7. Output flows as calculated by ASPEN compared to those supplied by RFAAP.

Stream: Mole Flow Lbmol/hr	WASTACID (Equilibrium Model)	WASTACID (Conversion Model)	Acid From Scrubber (RFAAP Data)	PRODUCT (Equilibrium Model)	PRODUCT (Conversion Model)	Gas to Vent Stack (RFAAP Data)
NO	6.8E-06	9E-3	-	0.22	0.06	0.06
NO_2	0.02	6E-3	-	0.035	9.7E-3	trace
NH_3	-	-	-	0	0	trace
O_2	4.0E-05	1.7E-6	-	132	132.1	132.06
N_2	7.9E-05	1.7E-6	-	498.7	498.8	496.8
H_2O	13.9	21.4	13.1	23.5	15.9	23.9
HNO_2	-	-	-	-	-	-
HNO_3	2.03	2.091	2.1	-	-	-
Total Flow lbmol/hr	18.0	25.6	20.8	654.4	646.8	654.8
Total Flow lb/hr	418	556	376	18624	18487	18631
Temperature F	89	80	86	350	350	350
Pressure psi	20	14	60	14.9	14.4	14.1

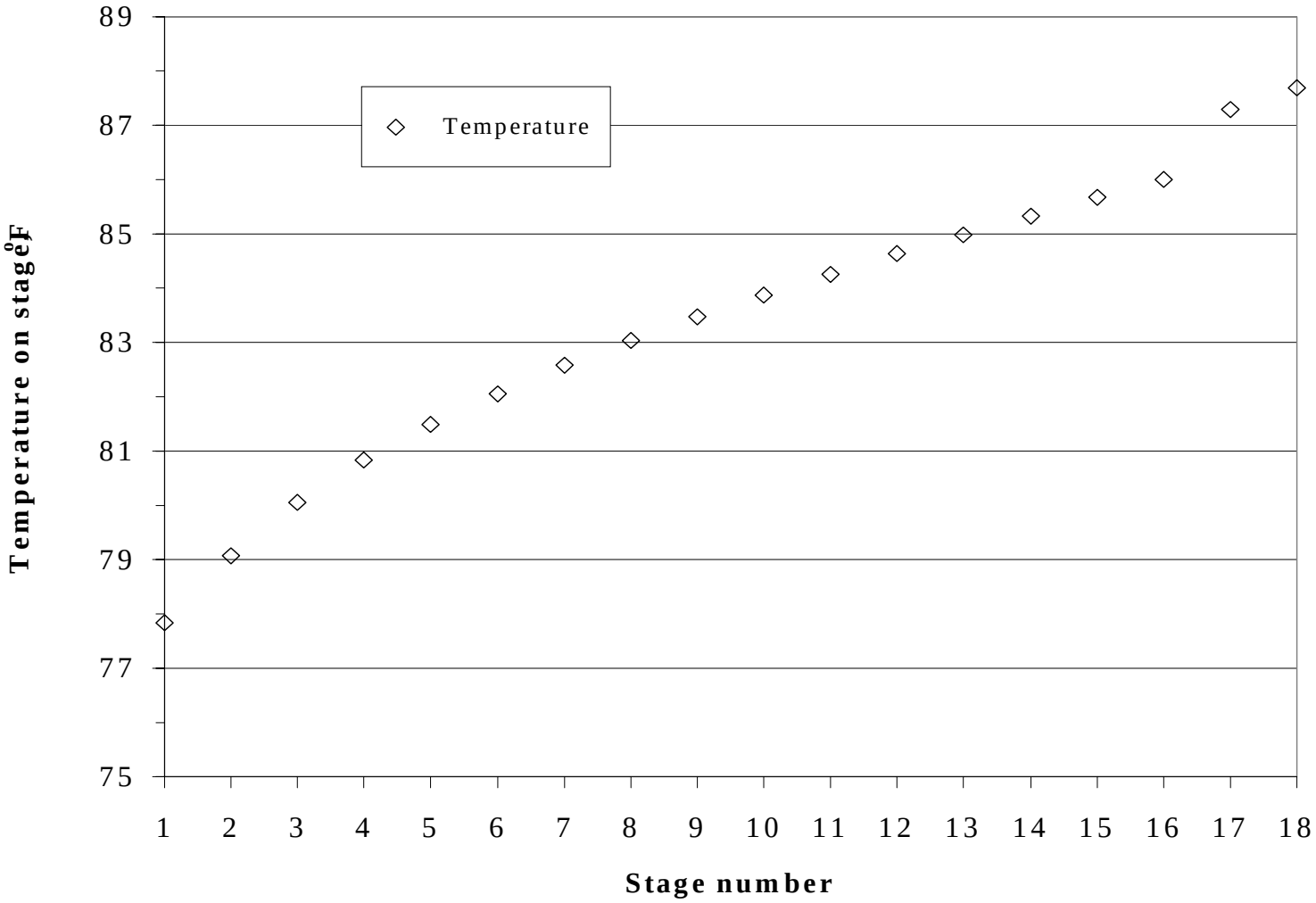

Figure 4.41. Column profile for stage temperatures for the second equilibrium model.

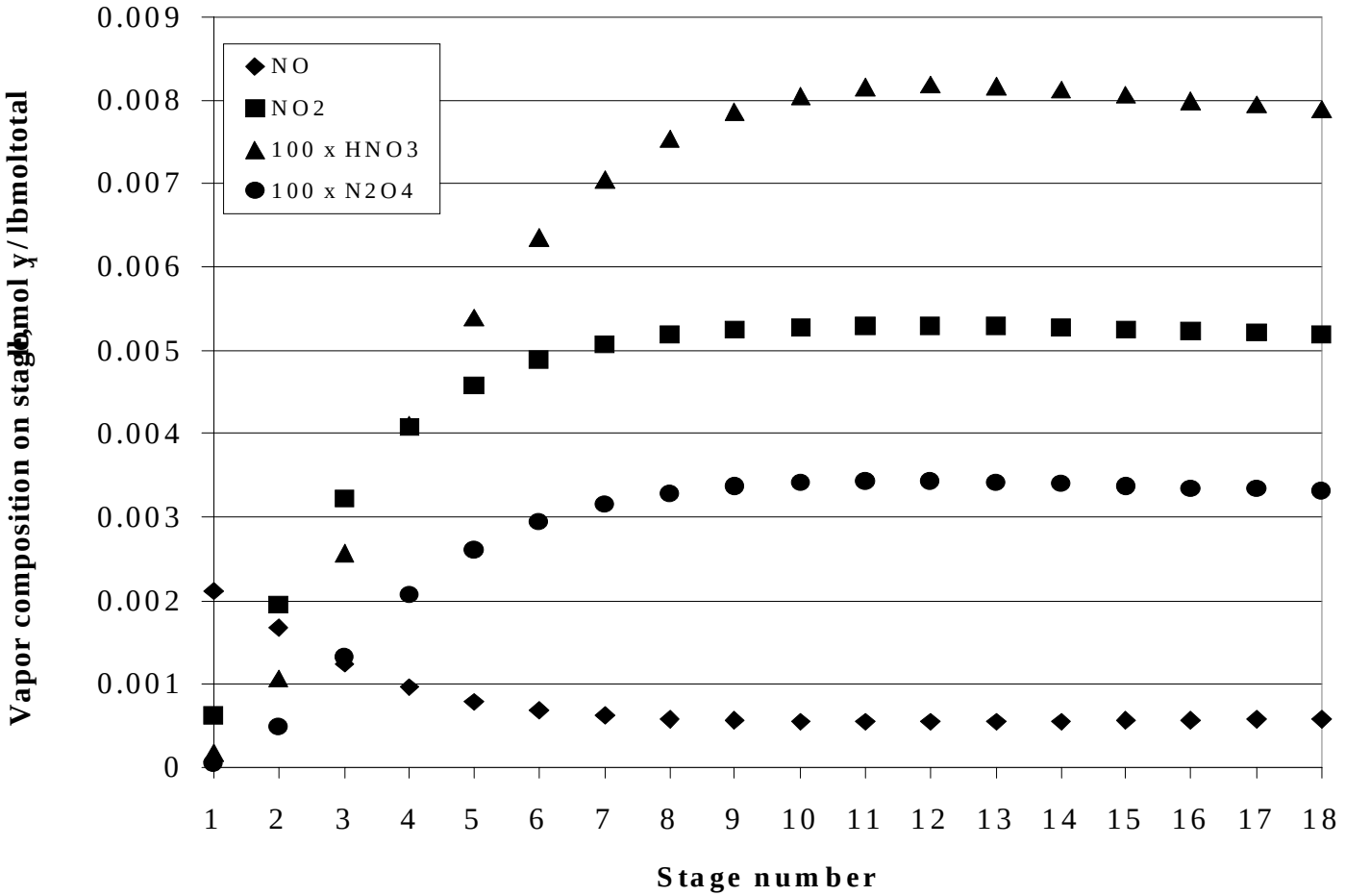

Figure 4.42. Simulation results for vapor-component stage compositions for the scrubber/absorber for the second equilibrum model.

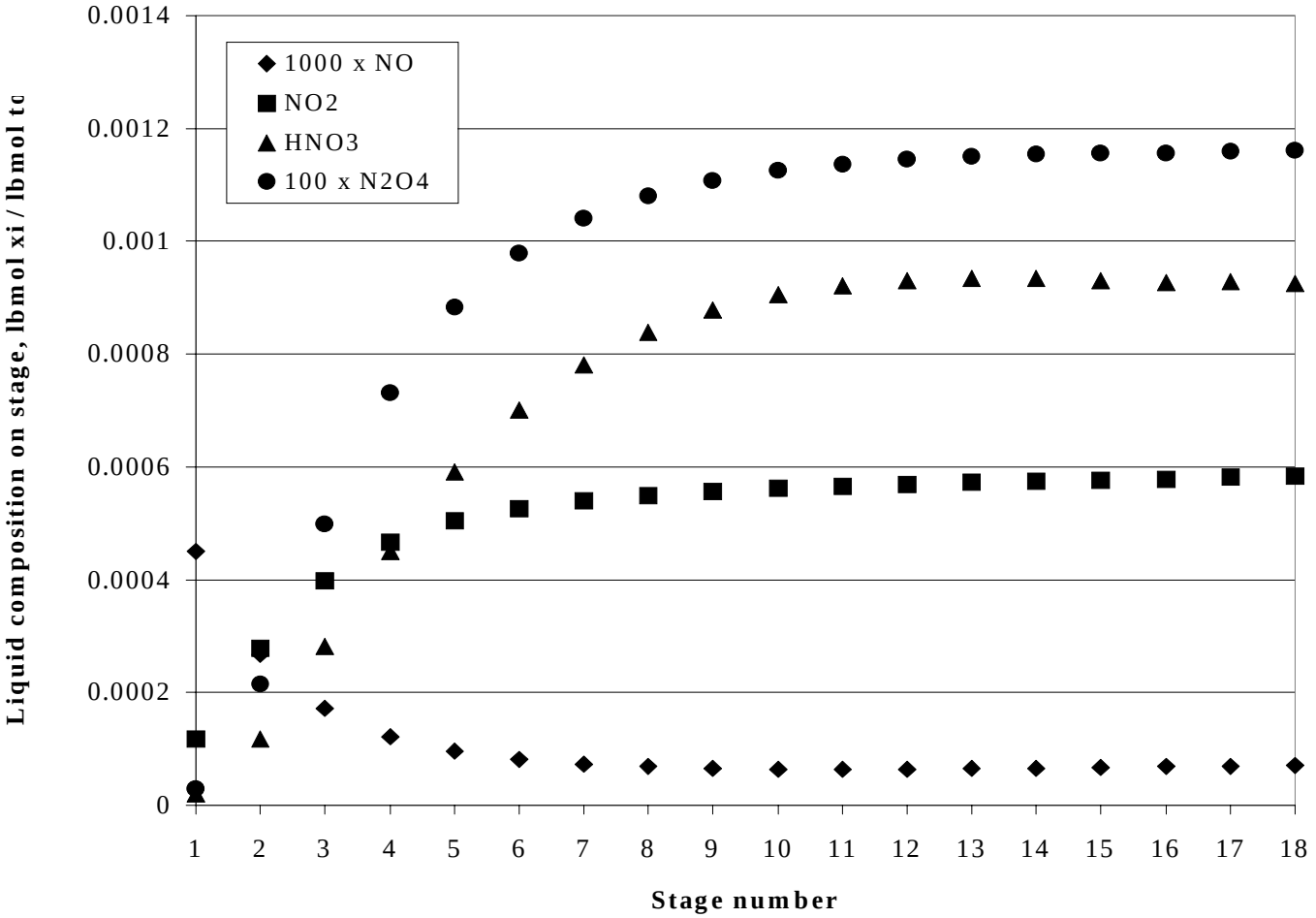

Figure 4.43. Simulation results for liquid-component stage compositions for the scrubber/absorber for the second equilibrum model.

4.3.4 Sensitivity Analyses

The above discussion of stage efficiencies underscores the differences between what the computer model tells us and what we know to be true in reality from experience and scientific knowledge. This section presents only those sensitivity analyses that add to the understanding of the column behavior over that of the first equilibrium model.

4.3.4.1 Column Cooling: Fume-Feed Temperature

We vary the temperature of the fumes from the nitrocellulose line prior to feeding it into the top of the column. Figure 4.44 shows the results for this test. We cannot achieve results for as wide a temperature range as in the first equilibrium model. However, we see that the second equilibrium model mimics the results of the first for the temperature range tested.

4.3.4.2 Top-Stage Pressure

Just as in the case of the first equilibrium model, varying the top-stage pressure affects the overall column pressure. In Figure 4.45, we see that the results for this test are analogous to those for the first equilibrium model.

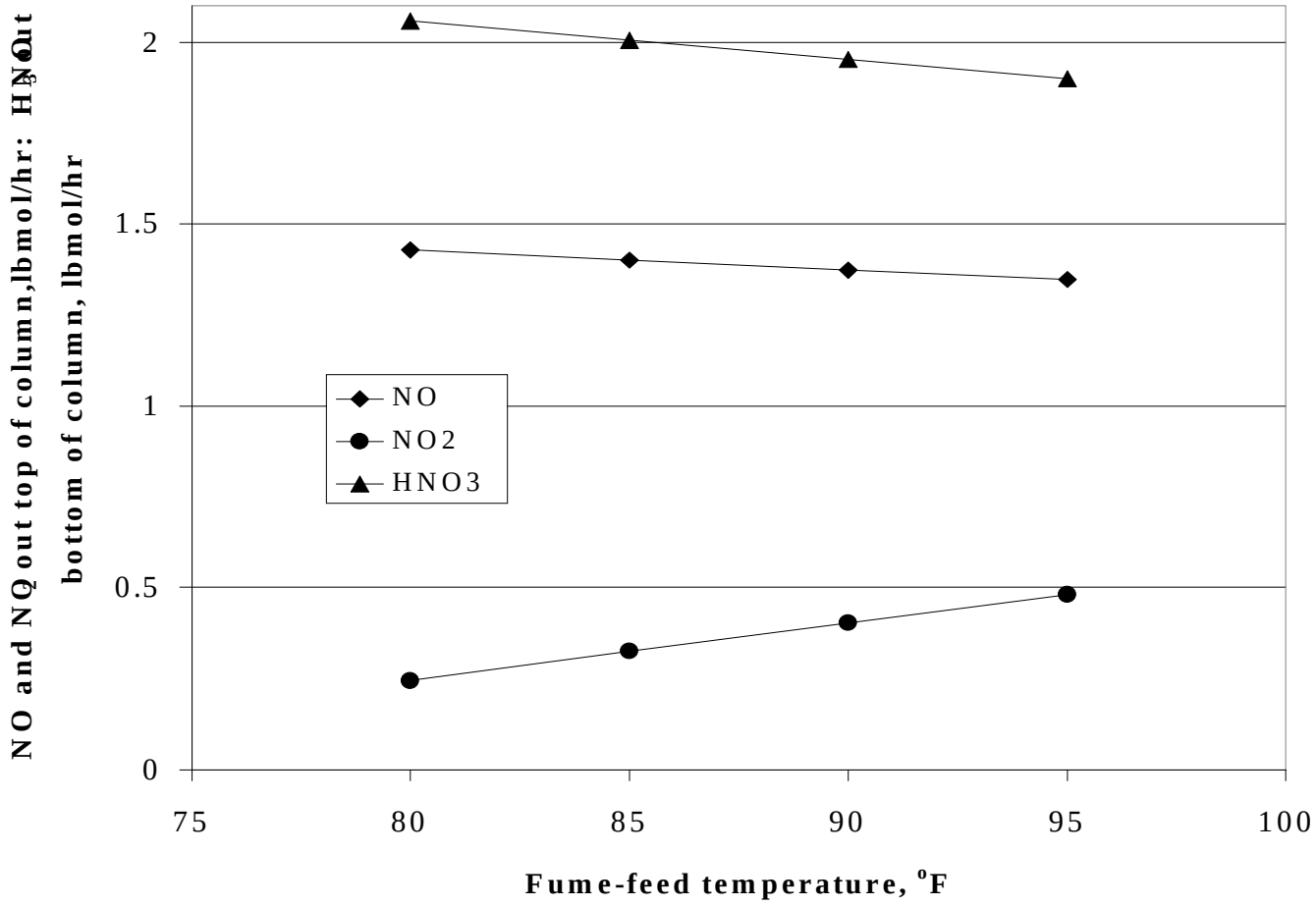

Figure 4.44. Sensitivity plot of the effect of fume-feed temperature on key components exiting the column.

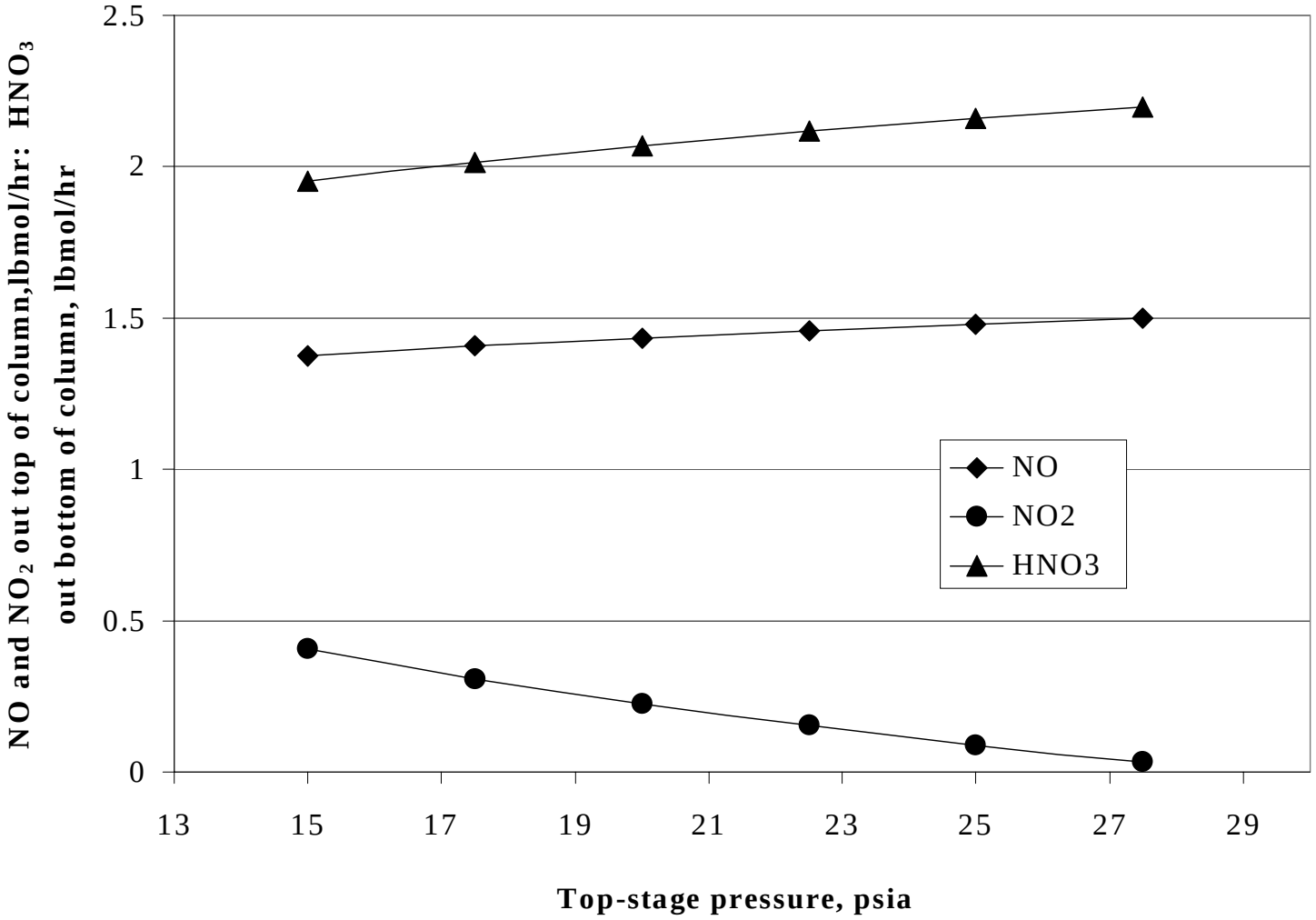

Figure 4.45. Sensitivity plot of the effect of top-stage pressure on key components exiting the column.

4.3.4.3 NO_2 Feed Flow Rate

We present a reaction profile of the scrubber/absorber column for the second equilibrium model. Figure 4.46 shows this reaction profile for NO_2. This plot is analogous to Figure 4.32 for the first equilibrium model. However, the results appear dramatically different. The preponderance of reaction activity is at the top and the bottom just like for the first equilibrium model. However, the activity for the second equilibrium model occurs much more at the top of the column. The middle contains virtually no reaction and the reaction at the bottom confines itself to a single stage. In fact, careful inspection shows that from stage 17 to approximately stage 12, NO_2 is actually produced within the column. How can this happen?

First, the use of vaporization efficiencies tends to push the reaction up the column. This probably represents an accurate picture of the true situation. NOx gases simply do not have time to absorb immediately and therefore rise through the column. The NO_2 absorbs gradually up the column, producing NO and nitric acid along the way. The NO rises and the nitric acid descends with the water. This descending nitric acid solution comes in contact with warmer fumes on its way down. The warmer fumes contain NO (fed initially as well as those produced on the bottom stage). Because reaction (4.4,5) is exothermic and because nitric acid and NO concentrations are high in the middle of the column, reaction (4.4,5) proceeds in the reverse direction, producing NO_2.

Does this sequence of events accurately depict the behavior of the real column at RFAAP? The answer is both yes and no. Even with vaporization efficiencies, the second equilibrium model remains an equilibrium model. Through the use of vaporization efficiencies, we simply shift the equilibrium farther to the gas for the components for which we specify these values (NO, NO_2, N_2O_4). Is this an accurate approximation? We do not know this answer, but we think it is a good assumption to make in the light of the literature and the results we obtain from it. Mass-transfer rates depend on driving force, that is, the concentration differences for the absorbing species. Large concentration differences suggest fast mass transfer. Therefore, the vaporization efficiencies we specify should be less for stages where the driving force is high. However, we do not know the degree to which they should vary and on which component driving force affects the vaporization efficiencies the greatest. Despite these drawbacks, constant vaporization efficiencies approximate the system quite well.

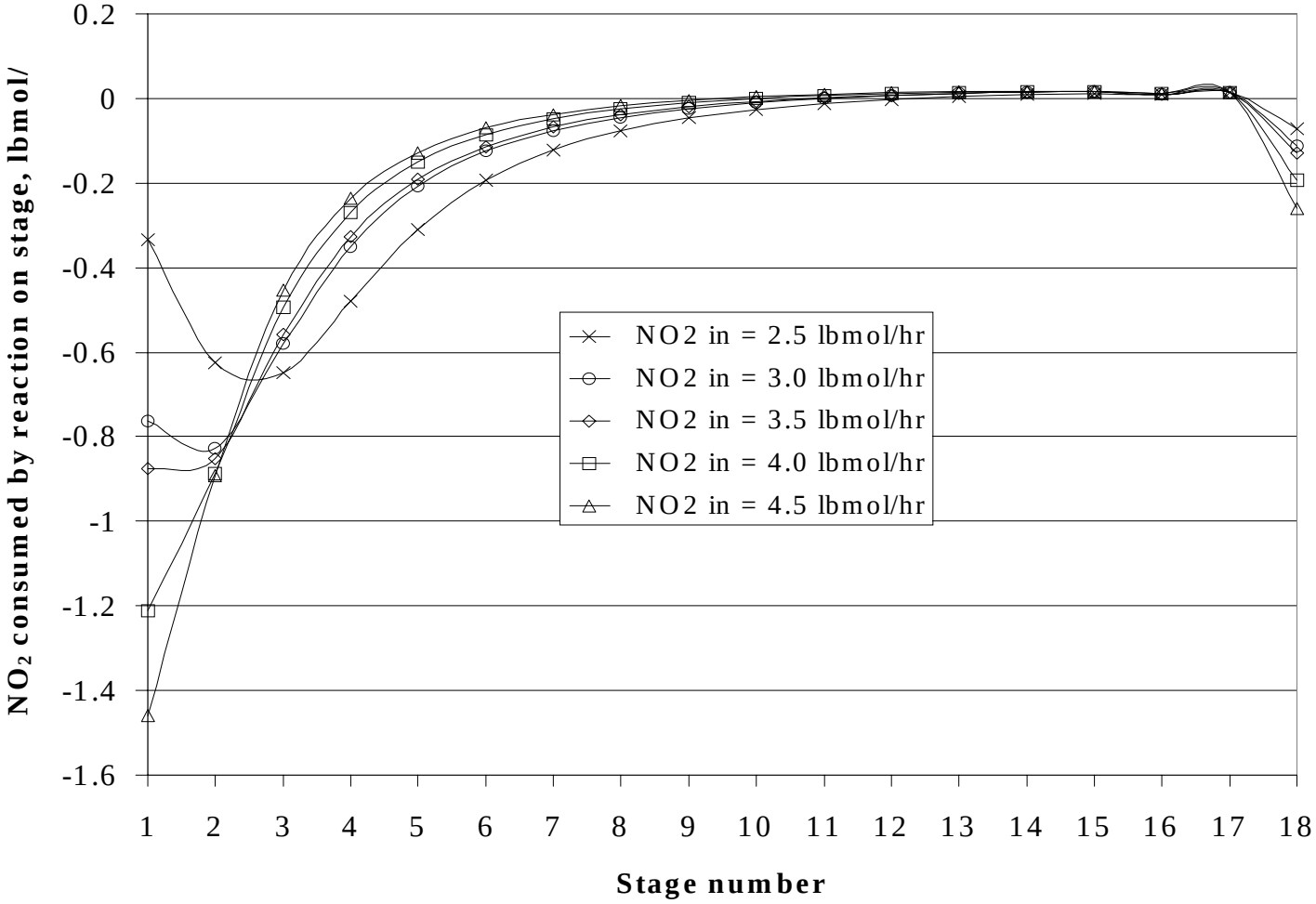

Figure 4.46. Stage-by-stage reaction profile for NO_2 in the scrubber/absorber for the second equilibrium model. Negative values correspond to NO_2 consumed by reaction, and positive values correspond to NO_2 production.

4.3.5 Advantages of the Second Equilibrium Model

The second equilibrium model gives us a better physical interpretation of how NOx absorption proceeds within the scrubber/absorber column. We see the component compositions in the vapor and liquid phases on each stage of the column and where the reaction produces and consumes the components. We can use this information for optimization of the column for promoting the elimination or production of certain species in sections of the column that are not performing to the maximum effect. For example, we see in Figure 4.46 that very little reaction occurs in the middle stages of the column. With this information, we can work with options to improve the reaction conversions in the middle stages.

Given the information on vapor- and liquid-stage composition profiles for the column, we can determine from which stages to take and add side streams. These side streams can likewise be used to promote reaction within the column.

4.3.6 Disadvantages of the Second Equilibrium Model

The second equilibrium model does not rectify the problems that we encountered in the first equilibrium model with the catalyst vessel. Therefore, this problem remains and, as stated previously, cannot be repaired within the confines of the equilibrium-reaction assumption. Neither has the second equilibrium model addressed the problems of nitric acid autocatalysis and the hydrogen peroxide effect. We require a kinetic study of the catalyst vessel reactions and the scrubber/absorber parameters for satisfactory treatment of these processes under the stated conditions.

The only accommodation that the equilibrium model makes for the time-dependent nature of NOx absorption is through the use of the vaporization efficiency. We assign the vaporization efficiency semi-arbitrarily as a singular value to individual components in the column, specifically NO, NO_2 and N_2O_4. The vaporization efficiencies utilized in the second

equilibrium model result from trial and error. We keep the values the same for the different components as well as for each stage for consistency and simplicity. Vaporization efficiency parameters remain constant until manually changed.

Though we would prefer to use Murphree efficiency over vaporization efficiency, the Murphree efficiency still represents an arbitrarily assigned parameter resulting from trial and error. Clearly, the manipulation of process parameters through sensitivity analyses and equipment retrofit trials affects only the equilibrium states of the reactions and absorption of the various components within the ASPEN simulation. There exists no visible effect on the rate of these processes, because the stage efficiencies are the only manifestation of this consideration, and they remain constant.

The equilibrium assumption for the reactions involved remains valid. However, we find the equilibrium assumption for vapor-liquid equilibrium unsatisfactory. Even the typical engineering expedient of assignment of vaporization efficiencies to account for column rate limitations becomes suspect for the unique NOx absorption system. We must view the results for the simulation in the light that unfortunately, our model cannot tell us the degree to which the parameters affect the stage efficiency. We must qualify each result arrived at from adjustment of parameters that we know from experience should affect stage efficiency.

From experience and our knowledge of thermodynamics, we know that increased pressure compresses the vapor and decreases the volumetric flow rate and vapor velocity through the column. Reducing vapor velocity increases the vapor residence time. Also, increased pressure raises component partial pressures, which in turn increases gas-phase reaction rates. Both of these factors lead to increases stage efficiency. However, the only visible effect from ASPEN is that of pressure on vapor-phase reaction equilibrium and component absorption. This aspect represents a major drawback for the equilibrium approach, because the efficiency has such a great effect on tower performance for the NOx absorption system. Therefore, for the results presented, we must assume that the efficiency of the column does not change. We tend to doubt the validity of this assumption.

Another drawback of the second equilibrium model that the reader will likely never see, and yet remains a very important aspect of computer modeling and simulation, is the increased computational complexity and instability of the simulation. The second equilibrium model requires greater simulation run times and converges less frequently than the first equilibrium model. This effect gives a good lesson of why we strive for the simplest computer model that gives accurate results. Even as simple a thing as using vaporization efficiencies to give eighteen stages increases computational complexity immensely.

4.4 Conclusions

4.4.1 Conclusions Regarding Process Parameters

Equilibrium modeled reactions provide an immensely improved way to model the NOx absorption process over stoichiometric conversion reactions. The equilibrium models provide us with great insight into the problem of NOx abatement as encountered at the RFAAP site. Primarily, they shed light on the multitude of process parameter adjustments and effects possible in the scrubber/absorber.

Mass transfer always increases with the number of stages. The amount of increase can vary considerably however. We have seen that there remains much room for improvement if the column can easily accept new stages or if a second column is not out of the question. For current conditions, diminishing returns quickly set in after the 20 to 25 total stages. However, for any greater NOx flow to the system, more stages will definitely be required to achieve results comparable to those observed currently.

As hypothesized, pressure and temperature strongly affect the performance of the scrubber/absorber. Increasing pressure and decreasing temperature, by any means available, reward the engineer with improved NOx absorption efficiency. This chapter addresses many different means of cooling the process. However, we make no mention of the practicality of any

of these methods, only the magnitude of effects associated with each. The chapter on retrofit options for the hybrid equilibrium/kinetic model addresses the issue of practicality and economic returns.

Cooling the filtered water shows very little effect. However, direct cooling of the column by a cooling jacket or special cooling stages, as well as cooling the fume feed gives very optimistic results for improved performance. Few such options exist for the pressurization of the column aside from purchasing blowers. Again, this chapter draws no conclusion as to the practicality of this approach.

Clearly, we should make a goal of feeding NOx to the column as concentrated as possible. Increasing the partial pressure of NOx species increases the total absorption, the percent absorbed, and the maximum possible nitric acid concentration in the fluid effluent. However, the practicality of demanding upstream sites to deliver their "waste" in an "uncontaminated" form gives us little encouragement. Still, it remains a goal for existing and NOx abatement processes in the design phase.

NOx removal increases considerably with an increase of filtered water fed to the top of the column. However, the nitric acid effluent becomes considerably diluted and quickly loses all recovery value. The ideal situation requires control of the water feed rate dependent upon the inlet NOx rate. The equilibrium model gives preliminary results for a control scheme of this kind.

The equilibrium model exposes the disappointing fact that most of the efforts to increase NOx removal also result in the dilution of the Nitric acid effluent. Increasing the filtered-water flow rate dilutes the acid for obvious reasons. Temperature and pressure affect the acid concentration by increasing the condensation of water into the liquid effluent stream under the conditions that likewise improve NOx removal.

4.4.2 Itemized Conclusions

1. For the conditions observed at RFAAP, NO oxidation proceeds at a negligible rate. Less than 10% of the NO fed to the column oxidizes within the column itself. However, one can make substantial improvements in the conversion by reducing temperature, increasing pressure, and increasing NO partial pressure.

2. The first and second equilibrium model results for the scrubber/absorber agree well with experimental results for a similar process (Thomas and Vanderschuren, 1996; Cheremisinoff and Young, 1977).

3. Cooling the fume feed presents a viable strategy for column cooling.

4. Cooling the fume feed from 90 ^{o}F to 50 ^{o}F eliminates virtually all the NO_2 from the fumes. Nitric acid converts to NO_2 in a one-to-one molar ratio to the NO_2 consumed.

5. Cooling the filtered water stream does improve NO_2 removal but not significantly compared to other options.

6. Increasing column top-stage pressure from 15 psia to 30 psia increases NO_2 removal efficiency from 92.0% to 97.6% and increases nitric acid production accordingly.

7. Increasing the filtered-water flow rate from 21 lbmol/hr to 30 lbmol/hr virtually eliminates all the NO_2 from the fumes stream.

8. Column cooling, increasing column pressure, and increasing the filtered water feed all aid in NOx elimination but also dilute nitric acid effluent, reducing its recovery value.

9. The reactions that eliminate NO_2 and produce nitric acid primarily occur in the top and bottom of the column. However, some disagreement persists between the first and second equilibrium models as to whether the predominant section is the top or the bottom.

10. The equilibrium model gives unstable results for the catalyst vessel.

4.5 Recommendations

1. We need a solution for the problems with the catalyst vessel. We recommend the research of a kinetic model for the reactions in this unit.

2. Care must be taken when viewing the results of the scrubber/absorber simulations in the light of the equilibrium assumptions used in the model. Recall that there is no provision given for the dependence of rates or stage efficiencies within the model itself. Keep in mind, therefore, that results give the maximum attainable NOx removal, whereas slow mass-transfer rates and column inefficiencies may hinder the response in an actual column.

3. The model does not take into account the widely theorized effect of nitric acid. Researchers claim that up to 30% of nitric acid by weight in the scrubbing liquid improves oxidation and absorption of NO. Higher pressures and lower temperatures may raise this mark. Proving this hypothesis requires experimental work in a laboratory or in the field.

4. Experimental literature states that adding hydrogen peroxide, H_2O_2, to the scrubbing solution improves NOx absorption by reducing the reversibility of reaction (4.4,5) thereby enhancing the catalytic effect of nitric acid. NOx absorption trials with hydrogen peroxide may prove beneficial in the actual process. Kinetic factors must be added to the simulation to show the effects of hydrogen peroxide and nitric acid catalysis.

4.6 Nomenclature

btu/hr	rate of energy flow
dx/dt	rate of change of the variable x with respect to time
E_M	Murphree efficiency
E_v	vaporization efficiency
k	equilibrium constant
K1	equilibrium constant for reaction 1
K_{eq}	equilibrium constant for chemical reaction
K_i	K value for the ith component, $K_i = y_i/x_i$
x_i	liquid composition of the ith component
x_{eq}	liquid composition of the ith component at equilibrium
y_i	vapor composition of the ith component
y_{eq}	vapor composition of the ith component at equilibrium

4.7 References

Cheremisinoff, P. N., and R. A. Young ed., *Air Pollution Control and Design Handbook, Part 2*, Marcel Dekker, Inc., New York (1977), pp. 628, 671-678.

Jethani, K. R., N. J. Suchak, and J. B. Joshi, "Modeling and Simulation of a Spray Column for NOx Absorption," *Computers in Chemical Engineering*, **16**, 11 (1992).

Matasa, C. and E. Tonca, *Basic Nitrogen Compounds: Chemistry, Technology and Applications, Third Edition*, Chemical Publishing Co., Inc., New York (1973), p. 442.

Miller, D. N., "Mass Transfer in Nitric Acid," *AIChE Journal*, **33**, 1351 (August 1987).

Newman, B. L. and G. Carta, "Mass Transfer in the Absorption of Nitrogen Oxides in Alkaline Solutions," *AIChE Journal*, **34**, 1190 (July 1988).

Peters, M. S. and K. D. Timmerhaus, *Plant Design and Economics for Chemical Engineers, Fourth Edition*, McGraw-Hill, Inc., New York (1991), pp. 661 – 677.

Suchak, N. J. and J. B. Joshi, "Simulation and Optimization of NOx Absorption System in Nitric Acid Manufacture," *AIChE Journal*, **40**, 944 (June 1994).

Thomas, D., and J. Vanderschuren, "Modeling of NOx Absorption into Nitric Acid Solutions Containing Hydrogen Peroxide," *Chemical Engineering Science*, **51**, 2649 (1996).

Thomas, D., and J. Vanderschuren, "The Absorption-Oxidation of NOx with Hydrogen Peroxide for the Treatment of Tail Gases," *Industrial Engineering and Chemistry Research*, **36**, 3315 (1997).